

Dissertation

**Optical quality after implantation of spherical or
aspheric intraocular lenses in hyperopic and emmetropic
patients**

submitted by

Dr.med.univ. Gernot Steinwender

for the Academic Degree of

Doctor of Medical Science (Dr.scient.med.)

at the

Medical University of Graz

Department of Ophthalmology

under the Supervision of

Univ.-Doz. Dr. med.univ. Navid Ardjomand

Univ.-Prof. Dr.med.univ. Andreas Wedrich

Univ.-Prof. Dr.med.univ. Oliver Findl, MBA

2018

Declaration

I hereby declare that this thesis is my own original work and that I have fully acknowledged by name all of those individuals and organisations that have contributed to the research for this thesis. Due acknowledgement has been made in the text to all other material used. Throughout this thesis and in all related publications I followed the guidelines of “Standards of Good Scientific Practice and Ombuds Committee at the Medical University of Graz”.

Disclosures

Part of this thesis has been published in Gernot Steinwender¹, Sanja Strini¹, Wilfried Glatz¹, Gerald Schwantzer², Bertram Vidic¹, Oliver Findl³, Andreas Wedrich¹, Navid Ardjomand¹. Depth of focus after implantation of spherical or aspheric intraocular lenses in hyperopic and emmetropic patients. J Cataract Refract Surg. 2017; 43(11): 1413-1419.

¹ *Department of Ophthalmology, Medical University of Graz, Graz, Austria*

² *Institute for Medical Informatics, Statistics and Documentation, Medical University of Graz, Graz, Austria*

³ *Vienna Institute for Research in Ocular Surgery, Karl Landsteiner Institute, Hanusch Hospital, Vienna, Austria.*

I confirm that all co-authors have explicitly agreed to the use of their data in this thesis. I confirm that I have obtained permission to reproduce figures and tables published in “Depth of focus after implantation of spherical or aspheric intraocular lenses in hyperopic and emmetropic patients. J Cataract Refract Surg. 2017; 43(11): 1413-1419” from the copyright holder Elsevier Inc..

Acknowledgments

Doctoral student Gernot Steinwender received funding from the Medical University of Graz through the Doctoral School “Sustainable Health Research”.

Graz, 13.11.2018

Table of contents

Abbreviations and Definitions	5
List of Figures.....	6
List of Tables.....	8
Abstract in German	9
Abstract in English.....	10
1 Clinical optics and optical quality	11
1.1 Refractive errors.....	12
1.1.1 Myopia	12
1.1.2 Hyperopia.....	14
1.1.3 Accommodation and presbyopia	15
1.1.4 Astigmatism	17
1.1.5 Higher-order aberrations	20
1.2 Functional testing of optical quality	34
1.2.1 Visual acuity.....	35
1.2.2 Contrast sensitivity	38
1.2.3 Depth of focus	40
2 Intraocular lenses	43
2.1 General indications	43
2.1.1 Cataract surgery.....	43
2.1.2 Refractive cataract surgery.....	49
2.2 Intraocular lens materials.....	50
2.2.1 Hydrophobic acrylic	50
2.2.2 Hydrophilic acrylic	51
2.2.3 Silicone.....	51
2.3 Intraocular lens design.....	52
2.3.1 Intraocular lens haptic design.....	52
2.3.2 Intraocular lens optic design	54
2.4 Intraocular lens power calculation	55
2.4.1 Sources of error	55
2.4.2 Formulas.....	56

2.4.3	Intraocular lens power calculation in short eyes	57
2.5	Aspheric intraocular lenses	58
3	Depth of focus after implantation of spherical or aspheric intraocular lenses in hyperopic and emmetropic patients	64
3.1	Introduction	64
3.2	Patients and methods	65
3.3	Results.....	68
3.4	Discussion	91
4	Bibliography	95

Abbreviations and Definitions

AL=axial length

BSS=balanced salt solution

CCC=continuous curvilinear capsulorhexis

CDVA=corrected distance visual acuity

CNVA=corrected near visual acuity

D=diopeters

DCIVA=distance corrected intermediate visual acuity

DCNVA=distance corrected near visual acuity

ELP=effective lens position

HOA=higher-order aberration

IOL=intraocular lens

K-value=keratometry value

PCO=posterior capsule opacification

PMMA= polymethylmethacrylate

RMS=root mean square

SA=spherical aberration

SE=spherical equivalent

UDVA=uncorrected distance visual acuity

List of Figures

Figure 1: Emmetropia with accommodation relaxed.....	11
Figure 2: Myopia with accommodation relaxed.....	13
Figure 3: Hyperopia with accommodation relaxed.....	14
Figure 4: Emmetropia with accommodation stimulated.....	16
Figure 5: Types of astigmatism.....	18
Figure 6: The conoid of Sturm.....	19
Figure 7: Change of astigmatism axis with age.....	20
Figure 8: Relation between light ray and wavefront.....	21
Figure 9: Light rays and wavefront in ametropia.....	22
Figure 10: Coma.....	23
Figure 11: Spherical aberration.....	24
Figure 12: Relation between pupil diameter and optical effect of aberrations.....	25
Figure 13: Principle of Hartmann-Shack aberrometry.....	26
Figure 14: Principle of Tscherning aberrometry.....	27
Figure 15: Pyramid with Zernike polynomials to the 5 th order.....	29
Figure 16: Interaction of defocus (Z_{-2}^0) and primary spherical aberration (Z_4^0).....	32
Figure 17: Enhanced depth of focus due to interaction of defocus and primary spherical aberration.....	33
Figure 18: Modified ETDRS visual acuity chart.....	36
Figure 19: Radner reading charts for near visual acuity testing. Reprinted by permission from Springer Nature BMC, Eye and Vision, Radner 2016 ³⁶	37
Figure 20: Typical contrast sensitivity curve.....	38
Figure 21: Pelli-Robson chart for contrast sensitivity testing.....	39
Figure 22: Exemplary defocus curves of eyes with monofocal and multifocal intraocular lenses (IOL).....	41
Figure 23: Creation of main incision.....	45
Figure 24: Creation of curvilinear capsulorhexis with a bent needle.....	46
Figure 25: Hydrodissection.....	47
Figure 26: Cracking the nucleus in half after creating a central groove with the phacoemulsification tip.....	48
Figure 27: Injecting the folded intraocular lens into the capsular bag through the anterior capsulorhexis.....	49

Figure 28: Different haptic designs.....	53
Figure 29: Scattergram of corneal 4th order spherical aberration RMS versus age.....	58
Figure 30: Scattergram of internal 4th order spherical aberration coefficients versus age.....	59
Figure 31: Scattergram of total eye higher-order aberrations RMS versus age.....	60
Figure 32: Image quality after implantation of spherical or aspheric intraocular lenses as a function of pupil diameter.....	62
Figure 33: Axial length [mm].....	75
Figure 34: Mean K-value [D].....	75
Figure 35: IOL-power [D].....	76
Figure 36: Corneal astigmatism [D].....	77
Figure 37: Photopic pupil diameter [mm].....	78
Figure 38: Mesopic pupil diameter [mm].....	78
Figure 39: RMS corneal higher-order aberrations [μm].....	79
Figure 40: RMS corneal spherical aberration [μm].....	80
Figure 41: RMS total eye higher-order aberrations [μm].....	81
Figure 42: RMS total eye spherical aberration [μm].....	81
Figure 43: Uncorrected distance visual acuity (UDVA) [logMAR].....	82
Figure 44: Manifest refractive spherical equivalent (MRSE) [D].....	82
Figure 45: Corrected near visual acuity (CNVA) [logMAR].....	83
Figure 46: Distance corrected intermediate visual acuity (DCIVA) [logMAR].....	83
Figure 47: Distance corrected near visual acuity (DCNVA).....	84
Figure 48: Photopic contrast sensitivity [logCS].....	85
Figure 49: Mesopic contrast sensitivity [logCS].....	85
Figure 50: Defocus curves of eyes with aspheric (dashed line) and spherical IOLs (solid line).....	88
Figure 51: Defocus curves of hyperopic eyes with aspheric (dashed line) and spherical IOLs (solid line).....	89
Figure 52: Defocus curves of emmetropic eyes with aspheric (dashed line) and spherical IOLs (solid line).....	90

List of Tables

Table 1: Patient characteristics for aspheric and spherical IOL group.	68
Table 2: Refractive outcome for aspheric and spherical IOL group.....	69
Table 3: Patient characteristics for hyperopic and emmetropic subgroup with an aspheric IOL.....	71
Table 4: Refractive outcome for hyperopic and emmetropic subgroup with an aspheric IOL.....	72
Table 5: Patient characteristics for hyperopic and emmetropic subgroups with a spherical IOL.....	73
Table 6: Refractive outcome for hyperopic and emmetropic subgroups with a spherical IOL.....	74
Table 7: Refractive outcome for the hyperopic patient group.....	87

Abstract in German

Ziel: Das Ziel war es zu untersuchen, ob hyperope Patienten mit kurzer Achsenlänge und hoher Intraokularlinsenstärke nach Implantation einer monofokalen sphärischen oder asphärischen Intraokularlinse (IOL) eine bessere Schärfentiefe erreichen können.

Methoden: In dieser randomisierten klinischen Studie wurden zur Kataraktoperation vorstellige Patienten nach der errechneten IOL-Stärke in eine hyperope (≥ 22.0 D) oder emmetrope (18.0 to 21.5 D) Subgruppe unterteilt und erhielten entweder eine asphärische (Tecnis ZA9003, Abbott Medical Optics) oder sphärische IOL (Sensar AR40e, Abbott Medical Optics). Postoperative erhobene Parameter waren korrigierte und unkorrigierte Distanzsehschärfe (CDVA, UDVA), distanzkorrigierte Intermediär- (DCIVA) und Nahsehschärfe (DCNVA), Root-mean-square(RMS)-Werte der Aberrationen höherer Ordnung (HOA) und der sphärischen Aberration (SA) der Kornea und des gesamten Auges, sowie photopische und mesopische Kontrastsensitivität.

Ergebnisse: Zweiundsechzig Augen von 62 Patienten wurden in diese Studie eingeschlossen, davon 34 Augen in der Gruppe mit asphärischen IOL (15 hyperope und 19 emmetrope Augen) und 28 Augen in der Gruppe mit sphärischen IOL (14 hyperope und 14 emmetrope Augen). UDVA, CDVA und Kontrastsensitivität zeigten keine signifikanten Unterschiede zwischen der asphärischen und sphärischen IOL-Gruppe, wohingegen DCIVA ($P = 0.004$) und DCNVA ($P = 0.001$) in der sphärischen IOL-Gruppe signifikant besser waren. Es zeigten sich keine signifikanten Unterschiede bezüglich DCIVA und DCNVA zwischen hyperopen und emmetropen Patienten, weder nach Implantation einer asphärischen oder einer sphärischen IOL.

Konklusion: Nach Implantation einer monofokalen sphärischen IOL lässt sich eine verbesserte Schärfentiefe ohne Herabsetzung von Distanzsehschärfe oder Kontrastsensitivität erreichen. Es zeigten sich keine signifikanten Unterschiede in der Schärfentiefe zwischen hyperopen und emmetropen Augen.

Abstract in English

Purpose: To evaluate, whether hyperopic patients with short axial length and high dioptric intraocular lens (IOL) power may achieve a higher depth of focus after implantation of a monofocal spherical or aspheric IOL than emmetropic patients.

Methods: In this randomized clinical trial patients presenting for cataract surgery were divided by calculated IOL power into a hyperopic (≥ 22.0 D) or emmetropic (18.0 to 21.5 D) subgroup, and received either an aspheric (Tecnis ZA9003, Abbott Medical Optics) or a spherical IOL (Sensar AR40e, Abbott Medical Optics). Postoperative measurements included corrected and uncorrected distance visual acuity (CDVA, UDVA), distance-corrected intermediate and near visual acuity (DCIVA, DCNVA), root-mean-square (RMS) values of corneal and total eye higher-order aberrations (HOA) and spherical aberrations (SA), and photopic and mesopic contrast sensitivity.

Results: Sixty-two eyes of 62 patients were enrolled in this study; 34 eyes in the aspheric IOL group (15 hyperopic and 19 emmetropic eyes) and 28 eyes in the spherical IOL group (14 hyperopic and 14 emmetropic eyes). UDVA, CDVA, and contrast sensitivity did not differ significantly among the aspheric and spherical IOL group, whereas DCIVA and DCNVA were significantly better in the spherical IOL group ($P = 0.004$, $P = 0.001$, respectively). No significant differences were found between hyperopic and emmetropic patients in DCIVA and DCNVA with both, aspheric or spherical IOLs.

Conclusions: Implantation of a monofocal spherical IOL resulted in an increased depth of focus without significant degradation of distance visual acuity or contrast sensitivity. There were no differences in depth of focus between hyperopic and emmetropic eyes.

1 Clinical optics and optical quality

This introductory chapter discusses the concepts of physiological optics that form the foundation for deeper understanding of the topics covered in the subsequent chapters and the purpose of the study.

Perfect imaging of objects on the retina via the dioptric system of the human eye is the basic condition for a true perception of the environment with our visual sense. In a real optical system like the human eye, the optical quality is limited by aberrations, diffraction and scatter. Thereof, the most important sources for degradation of retinal image quality are aberrations. A large majority of these aberrations can be compensated by spherical or cylindrical glasses, leading to satisfactory image quality.

Emmetropia is the refractive state in which rays of light from a distant object are focused on the retina in a nonaccommodating eye (Figure 1). It has to be noted that emmetropia in terms of geometric optic does not exist due to an inherent amount of measurable aberrations in every eye. However, if those aberrations are not detectable in subjective refraction measurement, physiological emmetropia is present.

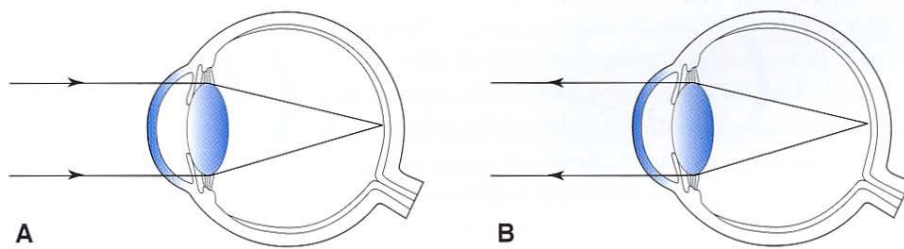


Figure 1: Emmetropia with accommodation relaxed. *A*, Parallel light rays from infinity focus to a point on the retina. *B*, Similarly, light rays emanating from a point on the retina focus at the far point of the eye at optical infinity. Reprinted by permission from American Academy of Ophthalmology, Basic and Clinical Science Course, Section 3, Clinical optics, Azar 2013-2014¹

1.1 Refractive errors

Refractive errors (= ametropia) are characterized by a discrepancy between refractive power and axial length of an eye.

In axial ametropia the eye has a normal refractive power, but objects do not focus on the retina because the axial length is too short or long. Axial ametropia induces a spherical refractive error, which can reach extreme amounts in high discrepancies.

Refractive ametropia is present, if objects do not focus on the retina in eyes with normal axial lengths and too strong or weak refractive power (either of the cornea or lens). Usually, refractive ametropia does not induce high refractive errors, except in the presence of pathologic conditions (keratoconus, cornea plana). Cornea and lens further are the sources of non-spherical refractive errors like astigmatism and higher order aberrations.

In most cases, mixed refractive errors are present if compared to average values.

1.1.1 Myopia

In myopia, or near-sightedness, parallel rays of light from a distant object are focused anterior of the retina in a non-accommodating eye. The far point is within a finite distance in front the eye (Figure 2). Therefore, distant objects are seen blurred, and near objects (at a distance depending on the extent of the myopia) are focused. Unlike hyperopia, myopia requires refractive correction at all ages and severity for clear focus.

In most myopic eyes, the axial length is too long relative to the refractive power. Thus, axial myopia is much more common than refractive myopia, which is caused by steep corneal radii (e.g. keratoconus) or a high refractive power of the crystalline lens (e.g. myopic nuclear cataract).

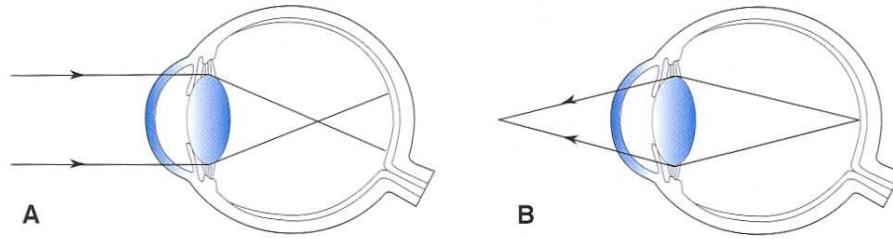


Figure 2: Myopia with accommodation relaxed. *A, Parallel light rays from infinity focus to a point anterior to the retina, forming a blurred image on the retina. B, Light rays emanating from a point on the retina focus to a far point in front of the eye, between optical infinity and the cornea. Reprinted by permission from American Academy of Ophthalmology, Basic and Clinical Science Course, Section 3, Clinical optics, Azar 2013-2014¹*

Myopia is corrected by reducing the total refractive power of the optical system with a diverging lens. Therefore, the level of myopia is given in negative diopters (e.g. -5 D), although the refractive power of the eye in this example is 5 D too high.

In cataract surgery, where the opacified crystalline lens is exchanged against an artificial intraocular lens (IOL), the required IOL power of that IOL to obtain a sharp image of a distant object on the retina is usually lower in long myopic eyes compared to emmetropic eyes with average axial lengths.

Myopia is the most common eye condition worldwide, with significantly increasing prevalence.^{2,3} A recent meta-analysis collecting refractive data from more than 68,000 participants revealed a prevalence of myopia from -0.75 to -6.0 D of 30.6 %, and high myopia (< -6.0 D) of 2.7 %.² Although less than in Southeast Asia, myopia is becoming more common in Europe too, particularly in young adults. In another meta-analysis age-standardized myopia prevalence increased from 17.8 % to 23.5 % in those born between 1910 and 1939 compared with 1940 to 1979.³ Myopia is a highly heritable trait, but also environmental factors like education, near work, urbanization, prenatal factors, socioeconomic state, cognitive ability, season of birth, light, and time spent outdoors.⁴ Increasing prevalence of myopia is of concern because, even if appropriately corrected, it

is associated with an increased risk of sight-threatening diseases, such as myopic maculopathy, retinal detachment, glaucoma, and cataract.⁵

1.1.2 Hyperopia

In hyperopia, or far-sightedness, parallel rays of light from a distant object are focused posterior of the retina in a non-accommodating eye (Figure 3). The (virtual) far point is within a finite distance behind of the eye and therefore distant objects are seen blurred. In contrast to myopia, in hyperopia the refractive error can be compensated physiologically by increasing the refractive power of the crystalline lens, a physiological mechanism called accommodation. Thereby, the focal plan is shifted onto the retina, and distant and near images can be seen clearly, although only with an accommodative effort of the ciliary muscle. This constant effort may cause so called asthenopic symptoms such as chronic headache and tiredness when reading.

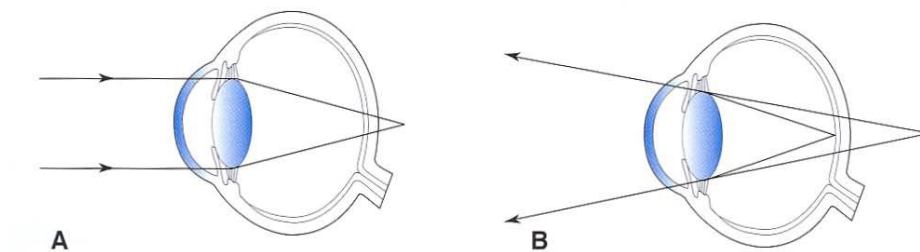


Figure 3: Hyperopia with accommodation relaxed. *A*, Parallel light rays from infinity focus to a point posterior to the retina, forming a blurred image on the retina. *B*, Light rays emanating from a point on the retina are divergent as they exit the eye, appearing to have come from a virtual far point behind the eye. Reprinted by permission from American Academy of Ophthalmology, Basic and Clinical Science Course, Section 3, Clinical optics, Azar 2013-2014¹

A hyperopic eye is too short relative to its refractive power. In most cases, axial hyperopia with normal corneal radii and a short axial length is present. Children usually have a

physiological hyperopia of +3 D, which normalises in the first 6 years due to growth of the bulbus.

As an analogy to myopia, hyperopia is corrected by increasing the total refractive power of the optical system with converging lenses, whereby the level of hyperopia is given in positive diopters.

In cataract surgery of short hyperopic eyes, the required IOL power to obtain a sharp image of distant objects on the retina is usually higher compared to emmetropic eyes with average axial lengths.

A prevalence of hyperopia of equal or greater 1.0 D of 25.2 % was found in a meta-analysis including more than 68.000 European participants.² Women were significantly more often hyperopic than men with a mean difference of 2.5 % across all ages, and there was less hyperopia in young participants compared to those in middle or older age. Regarding high hyperopia defined as equal or greater 3.0 D, the prevalence followed a similar pattern, affecting 1-3 % of younger and 10-13 % of older individuals.

1.1.3 Accommodation and presbyopia

The described concepts of emmetropia and refractive errors refer to objects at an infinite distance away. However, at most daily activities the objects of interest are situated at variable distances within finite space. To obtain a sharp image of those objects, the refractive power of the eye has to be adapted flexibly. This happens by dynamic changes of the eye's refractive power by altering the shape of the crystalline lens, a mechanism called accommodation.

The mechanism to achieve this alteration was described by v. Helmholtz.⁶ In the far-accommodated eye (focused on an object at infinite distance) the circular ciliary muscle is relaxed and tension on the zonular fibres leads to flattening of the lens curvature. Upon contraction of the ciliary muscle the tension on the zonular fibres relaxes, allowing the lens to become more spherical and thus, steepening the lens curvature. Hereby, and due to a change in the refractive index of the lens, the refractive power is increased (Figure 4).

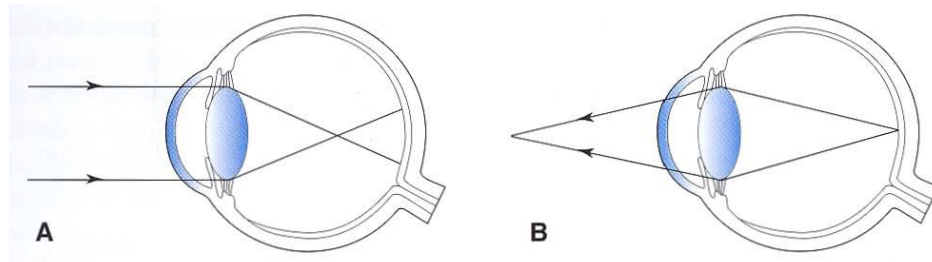


Figure 4: Emmetropia with accommodation stimulated. *A, Parallel light rays now come to a point locus in front of the retina, forming a blurred image on the retina. B, Light rays emanating from a point on the retina focus to a near point in front of the eye, between optical infinity and the cornea. Reprinted by permission from American Academy of Ophthalmology, Basic and Clinical Science Course, Section 3, Clinical optics, Azar 2013-2014¹*

Other mechanisms like the increase of depth of focus through pupillary contraction should be differentiated from the actual increase of refractive power and are referred to as pseudo-accommodation.

The amplitude of accommodation is the amount of change in the eye's refractive power that is produced by accommodation and it diminishes with age. This process is called presbyopia and it starts in young ages. Adolescents generally have 12-16 D of accommodation, whereas adults after age 50 have less than 2 D. The major cause of this gradual loss of accommodation is a progressive hardening of the lens with age, which inhibits ciliary muscle-induced changes of the lens shape.⁶

Presbyopia is corrected by convex lenses (plus lenses). However, an essential problem in presbyopia correction is, that a dynamic and highly flexible process is addressed by static measures. Reading glasses are only effective in a certain distance and make an emmetropic user myopic for distance vision. This problem can be reduced by progressive lenses, which offer a smooth transition between far and near correction, however, disturbing image distortions may occur with these lenses. Presbyopia correction with intraocular lenses after cataract surgery will be discussed in a following chapter.

1.1.4 Astigmatism

If an eye does not have the same refractive power in all meridians, rays of light are refracted in different distances to the retina depending on the meridian. Thus, such an eye forms 2 focal lines instead of a single point of focus. This kind of aberration is called astigmatism.

A classical *regular astigmatism* is present when the 2 principal meridians and thus, the 2 focal lines are oriented perpendicular. Since the axis of the principal meridians may vary, their orientation has to be specified by the position of the axis.

In most cases, astigmatism is caused by a toric shape of the cornea, whereby typically the curvature of the vertical meridian is steeper than that of the horizontal meridian (*astigmatism with-the-rule*). A condition, where the curvature of the horizontal meridian is steeper than that of the vertical meridian is called *astigmatism against-the-rule*. Furthermore, the axis can also lie in between the horizontal and vertical axis, then called *oblique astigmatism*. Also the crystalline lens has a certain amount of astigmatism, with the stronger refractive power usually in the horizontal axis, thereby often partially compensating for the corneal astigmatism. Frequently, a combination of astigmatism and other refractive errors is present. For example, an eye may have myopia of -6 D in one principal meridian and -7 D in the other. The amount of astigmatism (1 D in this example) results out of the difference in refractive power between the 2 principal meridians.⁷

Beside the classification regarding the axis orientation described above, astigmatic eyes further can be classified upon the relative locations of the focal lines (Figure 5). A *simple myopic astigmatism* is present, if 1 focal line lies anterior and the other is on the retina. In a *compound myopic astigmatism*, both focal lines lie anterior of the retina. If 1 focal line lies posterior of the retina and the other is on the retina, the condition is classified as *simple hyperopic astigmatism*. If both focal lines lie posterior of the retina, a *compound hyperopic astigmatism* is present. A *mixed astigmatism* is defined as a condition, where 1 focal line lies anterior and the other posterior of the retina.¹

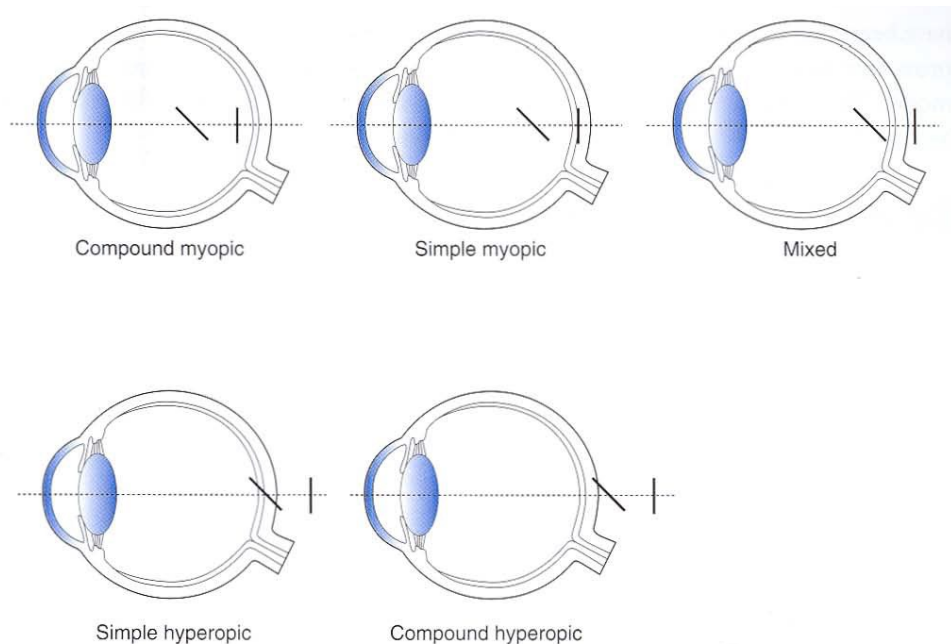


Figure 5: Types of astigmatism. The locations of the focal lines with respect to the retina define the type of astigmatism. The main difference between the types of astigmatism depicted in the illustration is the spherical equivalent refractive error. Reprinted by permission from American Academy of Ophthalmology, Basic and Clinical Science Course, Section 3, Clinical optics, Azar 2013-2014¹

For the correction of astigmatism cylindrical (or toric) lenses with astigmatic effect are used. The orientation of the correcting lens has to be with the stronger diverging axis of the lens according to the stronger refracting principal meridian of the eye. The axis is given in degree with the horizontal axis defined as 0° based on the TABO system.⁷

Those cylindrical lenses usually have a spherical component in most cases too. Since such spherocylindrical lenses are designed to compensate for the refractive errors of ametropic eyes, their optical effects are similar. Both refract light rays emanating from a single point source to a complicated geometric envelope of a pencil, which is called *conoid of Sturm* (Figure 6). It has 2 focal lines parallel to the principal meridians and all the rays pass through each of the focal lines. The cross sections of the conoid of Sturm are generally elliptical but vary in shape and area along its length. In the middle between the focal lines, there is a cross section of the conoid that is circular, which is called the circle of least confusion and represents the best overall focus of the spherocylindrical lens (or the eye,

respectively). The circle of least confusion marks the position of the average spherical power of all meridians, which is called the *spherical equivalent* of the optical system.¹

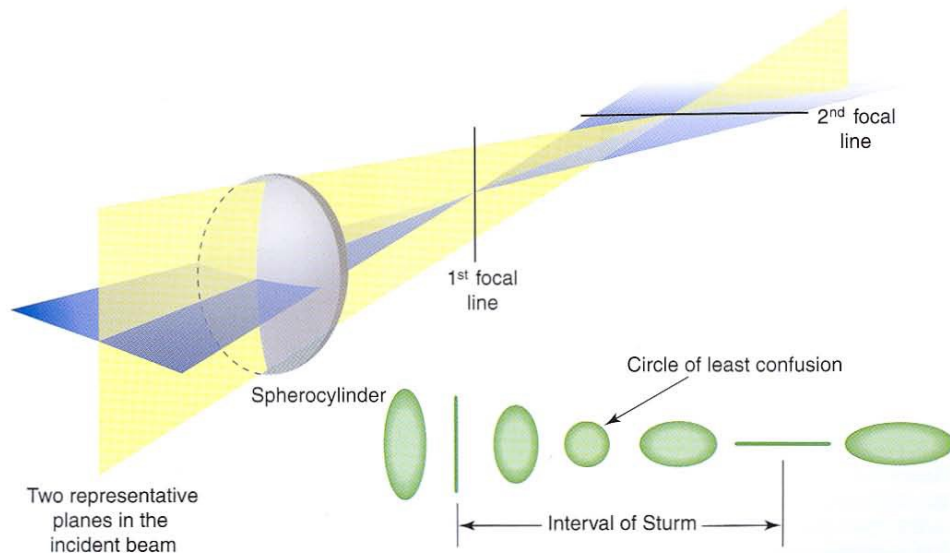


Figure 6: The conoid of Sturm. Reprinted by permission from American Academy of Ophthalmology, *Basic and Clinical Science Course, Section 3, Clinical optics, Azar 2013-2014*¹

Although a single focal point would provide a sharper retinal image, the conoid of Sturm with the confusion of light rays may offer a better depth of focus due to a certain range along the focal axis with “acceptable” blur. This pseudo-accommodative effect induces a better tolerability of defocus and explains the reduced dependency on reading glasses in presbyopic patients with small amounts of astigmatism.^{8,9}

In the present study, only eyes with preoperative astigmatism less than 1.5 D were included to avoid a factor that may confound analysis of depth of focus.

The age-standardized prevalence of astigmatism equal or greater 1.0 D in European eyes was 23.9 % in a meta-analysis. Astigmatism remained fairly stable 15 to 25 % in young and middle-aged participants, however, the prevalence in participants over 65 years of age increased to 51.1 %.²

These findings are in accordance with a study conducted by us to analyse cataract patients referred to our clinic.¹⁰ Of the 6900 included eyes with a mean age of 72.5 years, 38.3 %

had a corneal astigmatism of equal or greater 1.0 D. Furthermore, we observed a shift from with-the-rule astigmatism to against-the-rule astigmatism with age, which was also reported in other studies (Figure 7).²

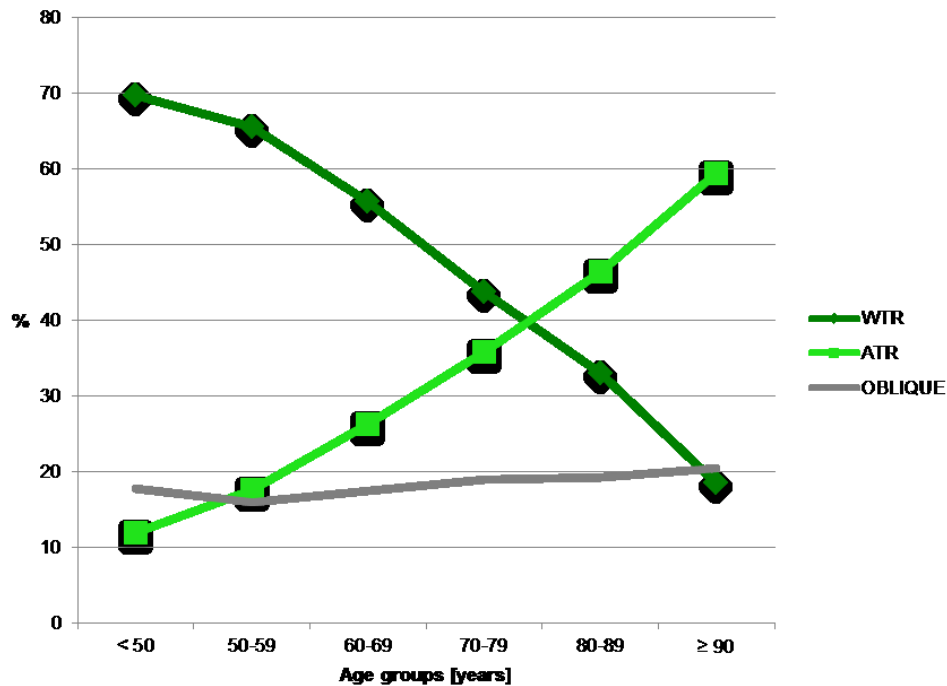


Figure 7: Change of astigmatism axis with age. WTR=with the rule, ATR=against the rule. Reprinted by permission from Springer, Ophthalmologe, Michelitsch 2016¹⁰

1.1.5 Higher-order aberrations

1.1.5.1 Wavefront

A perfect optical system brings all the rays from a single object point to a perfect point focus. Thus, when looking at a fixed star, an optically perfect eye would collect all rays of light emanating from that fixed star and entering the eye in a parallel way to one point on the retina.

In physics, a wavefront is the locus of points characterized by propagation of positions of identical phase, creating a 3-dimensional surface. If light is interpreted as an

electromagnetic wave and the wavefront is represented as a surface of identical phase, an object in infinite distance and therefore parallelly running light rays will form a flat surface. This surface is called wavefront.

As the wavefront is always perpendicular to single light rays and thus, is dependent on the direction of the light rays, it has a spherical shape in a perfect eye with convergent light rays (Figure 8).^{1,11}

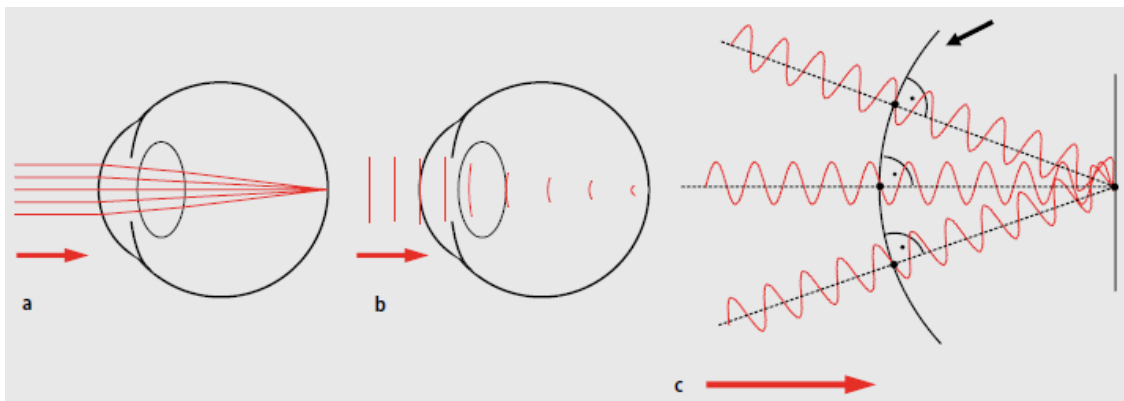


Figure 8: Relation between light ray and wavefront: *A*, Course of light rays in a non-accommodating ideal eye. *B*, Course of wavefront in the same eye. Outside the eye, the wavefront of parallel light rays is plane, inside the eye the wavefront of converging light rays takes on a spherical shape. *C*, Synoptic presentation: The wavefront connects light waves of positions of identical phase and is always perpendicular to the particular light ray. Reprinted by permission from Springer, *Ophthalmologie*, Bühren 2007¹¹

All deviations from a perfect optic are reflected by deviations from the ideal wavefront. These deviations are referred to as *wavefront error* or *wavefront deformation*, while single characteristic imaging errors are typically referred to as *wavefront aberrations*. The majority of these aberrations can be compensated by spherical or cylindrical lenses to acquire satisfactory vision. Other common aberrations, which are not correctable by spectacle glasses are called *higher-order aberrations* and include *coma* or *spherical aberration*.

In contrast to the wavefront in a perfect eye, the wavefront in a myopic eye is more curved as the light rays are more convergent, whereas in a hyperopic eye the wavefront is less curved compared to the ideal wavefront (Figure 9).

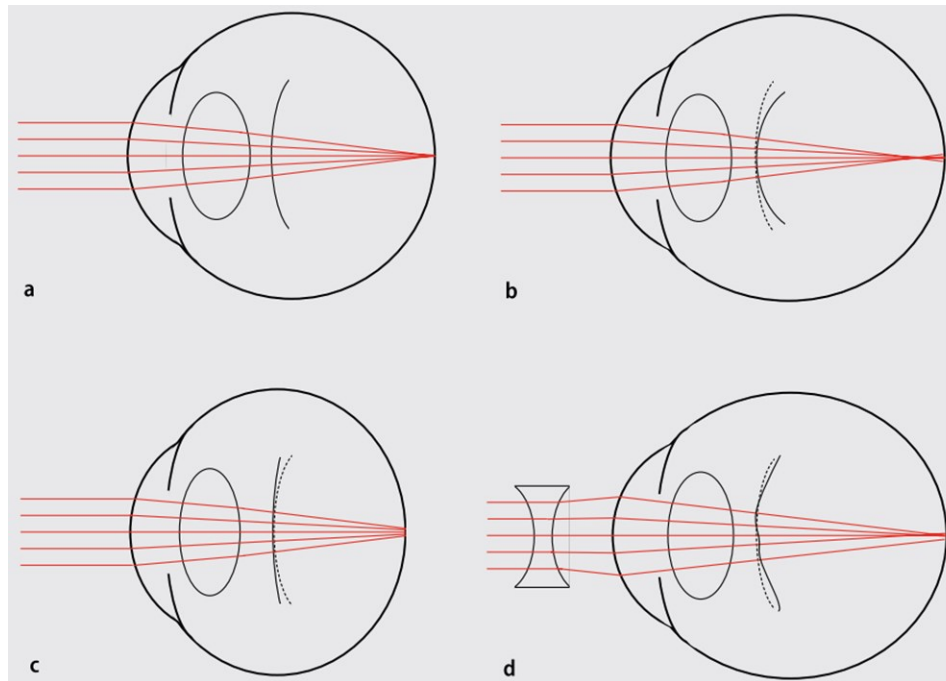


Figure 9: Light rays and wavefront in ametropia. *A, Ideal eye. B, Myopic eye: the wavefront is more curved than the ideal wavefront. C, Hyperopic eye: the wavefront is less curved compared to the ideal wavefront. D, Corrected myopic eye with higher-order aberrations: the wavefront is widely adjusted to the ideal shape by the correction, but some aberrations could not be fully compensated. Reprinted by permission from Springer, Ophthalmologe, Bühren 2007¹¹*

For that reason, in the present study only eyes with a postoperative refraction within ± 2.0 D were included to avoid confounding of depth of focus analysis.

1.1.5.2 Coma

Together with spherical aberration, coma is one of most important higher-order aberrations. As described above, higher-order aberrations are not correctable by spherical or cylindrical lenses.

Coma is an asymmetric variation of refractive power along an axis running through the pupillary center (Figure 10). Accordingly, also the wavefront is shaped asymmetrically. This asymmetrical distribution of refractive power is easily comprehensible with retinoscopy in eyes with coma by observing the typical “scissoring” reflex and the “oil drop” sign. The optical effect of coma is an asymmetrical distortion of the image. A point source of light would appear to have a tail like a comet.^{1,11}

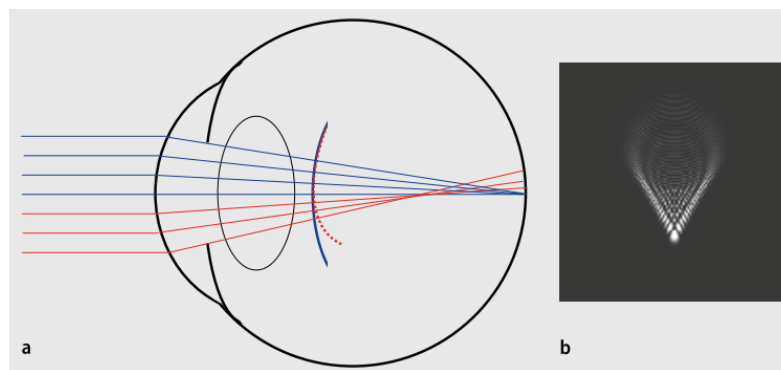


Figure 10: Coma. *A, Course of light rays and wavefront; aberrated light rays are drawn red. B, Visual impression when looking at a point source of light (point-spread-function). Reprinted by permission from Springer, Ophthalmologe, Bühren 2007¹¹*

1.1.5.3 Spherical aberration

The second important higher-order aberration is spherical aberration. This aberration is a rotationally symmetrical distributed deviation of refractive power from the peripheral to the central pupil (Figure 11). This means, that the periphery is more “myopic” or more “hyperopic” than the center. In retinoscopy, a “bull’s-eye” reflex is typically seen: the light reflex in the peripheral pupil moves contrary to the center. The optical effect is a blurred

image overlying the actual image, which is perceived as a blur – a halo surrounds the point source of light.^{1,11}

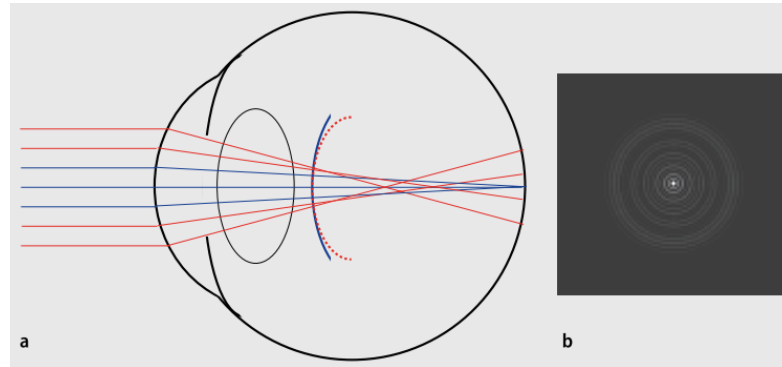


Figure 11: Spherical aberration. *A, Course of light rays and wavefront; aberrated light rays are drawn red. B, Visual impression when looking at a point source of light (point-spread-function). Reprinted by permission from Springer, Ophthalmologe, Bühren 2007¹¹*

Positive spherical aberration is present, if peripheral rays have a shorter focal length compared to more central rays. In an optical system with negative spherical aberration peripheral rays are less refracted than more central rays.

The amount of spherical aberration of the human cornea is positive and does not change significantly with age.¹² As the young crystalline lens has negative spherical aberration, the spherical aberration of cornea and lens are compensating each other.^{13,14} However, with increasing age the spherical aberration of the crystalline lens changes towards more positive values. Thus, the compensating effect diminishes and total spherical aberration of the eye increases.^{15,16}

1.1.5.4 Effect of pupil size

The optical effect of higher-order aberrations has a strong dependency on the pupil diameter: the larger the diameter, the stronger image quality is affected (Figure 12). In smaller pupils, the retinal image is less distorted by aberrations, but diffraction of light is becoming more important. Placing a pinhole aperture immediately in front of the eye

acting as an artificial pupil correspondingly reduces the size of the blur circle on the retina and therefore may improve visual acuity.^{1,11}

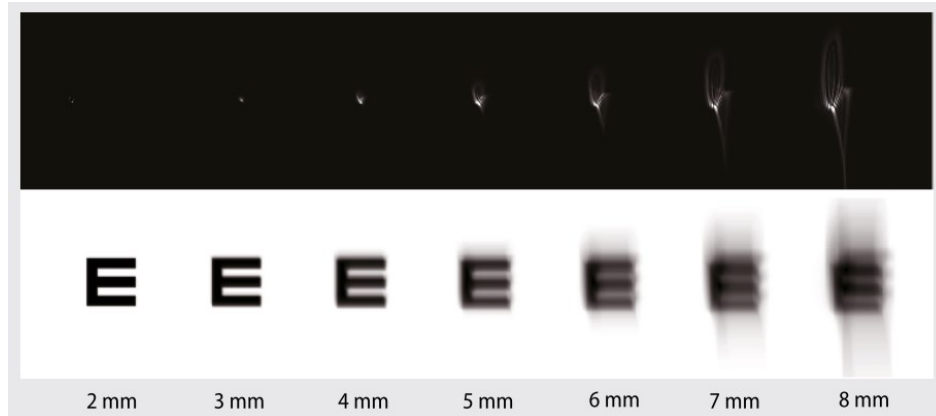


Figure 12: Relation between pupil diameter and optical effect of aberrations. Data of a normal eye (30 year old man). Point-spread-function is shown in the upper line and the simulated visual impression for a letter of visual acuity line 20/20 (decimal 1.0) in the lower line. Reprinted by permission from Springer, *Ophthalmologe, Bühren* 2007¹¹

In the present study, we used the same artificial pupil for every patient for contrast sensitivity testing to achieve a better comparability between the different groups. For this, we instilled pupil dilating drops and after 30 min we put a pinhole aperture with 5 mm diameter in the trial frame in front of the eye. Previous studies have recommended this technique, as contrast sensitivity is affected by pupil diameter as well as by spherical aberration.¹⁷

1.1.5.5 Measurement of wavefront error

The measurement of wavefront errors is called aberrometry. For the understanding of the operating principle of aberrometers and the interpretation of aberrometric measurements it is important to know, that in an ideal non-accommodating eye even after reversal of object and image positions (object inside the eye and light rays emanating from eye) the

wavefront outside the eye would be plane. Thus, all wavefront aberrations of an eye are detectable as deviations from a plane surface covering the entrance pupil of that eye.

Different sensors are used for wavefront measurements. Thereby, either a pattern is projected onto the retina and the wavefront error is deduced from the deformation of the pattern of the retinal image (Tscherning- Aberrometer, “ray tracing”, dynamic retinoscopy) or wavefront analysis is conducted based on the reflected light (Hartmann-Shack-sensor). In latter technique is the most popular one and was used in the present study.

1.1.5.1 Hartmann-Shack aberrometer

It is based on the reversal of object and image side. A low-power laser beam focused on the retina is used as point source (“object” of the aberrometry). An array of lenses sample parts of the wavefront and focus light on a detector with a camera (Figure 13). In an ideal eye, the emerging wavefront would be a flat plane. From the location of the focus on each detector the shape of the wavefront is calculated.¹⁸

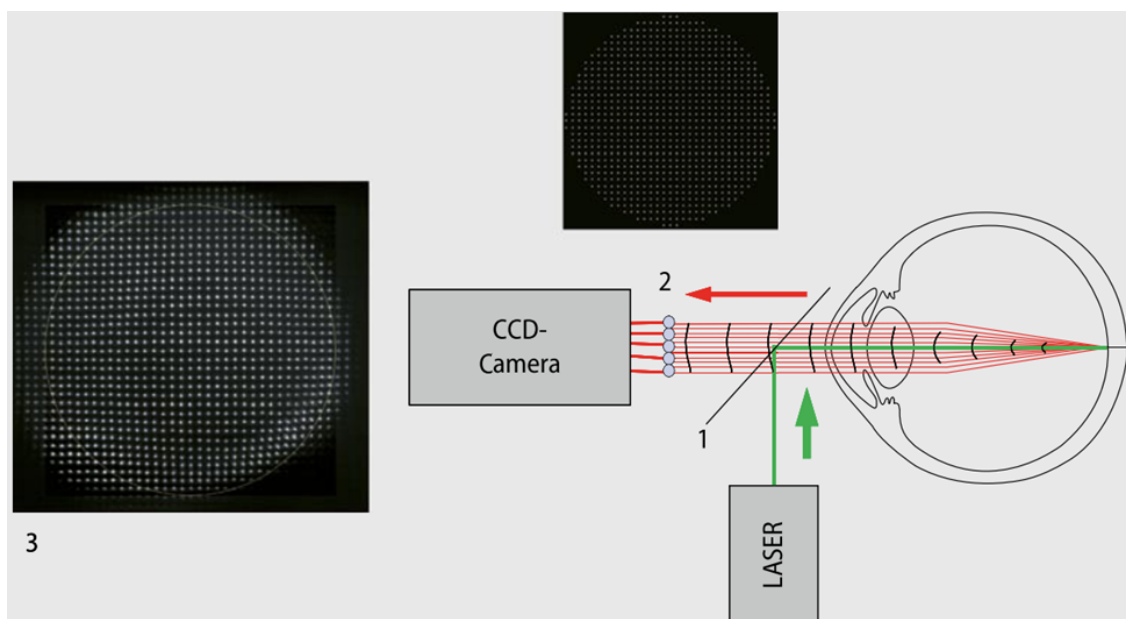


Figure 13: Principle of Hartmann-Shack aberrometry. Light entering the eye is coloured green, light emerging the eye is coloured red. 1, Beam splitter. 2, Microlens array. 3, Received camera image. Reprinted by permission from Springer, *Ophthalmologe*, Bühren 2007¹¹

1.1.5.5.2 Tscherning Aberrometer and “ray tracing”

With a Tscherning Aberrometer a point matrix is projected onto the retina and the retinal image is received by a camera (Figure 14). The shape of the wavefront is calculated from the dislocation of the points in the pattern. With “ray tracing” detected light beams are projected sequentially rather than simultaneously (as in a Hartmann-Shack device). This further improves the resolution of the measurement.¹⁹

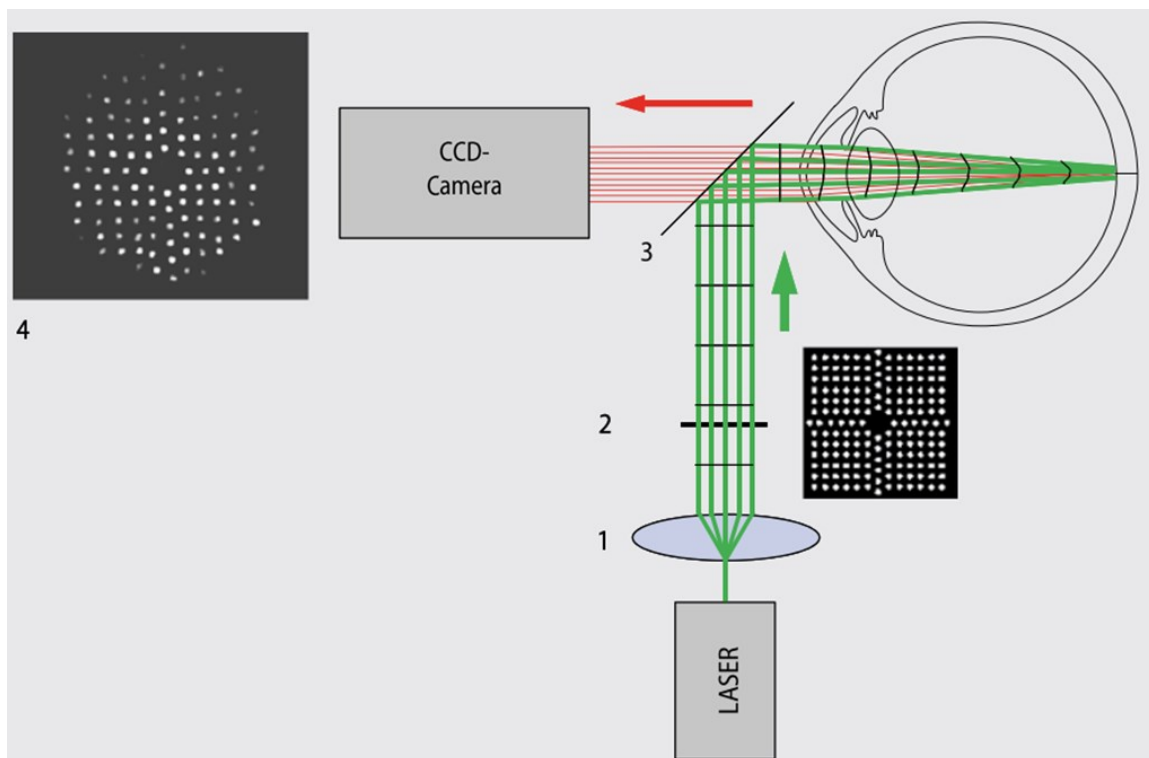


Figure 14: Principle of Tscherning aberrometry. Light entering the eye is coloured green, light emerging the eye is coloured red. 1, Collimator. 2, plate with small perforations. 3, Beam splitter. 4, Received camera image. Reprinted by permission from Springer, *Ophthalmologie, Bühren 2007*¹¹

Like all biometric measurements, aberrometry is a “snapshot” and thus is prone to fluctuations. Possible reasons for this are tear film break-up^{20,21} and microfluctuations of accommodation.

1.1.5.6 Interpretation of wavefront error

Measurement of wavefront deformation with one of the described techniques provides a difference value from the ideal wavefront for every data point (e.g. point of Hartmann-Shack pattern). Based in that raw data, an (approximative) wavefront map could be created. However, information would be limited with that approach for 2 reasons: firstly, because data between the data points has to be interpolated, and secondly, because wavefront maps provide only qualitative information. Thus, today it is more popular to describe wavefront deformation by means of polynomials developed by Frits Zernike.

1.1.5.6.1 Zernike polynomials

With the polynomials formulated by Zernike, a wavefront error can be reconstructed by mathematical approximation to the measured raw data and decomposed into its components.²² The separate functions can be arranged as a pyramid and build on one another (Figure 15).

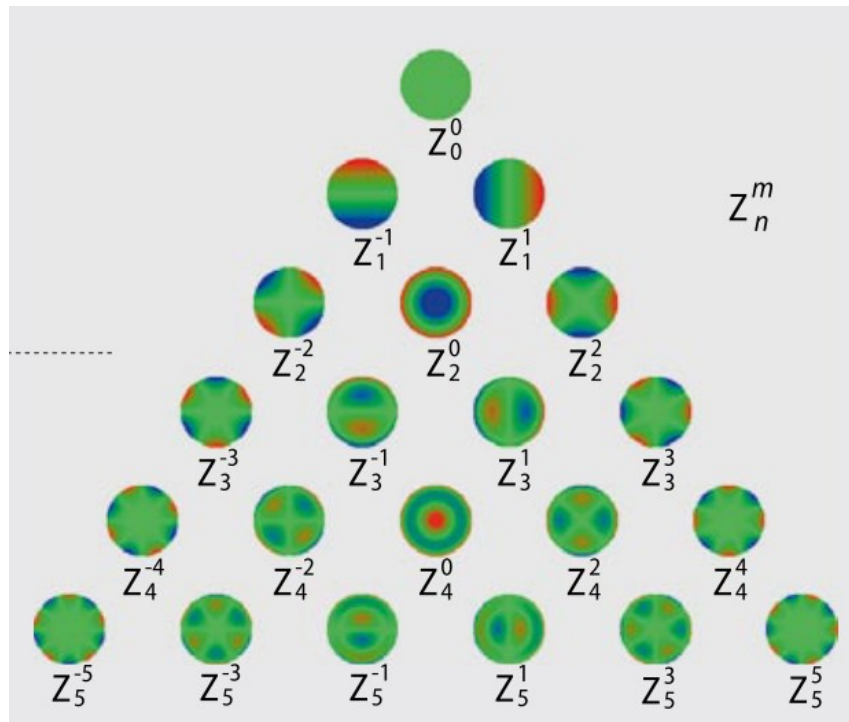


Figure 15: Pyramid with Zernike polynomials to the 5th order. The dashed line divides „lower-order aberrations“ (upper part) from „higher-order aberrations“ (lower part). Reprinted by permission from Springer, *Ophthalmologe*, Bühren 2007¹¹

The functions are order vertically by radial degree and horizontally by azimuthal degree. Every polynomial is clearly defined by 2 indices: n indicates the radial degree (polynomial component), and m indicates the azimuthal degree (angular frequency, sinus or cosinus component).²³ As the number of Zernike polynomials is unlimited, the more polynomials are used the more accurate a wavefront error can be described. Although wavefront decomposition with Zernike polynomials is widely used and understood, the method represents a compromise, which may lead to undercorrection if the number of used polynomials is too low (underrepresentation of high frequencies).²⁴ However, usually in the clinical practice polynomials up to the 5th or 6th order are used only.

Beside the Zernike polynomials, other decomposing techniques like *zonal reconstruction* or *Fourier reconstruction* exist, but the Zernike technique is the most commonly used, mainly because it is easy understandable. This reflects the fact that some Zernike polynomials represent well-known imaging errors like tilt, defocus, stigmatism, spherical aberration or coma. Other polynomials like trefoil, tetrafoil, and pentafoil are derived from astigmatism and represent 3, 4, or 5-wing equivalents to the conventional 2-sided

astigmatism. Aberrations of the 1st and 2nd order can be corrected with spectacle glasses and are called *lower-order aberrations*. Aberrations with 3rd order or higher are more called *higher-order aberrations* and are more complex and of higher frequency.¹¹

1.1.5.6.2 Corneal wavefront

Beside using data obtained by aberrometry, also topography- or tomography-derived elevation data of the cornea can be used for Zernike decomposition.²⁵ A better term for this method would be “Zernike decomposition of corneal elevation data” rather than “corneal wavefront”.

The technique offers isolated characterisation of the optical effect of the anterior corneal surface (topography), or even the entire cornea additionally including the posterior surface (tomography). Typical applications are conditions where the cornea is the major cause for aberrations (e.g. irregularities after corneal refractive surgery) and a potential advantage is that the analysed area is not restricted to the entrance pupil.

1.1.5.6.3 Wavefront function

For quantification of a wavefront error, a wavefront function is calculated, which gives separate polynomials different weightings by using coefficients. These coefficients are the values which are displayed by the aberrometers software. They can be positive or negative and are given in μm . The higher the coefficient, the more dominant is the imaging error described by the actual polynomial.²³

Non-symmetrical polynomials of the same order with opposite +/- sign represent the same optical imaging error, but differ in the spatial orientation. Only addition of both coefficients results in a vector with a certain axis position.

It has to be emphasized, that coefficients are only true for the pupil diameter, which was used for wavefront reconstruction. Thus, the pupil diameter always has to be indicated with the measurements and considered for the interpretation of the aberrometry.

1.1.5.6.4 Interactions of Zernike polynomials

Although in the clinical practice lower-order and higher-order aberrations are usual divided, from a physiological and optical point of view a wavefront error should always be

understood as a functional unit. The reason for this is that every coefficient only represents the proportion of aberrations from the total wavefront error, and but the optical effect is determined by the entire shape of the wavefront. Thus, the effect of a certain Zernike coefficient is always dependent of the level of other coefficients of the wavefront error. Lower- and higher-order aberrations may affect each other via such interactions.¹¹ As an example, Figure 16 illustrates the interaction between spherical aberration and defocus. With respect to the presented study, two important examples for that effect regarding spherical aberrations and defocus are described in more detail.²⁶ If both aberrations with the same +/- sign are present in a wavefront in a ratio of approximately 3:1, the resulting image quality would be better than if only one of these aberrations is present.

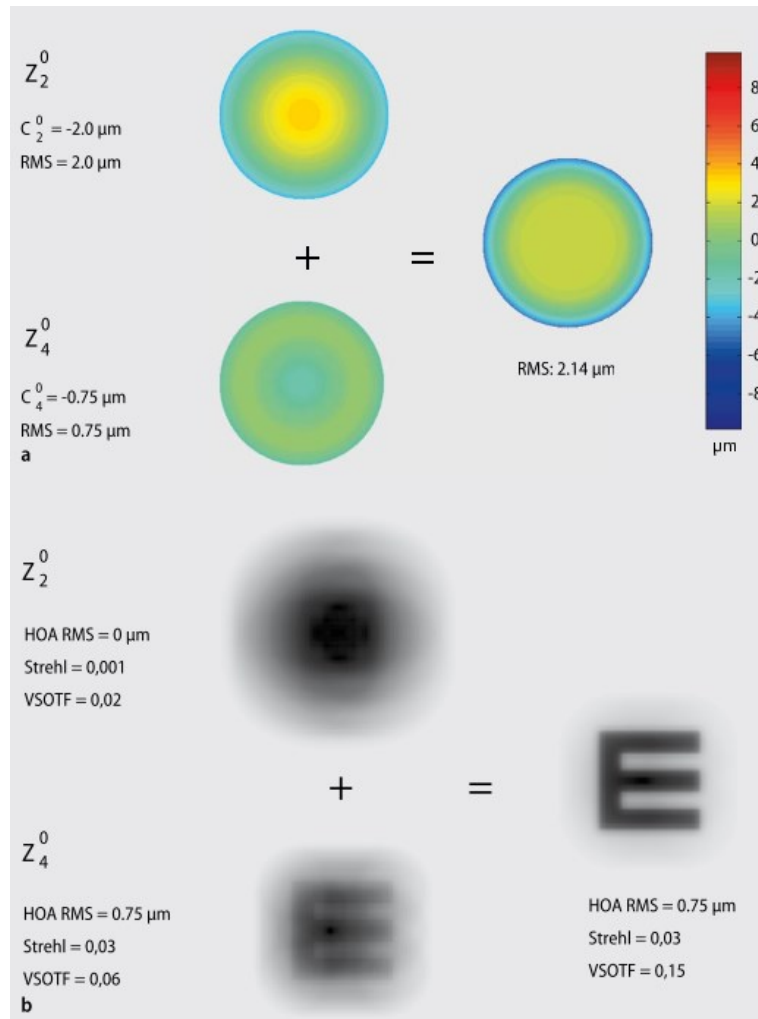


Figure 16: Interaction of defocus (Z_2^0) and primary spherical aberration (Z_4^0). If primary spherical aberration of $-0.75 \mu\text{m}$ is added to defocus of $-2.0 \mu\text{m}$, the resulting wavefront is more plane and simulated image quality is improved. Reprinted by permission from Springer, *Ophthalmologe, Bühren 2007*¹¹

Thus, increase of a particular Zernike polynomial does not have to degrade the image quality. Furthermore, the aim of subjective refraction is not to be equated with the situation of that lower-order aberrations are zero.

Another important example for an advantageous effect of higher-order aberrations is enhanced depth of focus due to spherical aberration. Figure 17 illustrates the described relation.

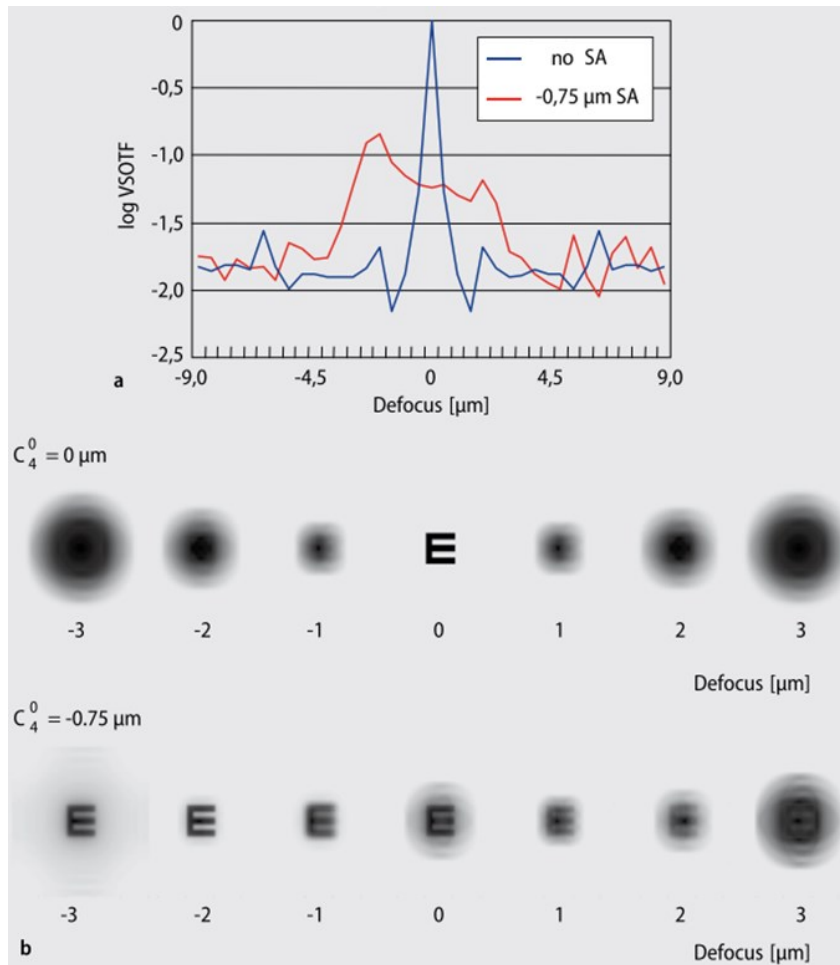


Figure 17: Enhanced depth of focus due to interaction of defocus and primary spherical aberration. *A*, The defocus curve shows that in eyes without spherical aberration (SA, blue curve) the image quality decreases significantly even in presence of low defocus; in eyes with spherical aberration (red curve) maximum image quality is reduced but depth of focus is increased. *B*, Simulated image quality: increased depth of focus in eyes with spherical aberration (lower line). Reprinted by permission from Springer, *Ophthalmologe*, Bühren 2007¹¹

A perfect eye without any aberration is more prone to defocus than an eye with spherical aberration.^{11,27,28}

1.1.5.6.5 RMS values

The most important clinical and scientific application of wavefront analysis is the objective evaluation of the quality of the retinal image. Hence, a measurement should provide values for intuitive interpretation of the examiner.

All Zernike coefficients of a measurement in total offer detailed information about the wavefront error and imaging quality, however, the quantity of data may be confusing and complicates further statistical processing. But also the use of single coefficients for evaluation of image quality may be problematic due to complex interaction phenomena mentioned earlier.

A very clear and thereby popular representation of wavefront errors is the calculation of *root mean square-values (RMS)* of the wavefront error, which is determined as the square root of the arithmetic mean of the squares of the coefficients. The RMS value of the total wavefront error includes the mean deviation of all Zernike coefficients from the ideal wavefront, thus it is the standard deviation of the wavefront error, indicated as μm . The minimal value of 0 means complete alignment with the ideal wavefront, and higher values indicate a stronger deformation.

The RMS value of higher-order aberrations (*RMS HOA*) is often used as a well applicable criterion for the optical quality of a corrected eye. Despite its popularity, the RMS HOA value gives only a pure quantitative information and neither takes into account different optical effects of certain aberrations nor reflects interactions between aberrations.^{29,30}

A further, more differentiating application is the calculation of RMS values of certain Zernike orders or homologous aberrations like coma-RMS or spherical aberration-RMS. This method provides a better qualitative evaluation due to summarization of aberrations with related characteristics.¹¹

Hence, we used the latter approach in the present study to evaluate the amount of corneal and total eye spherical aberration in our patients.

1.2 Functional testing of optical quality

There are a multitude of ways for functional testing of visual perception, like testing of visual acuity, contrast sensitivity, straylight, colour perception, and visual field. Compared to aberrometric measurements, results of functional tests are subject to significant complex

influences. Despite pathologies of the retina or the optic nerve, results are affected by retinal and cortical stimulus processing as well as by interindividual differences in pattern recognition, intellectual abilities, concentration, and other variables.⁷

1.2.1 Visual acuity

Visual acuity testing is the most common functional testing method. Visual acuity is defined as the smallest visual angle at which 2 separate objects can be discriminated (minimum separable threshold).

In the German-speaking world, visual acuity is usually indicated in *decimal notation*, represented as the reciprocal of the smallest visual angle in arc minutes.

For scientific publications, decimal acuity is increasingly converted to the *base 10 logarithm of the minimum angle of resolution* (logMAR). This is necessary for determining a mean visual acuity of a series, as different lines of decimal acuity are not related to one another by size in a geometric or logarithmic way.

Certain letters (“round” letters like O, C, or G) are inherently harder to recognize than others (such as J, A), because there are more alphabetical letters with which they could be confused. Thus, alternative visual acuity charts have been developed, whereby the chart used in the *Early treatment of diabetes retinopathy study* (ETDRS) is the most popular one.³¹ In this chart, every line has the same number of letters and the gradation of steps occurs logarithmically (Figure 18). This means that a decimal step on the logMAR scale always shows the same proportions of letters, which is not the case in usual decimal charts.

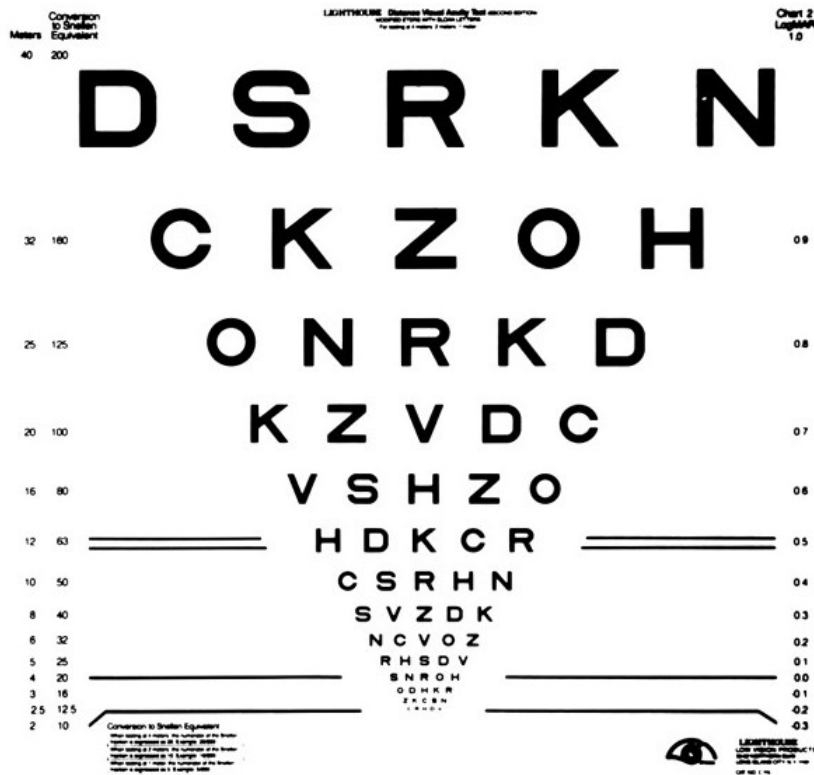


Figure 18: Modified ETDRS visual acuity chart. The chart is intended for use at 6m, but can also be used at 3 m or 1.5 m with appropriate scaling. Reprinted by permission from BMJ Publishing Group Ltd., British Journal of Ophthalmology, Laidlow 2003³²

In clinical practice, visual acuity means the threshold value obtained by testing under photopic conditions and with optotypes presented in the distance.

Optotypes for visual acuity testing may be standardized letters, numbers or other symbols like the Landolt ring (C) or the Snellen-E. However, the determined threshold value represents only a small part of all visual tasks. In daily life, there are often different conditions present, like low luminance, low contrast, glare or other object distances. Thus, visual acuity is not the only parameter to evaluate visual function or optical quality. Further specific questions require visual acuity testing with low contrast optotypes or with variable luminance to test under mesopic conditions.⁷

In the present study, an ETDRS logMAR visual acuity chart was used for testing distance visual acuity under photopic conditions (target luminance of 85 cd/m²).

Near visual acuity testing represents a distinct entity. As reading is the most common near task in daily life, many tests are designed as reading charts. Thus, the demanded task for is much more complex compared to distance visual acuity testing with simple detection of single optotypes. The determined parameter is dependent on the used near visual acuity chart and could be indicated as visual acuity, reading velocity, or critical font size.³³ In the present study, near visual acuity was measured using the Radner Reading visual acuity chart (Precision Vision, La Salle, USA, Figure 19) at 40 cm under photopic conditions (target luminance of 85 cd/m²).^{34,35}

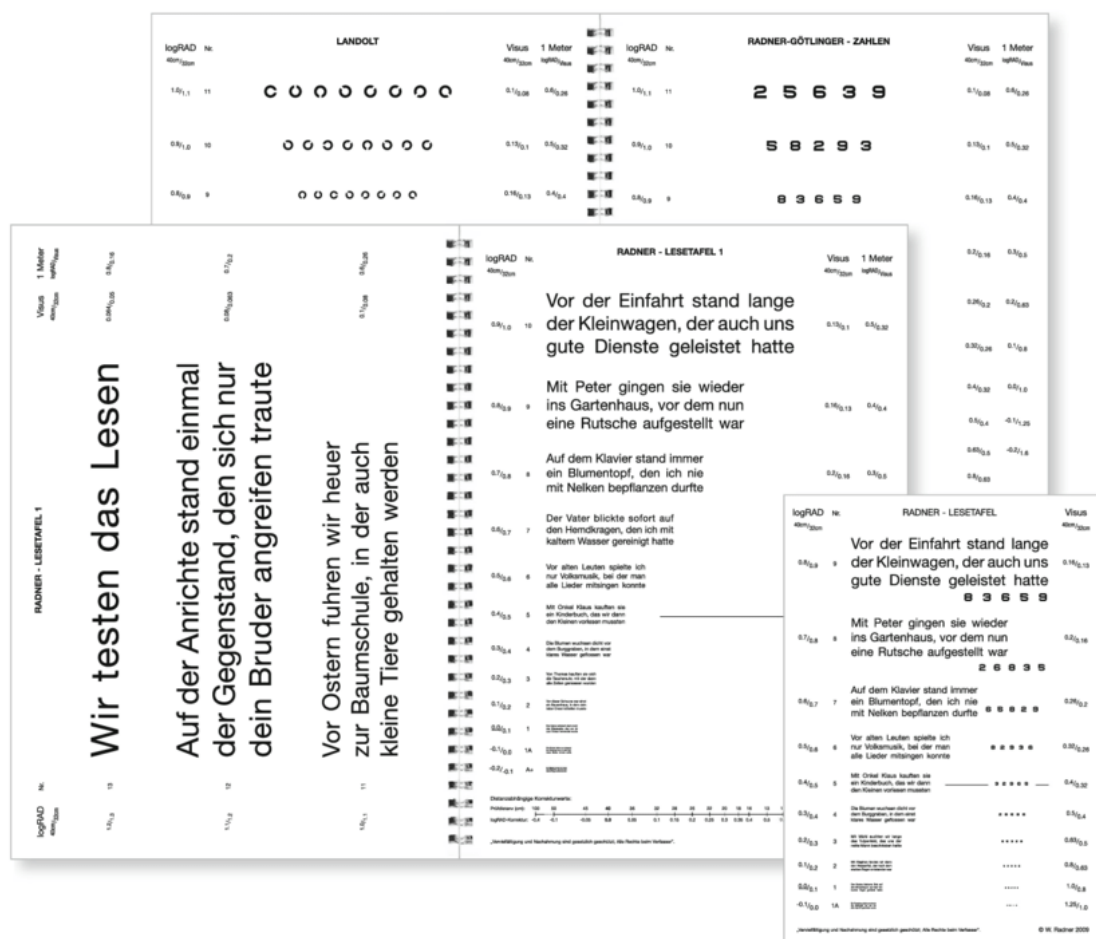


Figure 19: Radner reading charts for near visual acuity testing. Reprinted by permission from Springer Nature BMC, Eye and Vision, Radner 2016³⁶

1.2.2 Contrast sensitivity

Contrast sensitivity is the ability of the visual system to detect differences in luminance.³⁷ In contrast to visual acuity testing where optotypes of different size but with same contrast level are used, in contrast sensitivity testing patients have to detect optotypes of the same size but with different contrast levels. Contrast sensitivity is indicated as the reciprocal of the minimum contrast that can be resolved by the patient (contrast threshold). If a contrast of 1 % is resolved, the contrast sensitivity is 100; if a logarithmic scale is used it would be $2 \log CS (10^2)$.

If contrast sensitivity is indicated as a function of optotypes size, a curve named *contrast sensitivity function* is obtained. This curve shows that contrast sensitivity is strongly correlated to optotypes size and decreases if smaller optotypes are used (Figure 20). In other words, for the resolving small objects maximum contrast is necessary.⁷

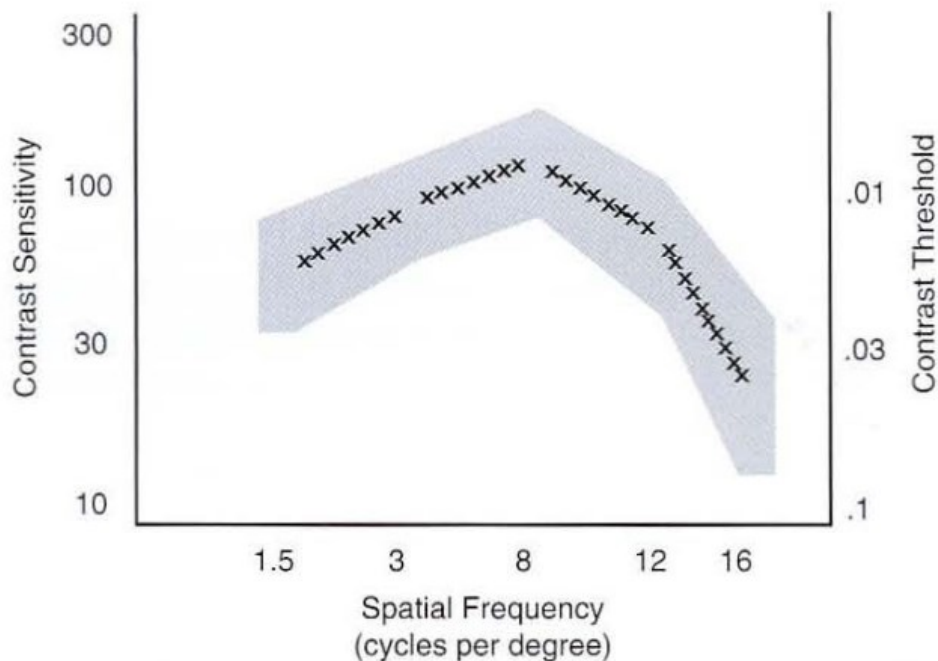


Figure 20: Typical contrast sensitivity curve. The curve is noted as x-x-x. The shaded area represents the range of normal values for 90% of the population. Reprinted by permission from American Academy of Ophthalmology, Basic and Clinical Science Course, Section 3, Clinical optics, Azar 2013-2014¹

Under photopic conditions, a small pupil diameter together with a high neuronal contrast sensitivity result in maximum optical quality. With intermediate luminance the effect of aberrations gain in significance, while under low-mesopic conditions the limiting factor is the neuronal contrast sensitivity.³⁸ However, higher-order aberrations primarily affect low contrast-visual acuity.^{39,40}

In the present study, we tested contrast sensitivity was measured with the Pelli-Robson contrast sensitivity test (Clement Clarke International, London, United Kingdom) under photopic (85 cd/m²) and mesopic (3 cd/m²) conditions with distance correction. The Pelli-Robson is contrast sensitivity chart with optotypes of a fixed spatial frequency and reducing contrast (Figure 21).⁴¹



Figure 21: Pelli-Robson chart for contrast sensitivity testing. Reprinted by permission from White Rose University Press, *British and Irish Orthoptic Journal*, Milling 2014⁴²

The test was performed at a viewing distance of 3 m, which corresponds to a spatial frequency of approximately 3 cycles per degree (cpd).⁴³ To exclude any influence of pupil size on contrast sensitivity, testing occurred in mydriasis with a 5.0 mm artificial pupil in the trial frame in front of the eye.¹⁷

1.2.3 Depth of focus

The depth of focus of an optical system like the human eye is the variation in object distance that can be tolerated without incurring an objectionable lack of image sharpness. Existing depth of focus can restore good near and distance visual acuity even in eyes after cataract surgery with implantation of a monofocal intraocular lens (IOL). The main factors contributing to good depth of focus are astigmatism, small pupil size and higher-order aberrations.^{44–48}

There are different examination methods to evaluate pseudophakic depth of focus.⁴⁹

1.2.3.1 Distance corrected intermediate visual acuity

With this test, visual acuity is measured with an out-of-focus scenario. The focus of an eye is fixated to infinity (distance corrected) and then visual acuity at 1 m is measured. This approach has previously been used to determine the delayed onset of presbyopia in patients with high spherical aberration after corneal excimer laser surgery for myopia correction⁵⁰ and in another study evaluating pseudophakic depth of focus⁵¹.

In the present study, this parameter was our primary outcome parameter. For testing, we used the Radner Reading visual acuity chart at 1 m distance under photopic conditions.

1.2.3.2 Distance corrected near visual acuity

Similar to the test described above, in this test visual acuity was tested with distance correction, but at near instead of intermediate distance.

In the present study, we used the Radner Reading visual acuity chart at 40 cm distance under photopic conditions.

1.2.3.3 Defocus curve

Defocus curves are a popular method of evaluating the subjective range of clear vision in presbyopic or pseudophakic patients. Thereby, optical modification of the focal demand to view a distant object by placing lenses in front of the eye and then measure visual acuity with each particular lens is conducted (Figure 22). It has been shown to be a repeatable and reliable method of measuring accommodation.^{52,53} The more physical alternative to this test is to actually measure visual acuity at different distances from the eye, which can be impractical.⁵⁴

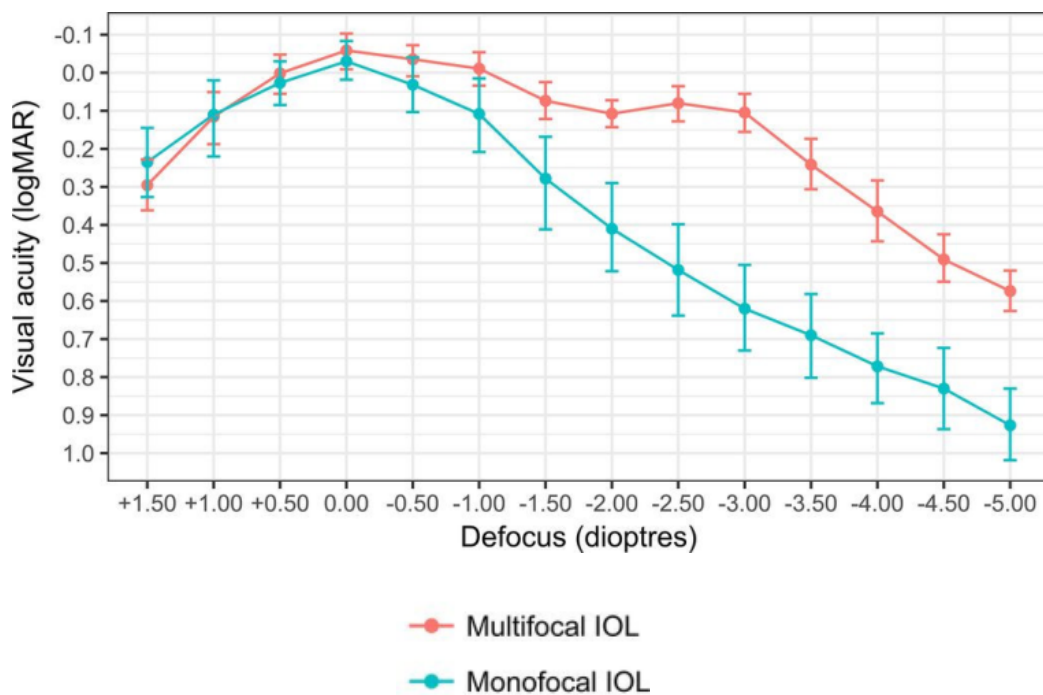


Figure 22: Exemplary defocus curves of eyes with monofocal and multifocal intraocular lenses (IOL). The monofocal IOL group demonstrates maximum visual acuity without any defocus and a gradual decline in acuity with increased defocus in both directions. The multifocal IOL also demonstrated maximum distance acuity without any defocus, but there was only a slight reduction in acuity with myopic blur. Reprinted by permission from BMJ, *BMJ Open Ophthalmology*, Lenton 2018⁵⁵

However, it has to be stated that defocus curves also tend to overestimate the amplitude of accommodation in comparison to the more physical method, primarily through an increase in depth of focus due to inevitable pupillary constriction from the accommodative stimulation, and possibly through minification effects of negative lenses.^{56,57}

Furthermore, appropriate methodology of presenting letter sequences on acuity charts and the order of lens presentation is necessary to avoid influences on the outcome due to memory effects.⁵⁴

In the present study, defocus curves were assessed by reading ETDRS logMAR visual acuity charts under photopic conditions with levels of defocus between -1.5 D and 1.5 D induced by trial lenses in steps of 0.5 D.

2 Intraocular lenses

The first intraocular lens (IOL) was implanted in 1949 by the English ophthalmologist Harold Ridley in London. Remarkably, he anticipated the later development of IOL implantation with 2 of his decisions: by using extracapsular cataract surgery (ECCE) with preservation of the posterior lens capsule, and by placing the IOL in the posterior chamber. Although the use of IOLs was strongly opposed by other ophthalmologists initially, after years of further development of the IOL it became the standard it is today.¹

Beside implantation of an IOL, which is the best form of refractive correction after lens removal, alternative possibilities include aphakic spectacles or contact lenses. Aphakic spectacles induce side effects like visual field impairment and image magnification, and contact lenses require daily insertion and removal, which can be problematic especially in older patients.¹

2.1 General indications

2.1.1 Cataract surgery

The crystalline lens and the cornea represent the major refracting media of the optical system of the human eye. Clarity of those optical media is essential for optimal optical quality, as otherwise an adequate projection of a fixated object is not possible. The most common pathology of the crystalline lens is opacification due to cataract. Today, surgical removal of the opacified lens with implantation of an IOL is the only available therapy.

Cataract is defined as congenital or acquired opacification of the crystalline lens. By affecting worldwide more than 20 millions of people considered as blind, it is the most common cause for blindness.⁵⁸ It is expected that the incidence of age-related cataract will further increase as the world's population ages.⁵⁹ Thus, cataract surgery is the most frequently performed surgical procedure in medicine.

The techniques and results of cataract surgery have changed dramatically throughout the past decades. Modern cataract surgery primarily comprises extracapsular cataract extraction (ECCE) with preservation of the posterior lens capsule and implantation of the IOL in the capsular bag.⁶⁰ The opacified lens material usually is extracted after emulsifying

the hard central nucleus by ultrasound waves (phacoemulsification). Then the IOL is implanted in the capsular bag. Today, due to the small corneal incisions postoperative rehabilitation is very short and surgically induced astigmatism (corneal astigmatism) is low. Each surgical step is briefly described in the following sections.

2.1.1.1 Incisions

Wound construction in cataract surgery has evolved greatly over time. With introduction of phacoemulsification and innovative IOL design, incision size was constantly reduced. As a consequence, since the middle of the 90ies suture-less cataract surgery was enabled.⁶⁰

The most common incision types include clear corneal incisions (Figure 23) and scleral tunnel incisions. The position of the incision can be temporal or superior, whereby the temporal incision has become the most predominant position used in cataract surgery.⁶¹ As in our study, some surgeons try to perform the incision on the steep meridian of the present corneal astigmatism to partially neutralize for it.

Incision size is dependent on the size of the used instruments, especially the phacoemulsification handpiece and the IOL injector. Today, the incision size in width is around 2.0 mm or less. The decrease in incision size lead to a self-sealing nature and stability of the wound, minimal astigmatism induction, and rapid visual recovery.⁶²

Via the created wound and additional smaller side incisions, the instruments are inserted into the eye during surgery. At the end of surgery and after removal of the instruments, the internal portion of the corneal lamella is pushed against the external portion by the intraocular pressure providing watertight wound closure. Thus, sutures for closure are not required in most cases.⁶⁰

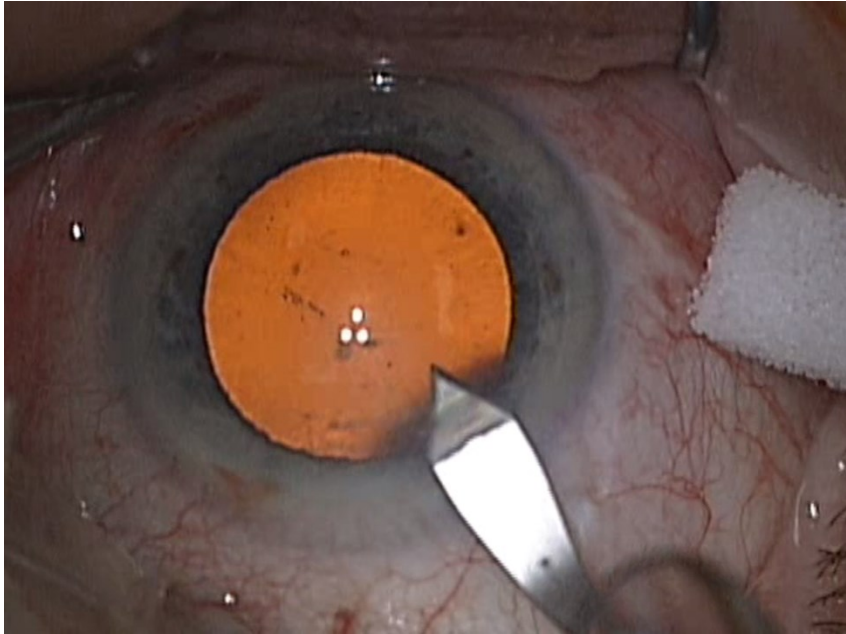


Figure 23: Creation of main incision.

2.1.1.2 Capsulorhexis

An essential step for the development of modern phacoemulsification techniques was the introduction of continuous-tear curvilinear capsulorhexis (CCC) by Gimbel and Neuhann in the 1990ies.⁶³ This method provided a high reproducibility and prevention of uncontrolled tearing of the anterior capsule. Hence, the technique is considered the “gold standard” for opening the anterior lens capsule.

The technique starts with injection of ocular viscoelastic device (OVD) into the anterior chamber after the creation of a corneal or scleral incision. Filling the anterior chamber with OVD is important to counteract forward pressure of the vitreous, and thus to minimize the tendency for the capsular tear to extend towards the equator. A bent needle or capsule forceps are used to make an initial puncture at the desired center of the CCC. The opening is then extended to create a triangular tear of the planned length. After turning the flap over, a circular capsulotomy is created by applying tearing forces to the tearing edge (Figure 24). The CCC is completed by drawing the tear inwards until the 2 torn ends join.⁶⁰ The CCC is stable and very resistant to radial tears compared to other opening methods.⁶⁴ The ideal diameter of the final capsulorhexis should be only about 1 mm smaller than the IOL and concentric with the IOL so that no portion of the capsulorhexis edge can fuse to

the posterior capsule.⁶⁰ The capsulorhexis is one of the most important steps of cataract surgery.

In the present study, the CCC was created by a bent needle and the intended capsulorhexis size was 5 mm.

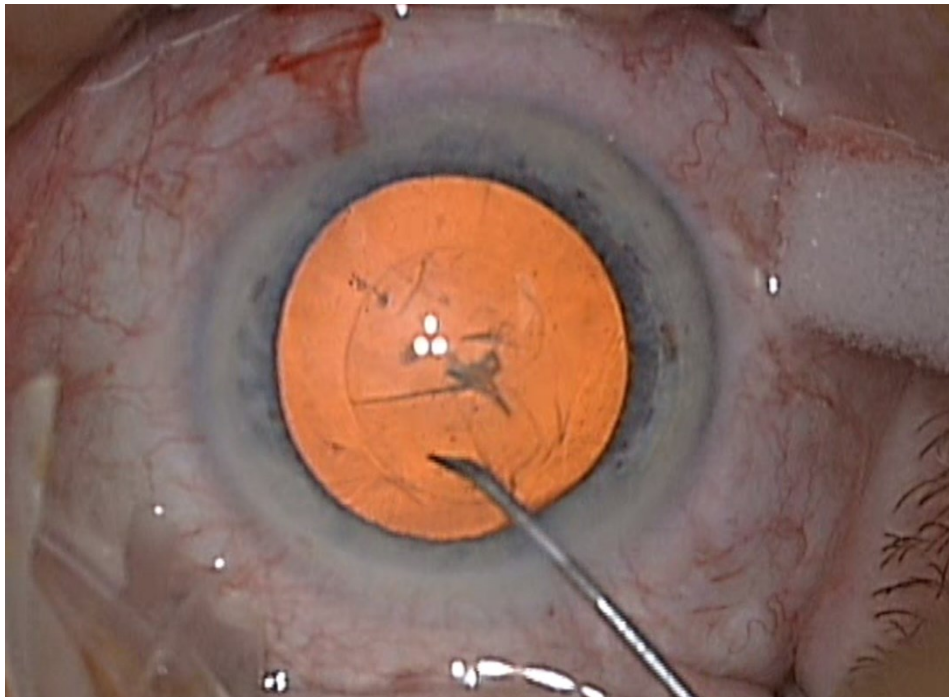


Figure 24: Creation of curvilinear capsulorhexis with a bent needle.

2.1.1.3 Hydrodissection

Hydrodissection was first described by Faust.⁶⁵ The aim of hydrodissection is the separation of cortex from the capsular bag as completely as possible. Balanced salt solution (BSS) is injected by a cannula which is placed right under the edge of the capsulorhexis between the anterior capsule and the cortex (Figure 25). Hydrodissection is a critical step for the following mobilization of the lens nucleus and its removal.⁶⁰

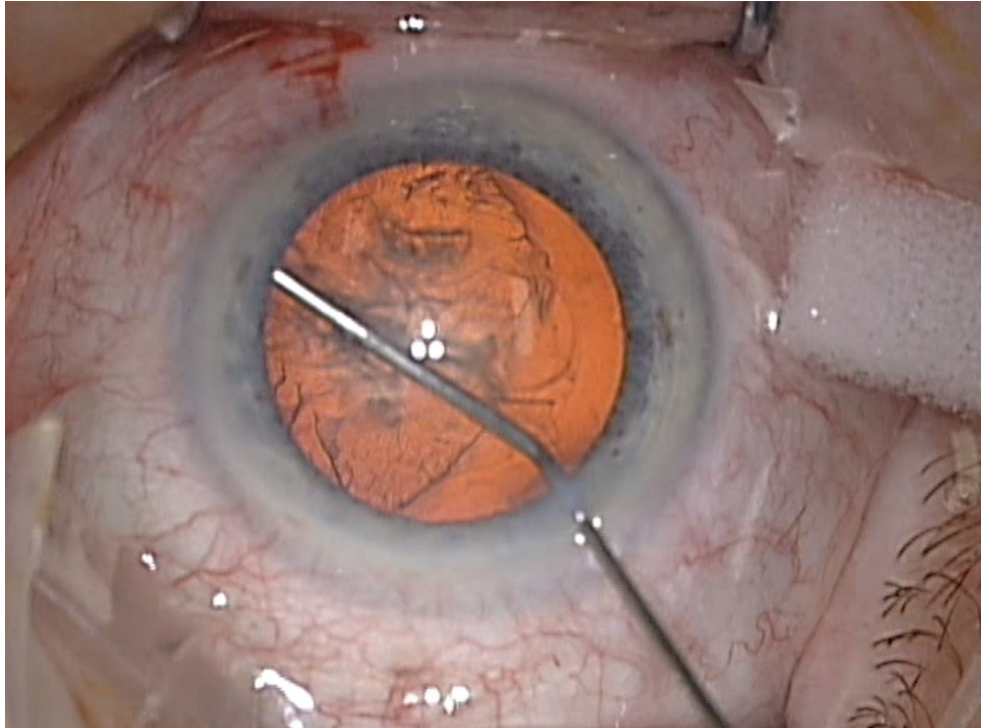


Figure 25: Hydrodissection.

2.1.1.4 Phacoemulsification

Charles Kelman revolutionized the surgical removal of cataract by introducing phacoemulsification in the 1960ies and 1970ies. Phacoemulsification is a small incision surgical procedure using ultrasound energy to break up and liquefy the hard lens nucleus, and then aspirate the lens fragment through the small incision.⁶⁶

The phacoemulsification handpiece is made of titanium and vibrates with a certain ultrasound frequency to break the nucleus into lens fragments. During liquefaction, fluid is injected into the anterior chamber to aspirate the small lens fragments. The nucleus is divided in half (Figure 26) and then typically into quarters, enabling the safe and efficient disassembly and removal of the nucleus. To aspirate the remaining cortex portions in the capsular bag the phacoemulsification handpiece is replaced by an irrigation/aspiration handpiece without sharp edges for reduced risk of capsule rupture. Today, manufacturers have optimized the probes and pump systems for better control of fluidics.⁶⁰

In the present study, surgeons used a phaco devices with peristaltic pumps and irrigation/aspiration was performed with coaxially positioned probes.

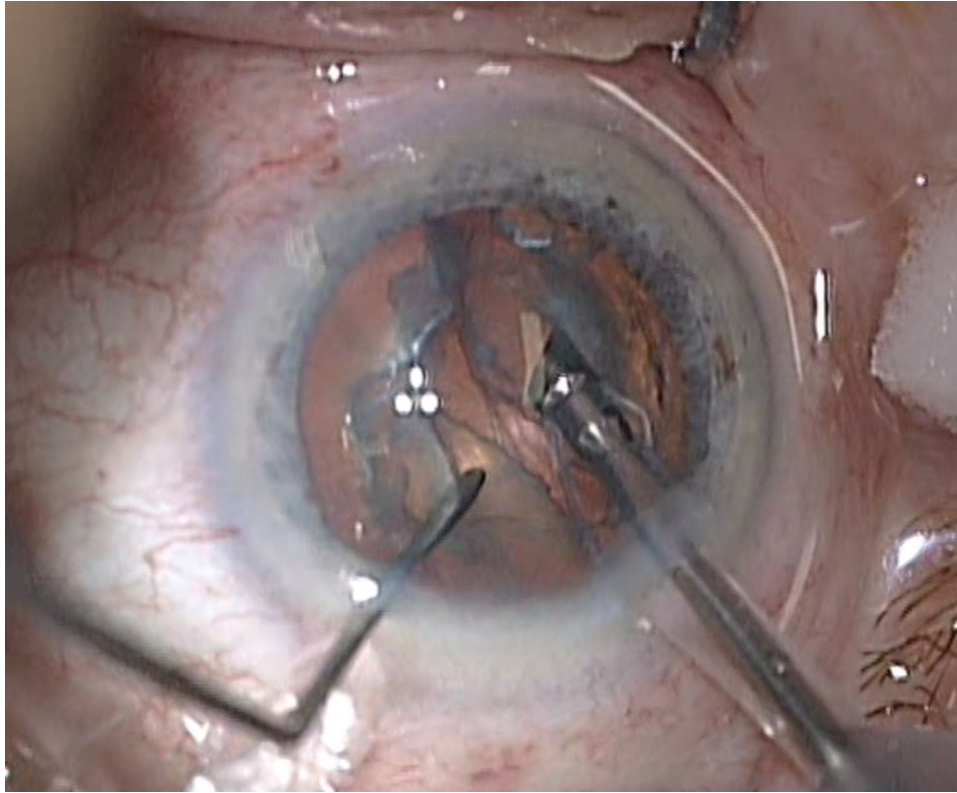


Figure 26: Cracking the nucleus in half after creating a central groove with the phacoemulsification tip.

2.1.1.5 Intraocular lens implantation

In modern-day cataract surgery, most commonly used intraocular lenses are foldable, allowing injection into the eye through a small incision. At the time of introduction of foldable IOLs, insertion was accomplished using folding forceps and inserters. Later, the procedure was simplified by the use of cartridge injectors.

After filling the anterior eye segment with OVD, the IOL is injected into the eye (Figure 27), unfolds within the eye, and is positioned in the capsular bag.

In principle, IOLs consist of a central optical part and 2 to 4 elastic side structures, called haptics, to hold the lens centered in the capsular bag.⁶⁰

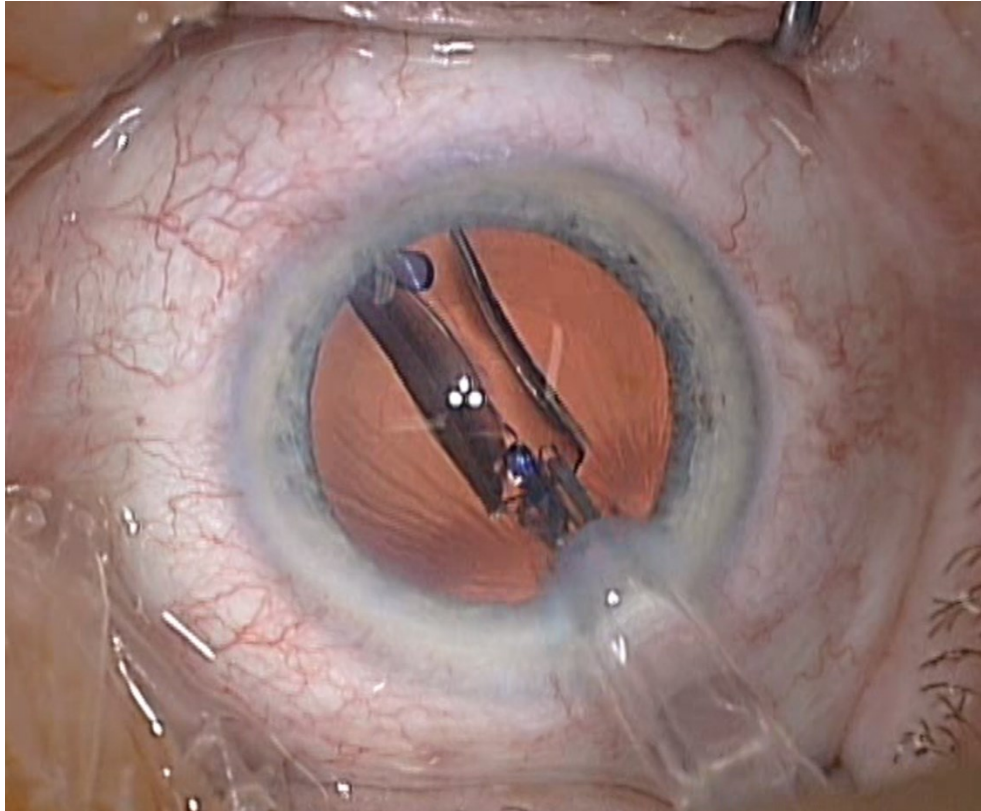


Figure 27: Injecting the folded intraocular lens into the capsular bag through the anterior capsulorhexis.

2.1.2 Refractive cataract surgery

The term “refractive lens exchange” means optimized surgery in consideration of refractive error like surgically induced astigmatism or pre-existing astigmatism, and the use of special IOLs, like multifocal IOLs (additional correction of near and/or intermediate vision) or toric IOLs (additional correction of astigmatism). Thereby, corneal astigmatism can be addressed by positioning of the incision. A fundamental requirement for successful cataract surgery is comprehensive and precise preoperative diagnostics. Depending on the planned surgery, further topographic analysis of the cornea may be necessary in addition to IOL-power calculation (biometry).

2.2 Intraocular lens materials

Treating perforated eyes of aviators struck by splinters from aircraft cockpit canopies during combat in World War II, Harold Ridley noticed acrylic plastic to be inert in eyes. Hence, he developed the first IOLs out of polymethacrylate (PMMA).

The introduction of modern phacoemulsification techniques allowing removal of cataract through smaller incisions lead to the development of foldable materials such as hydrophobic acrylic, hydrophilic acrylic, and hydrophobic silicone.

2.2.1 Hydrophobic acrylic

2.2.1.1 Polymethylacrylate

In modern cataract surgery, rigid non-foldable polymethacrylate (PMMA) IOLs play only a minor role because of large wound size. However, they play a role in developing countries where extracapsular cataract extraction (ECCE) with manual expression of the nucleus is the technique of choice. Furthermore, PMMA IOLs are still used for situations requiring placement in the ciliary sulcus, since their overall rigidity results in good centration and resistance to tilt.⁶⁷

2.2.1.2 Foldable hydrophobic acrylic

Foldable hydrophobic acrylic IOLs are currently the most used IOLs.⁶¹ The name comes from a very low water content, and with its high material memory it is optimal for the haptics of a one-piece open-loop IOL. It unfolds in the eye in a controlled fashion and has shown excellent biocompatibility.⁶⁸

A drawback of this material is the possibility of intralenticular changes such as small water inclusions in the optic material. However, these so called glistenings predominantly occur in the IOL material of one manufacturer (Acrysof, Alcon Fort Worth, TX) and rarely have an effect on visual function.⁶⁹

Another drawback has been dysphotopsias due to the high refractive index of the material. Positive dysphotopsia is edge glare due to internal reflections, mainly in reported in eyes with large pupils. Negative dysphotopsia, typically a scotoma in the temporal peripheral visual field, is reported by a smaller proportion of patients.⁷⁰

In the present study, both the Tecnis ZA9003 (Abbott Medical Optics, Ettlingen, Germany) IOL and Sensar AR40e (Abbott Medical Optics) were made of foldable hydrophobic acrylate.

2.2.2 Hydrophilic acrylic

This material group is quite heterogeneous and has a high water content. It has been shown, that compared to hydrophobic acrylic IOLs hydrophilic acrylic lenses have a higher tendency to develop posterior capsular opacification (PCO), a fairly common complication (also called “secondary cataract”) resulting from the growth and abnormal proliferation of lens epithelial cells on the posterior capsule.⁷¹

Opacification of the optic material was reported in some hydrophilic acrylic IOLs of different companies, although the majority of IOLs of other companies have never shown such problems.⁷²

2.2.3 Silicone

Although the first foldable IOLs were made of silicone, since then the use of such IOLs continuously declined. The main reason therefore is that the material cannot be used for one-piece IOLs with open-loop haptic and hence, the required 3-piece IOL design carries the risk of tearing the optic-haptic-junction during injection in small incision.⁶⁷

2.3 Intraocular lens design

Today a diverse range of IOL designs is available. Basically, all IOLs consist of 2 parts: a central optical part called *IOL optic*, and 2 to 4 side structures for the fixation in the capsular bag, the ciliary sulcus or the anterior chamber angle, the so called *haptics*.

2.3.1 Intraocular lens haptic design

2.3.1.1 Plate haptic

Today, plate haptics (Figure 28) are used mostly in hydrophilic IOLs, usually in combination with small loop-like haptics at the 4 corners for a better adaption to capsular bag size. Due to the design there is no complete fusion of the anterior and posterior capsule along the plate haptic axis, making those IOLs more prone to migration of lens epithelial cells onto the posterior capsule and thus posterior capsule opacification.⁷³

2.3.1.2 Open-loop haptic

These IOLs are fixated in the capsular bag by exerting a centripetal pressure on the capsular bag fornix, or the ciliary sulcus in case of sulcus implantation. Important factors for good IOL centration after implantation in an eye are the haptic rigidity, which is the resistance against forces bending the loops centrally, and the haptic memory, which is the ability to maintain its original configuration after having been bent.

Multi-piece IOLs usually consist of 2 different materials (optic and haptics), whereby the most common haptic materials are PMMA, polyvinylidene, polyimide, and less frequently polypropylene.⁶⁷

The haptic shape of the first modern IOL was the *j-loop design*, which may result in stress folds of the posterior capsule due to pinpointed contact with the capsular bag equator. Further modifications lead to the development of *modified j-loops* and *c-loops* with different lengths (Figure 28).⁷⁴

In contrast to multi-piece IOLs, which have to be assembled by hand, **single-piece IOLs** are produced from one material in a single step. Thus, beside lower production costs those IOLs are more resistant to damage when used with injectors.

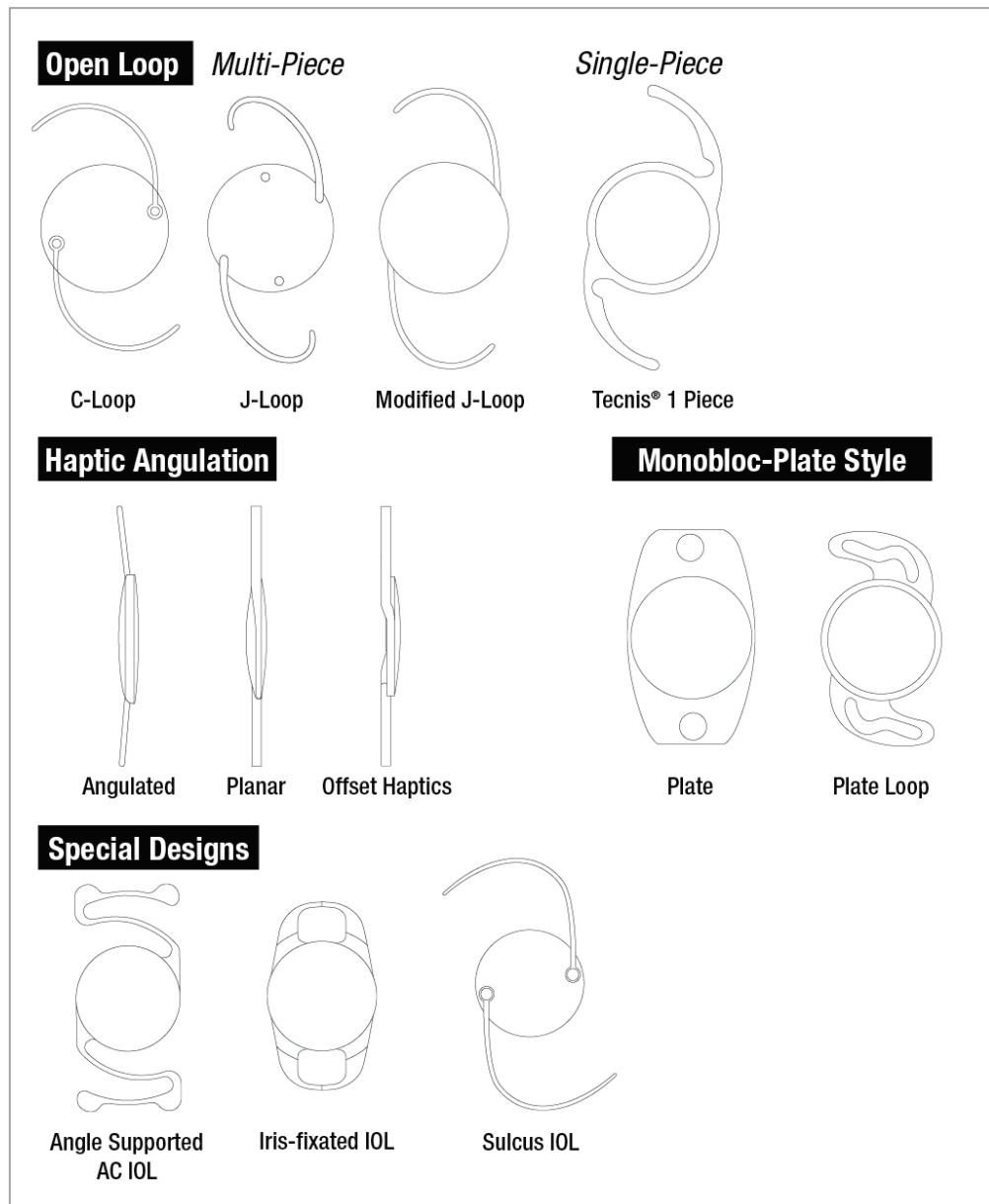


Figure 28: Different haptic designs. Reprinted by permission from D. Michel Colvard, *Achieving Excellence in Cataract Surgery*, Findl 2009⁶⁷

It has been shown that a sharp edge of the optic has a preventative effect against PCO because it reduces migration of lens epithelial cells onto the posterior capsule.^{75,76} To

maximize this effect by pushing the IOL backward against the posterior capsule, an angulated design of the haptic could be useful. The original intention of **haptic angulation** (Figure 28) was to reduce iris shave in cases where the IOL was placed in the sulcus. Many modern IOLs show haptic angulations of 5 to 10 degrees, however, the PCO-preventing effect remains controversial.⁷⁷

In the present study, both IOLs used were 3-piece IOLs with an overall length of 13 mm. Both IOLs had PMMA haptics designed as a modified c-loop and an angulation of 5 degrees.

2.3.2 Intraocular lens optic design

As already mentioned previously, the optic **edge design** plays an important role in the prevention of PCO.^{75,76} The preventive effect lies in the discontinuous capsular bend induced by the mechanical pressure, which inhibits lens epithelial cell migration on the posterior capsule. As a consequence, eyes with sharp-edge IOLs developed significantly less PCO compared to eyes with a round posterior optic edge.⁷⁸ However, there are also disadvantages of a sharp optic edge like an increased risk for positive dysphotopsia, a persistent edge-glare phenomenon reported after implantation of IOLs with sharp optic edge and a high refractive index.^{79,80} However, some newly developed IOLs provide a round anterior and a sharp posterior optic edge to avoid such disturbing dysphotopsias.⁸¹ Round edge IOLs disperse the rays of light over a larger retinal area, inducing less glare.

Most current IOLs have a symmetrical **biconvex optic** design with identical radius of curvature of the anterior and posterior lens surface. In IOLs with an asymmetric biconvex optic, the relatively flat posterior lens surface remains almost unchanged throughout most of the power range while the anterior lens curvature varies for IOL power. Hence, upside down IOL implantation will lead to higher postoperative refractive errors in those asymmetric biconvex IOLs compared to symmetric biconvex IOLs.⁶⁷

The effective **optical zone** of most modern IOLs is 6 mm. Thus, IOLs with higher dioptric power (as required in short hyperopic eyes) will have a thicker optic than lower power IOLs. This may have an impact on folding of the IOL or requires different shooters depending on IOL power.

In the present study, the used IOLs have a “half-rounded edge design” with a 360° square posterior edge and a round anterior edge. The optic of both IOLs is designed biconvex with an anterior aspheric surface and the optical zone is 6.0 mm.

2.4 Intraocular lens power calculation

The postoperative refraction, and consequently the achieved spectacle independency after cataract surgery is a substantial criterion for the quality of surgery and the subjective patient satisfaction.

Fifty years ago, Fyodorov published the first theoretical IOL calculation formula.⁸² Since then, remarkable progress in accuracy of measurements and power calculation formulae improved results to level, that more than 73 % of eyes are within ± 0.5 D postoperatively.⁸³

2.4.1 Sources of error

Axial length: Acoustic measurement with A-scan-ultrasonography, using 10 MHz probe frequency and the contact method, has a mean tolerance of about 0.2 mm, corresponding to 0.75 D in the spectacle plane. Significantly better results are achievable with immersion ultrasonography technique due to the absence of corneal indentation.⁸⁴ Introduction of partial coherence tomography (e.g. IOL Master, Carl Zeiss, Jena) has further improved the mean error to 0.03 to 0.05 mm, corresponding to 0.15 to 0.2 D in the spectacle plane.^{85,86} Accuracy is expected to be at least comparable with newer devices using optical coherence tomography (e.g. IOL Master 700, Carl Zeiss).

Keratometry: Usually corneal curvature is calculated from paraxially measured radii of the anterior corneal surface. For this, some assumptions have to be made, like presence of a sphere or prolate asphericity and a constant ratio between anterior and posterior corneal surface. Each of these parameters causes an error of about 0.125 D.⁸⁶

Intraocular lens position: The axial position of the IOL may be the major source of error with the use of modern biometry devices.^{86,87} The mean error is 0.45 D in an average eye, which could even increase in short eyes.

Refraction: Measurement of postoperative refraction is subjective to the patient and the examiner, while also other factors like room illuminance may have an influence. The mean error of postoperative refraction was reported to be between 0.28 to 0.39 D.^{86,88}

Formulae: Approximations regarding paraxial beams and thin lenses are not accurate for the human eye. Another source of error is the corneal model with the refractive index of 1.3375. The assumption of the estimated lens position (ELP) is made with the preoperatively measured parameters axial length and keratometry (Holladay, Hoffer Q, SRK/T) or axial length and anterior chamber depth (Haigis). The prediction is adapted by so called constants, which enable to fudge the mean prediction error of a certain cohort to zero. Hence, these constants are fudge factors not only for the ELP, but also for other parameters like false refractive indices, pupil size (aberrations), decentration and tilt of the IOL, pseudo-accommodation, asphericity of cornea and lens, atypical ratio between anterior and posterior eye segments, surgical technique and so on. This means that a systematic error is compensated through another variable and the contribution of single errors is not transparent.⁸⁹

2.4.2 Formulas

Traditionally IOL calculations are classified by generation, which worked well for common formulas that are predominantly vergence formulas. However, the introduction of newer formulas that work differently, for example ray tracing or artificial intelligence, make things more complex. Thus, a newer classification was proposed recently⁹⁰:

Historical/refraction based: The first attempts at calculating IOL power were simple formulas based on preoperative spherical equivalent. This approach is obviously obsolete.

Regression: Previous data is analysed without using theoretical optics.

SRK and *SRK II*: linear regression

Vergence: These are by far the greatest in number and are based on Gaussian optics. The major weakpoint and the part differing strongest between different formulas is the accurate estimation of the ELP. Vergence formulas can be subclassified by the number of variables used:

2-variable formulas: *Holladay 1, SRK-T, Hoffer Q*

3-variable formulas: *Haigis, Ladas Super Formula*

5-variable formulas: *Barrett Universal II*

7-variable formulas: *Holladay 2*

Artificial intelligence: These formulas are basically regression formulae using huge databases and sophisticated statistical models to find relationships not apparent in theoretical formulas.

Clarke neural network

Hill-RBF (radial basis function)

Ray tracing: Basically, this method is a systematic application of the Snellen law at all refractive interfaces of the eye. Hence, not only the posterior corneal surface is taken into account but also instead of approximation of an infinite thin lens the crystalline lens is considered as a thick lens with an anterior and posterior surface.

Okulix

Phacooptics (Olson)

2.4.3 Intraocular lens power calculation in short eyes

IOL power calculation in short eyes is challenging for several reasons: the allowed tolerances for IOL power are higher, measurement errors have a stronger effect compared to more normal eyes, and the prediction of ELP is more critical. A change in the axial position of 0.1 mm has a 2.5 times higher effect in a +35 D IOL compared to a +20 D IOL. In addition, in very short and very long eyes the anatomy of the anterior segment does not correlate with the total size of the eye.⁹¹

Clinical studies reported varying results for different formulas in short eyes. Haigis formula was superior in a meta-analysis⁹², Carifi et al found the best results with the Hoffer Q formula⁹³, and Gökce et al reported no differences in the median absolute error after adjusting the mean numerical refractive prediction error to zero.⁹⁴

In the present study, the same IOL power calculation formula (SRK-T with optimized constants) was used for all patients to avoid a confounding factor for the comparison between emmetropic and hyperopic patients.

2.5 Aspheric intraocular lenses

In photography, to obtain great images cameras with aspheric lenses are used for many years. This concept was adopted in ophthalmology with the introduction of precisely made IOLs with aspheric optics in 2002.⁹⁵

The traditional IOLs are spherical, meaning that they have the same constant curvature on the optic, basically as being carved out of a sphere of glass. Those spherical IOLs have a higher power in the periphery than in the center, hence inducing positive spherical aberration. In contrast, aspheric IOLs with zero spherical aberration have a variable curvature, creating lenses with even power from the center to the edge. They are more technically challenging to produce; however, the intention is to obtain a better optical quality. Aspheric IOL are also available with a negative degree of spherical aberration whereby the IOL refractive power is higher in the center than in the periphery.⁶⁰

Spherical aberration is the only higher-order aberration of the cornea that has a non-zero mean in normal eyes.^{96,97} The average cornea has a spherical aberration of $+0.27 \mu\text{m}$, remaining relatively stable throughout the lifetime (Figure 29).⁹⁸

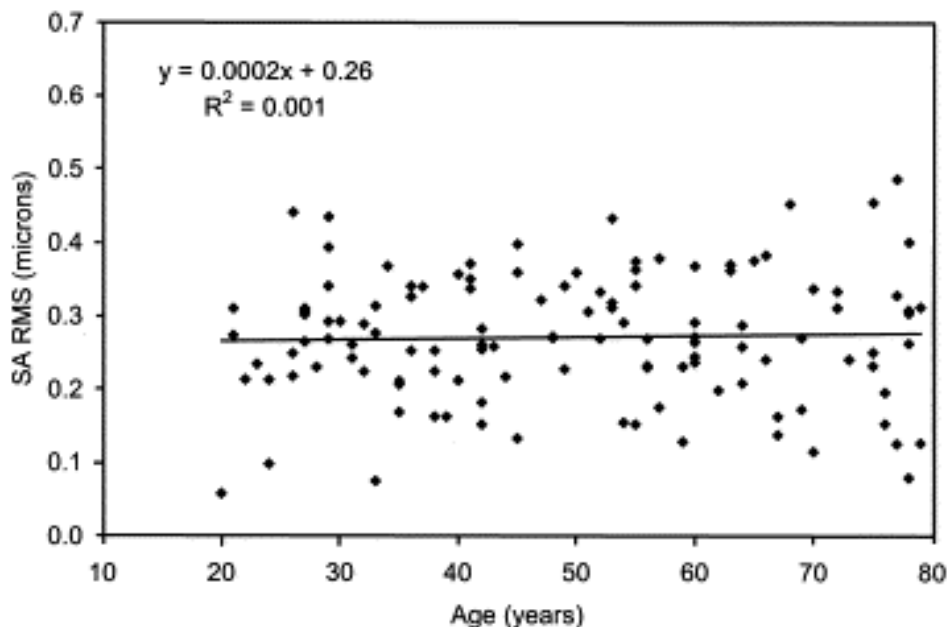


Figure 29: Scattergram of corneal 4th order spherical aberration RMS versus age. Reprinted by permission from Elsevier, *Journal of Cataract and Refractive Surgery*, Wang 2003⁹⁸

This small degree of positive spherical aberration of the cornea is typically counterbalanced by the young crystalline lens which has a small degree of negative spherical aberration. Thus, an eye with a total of zero spherical aberration is produced.

However, with age the crystalline lens changes towards a less negative spherical aberration⁹⁹ (Figure 30) and the total eye develops a small degree of positive spherical aberration.

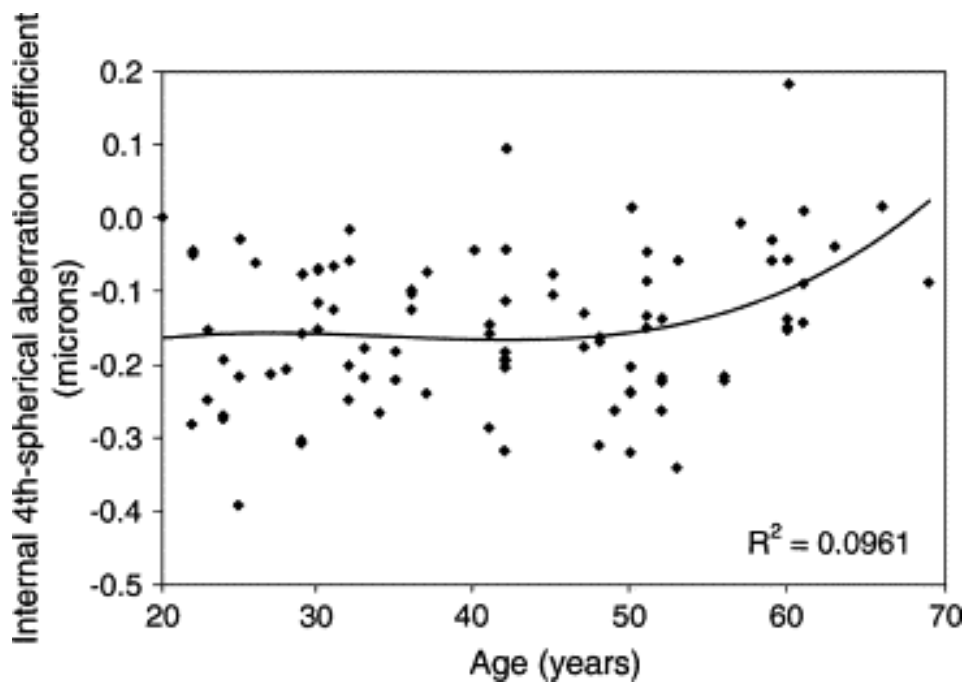


Figure 30: Scattergram of internal 4th order spherical aberration coefficients versus age. Reprinted by permission from Elsevier, *Journal of Cataract and Refractive Surgery*, Wang 2003⁹⁹

As a consequence, also the higher-order aberrations of the eye increase with age (Figure 31). This may even be useful because it may increase the depth of focus as the eye becomes presbyopic.⁶⁰

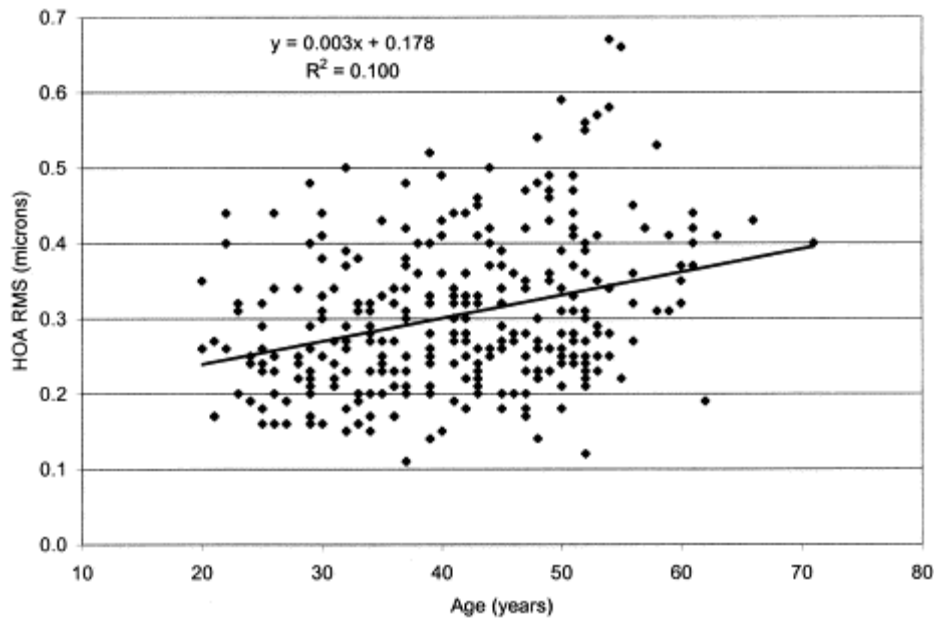


Figure 31: Scattergram of total eye higher-order aberrations RMS versus age. Reprinted by permission from Elsevier, *Journal of Cataract and Refractive Surgery*, Wang 2003¹⁰⁰

In selecting an IOL for the eye, we have a choice of 3 different IOL types:

Spherical IOLs: All spherical IOLs produce positive spherical aberration. Thereby, the degree of positive spherical aberration correlates with the dioptric IOL power and the size of the optical zone (e.g. *AMO Sensar AR40e*, *Alcon AcrySof SA60*).

Spherical aberration-neutral aspheric IOLs: These IOLs induce no spherical aberration. As in the optical system of the eye spherical aberration is only produced by the cornea, the total eye spherical aberration is positive (e.g. *Bausch & Lomb SofPort*, *Rayner C-flex 970 C*).

Spherical aberration-compensating IOLs: The spherical aberration of these IOLs is designed complementary to the spherical aberration of the cornea. If the manufacturer assumes a corneal spherical aberration of +0.2 μm , the IOL is designed with -0.2 μm spherical aberration. (e.g. *Alcon Acrysof SN60WF*, *Hoya AF-1*)

Since the introduction of aspheric IOLs, clinical studies have reported controversial results. As expected, the theoretical concept was confirmed as spherical aberration after implantation of aspheric IOLs was lower than after implantation of traditional spherical

IOLs.¹⁰¹⁻¹⁰³ However, total eye higher-order aberrations were not always significantly lower in eyes with aspheric IOLs. Investigating retinal image quality with a parameter like the *visual Strehl ratio based on the optical transfer function (VSOTF)*, eyes with aspheric IOLs were superior.^{102,104} While an advantage of aspheric IOLs in photopic high-contrast visual acuity was shown only very rarely, superiority of aspheric IOLs was reported for low-contrast acuity. Especially contrast sensitivity under mesopic conditions was better in eyes with aspheric IOLs.^{101,105}

A meta-analysis including more than 4000 eyes of 43 randomized controlled trials comparing aspheric and spherical IOLs found a statistically significant better corrected distance visual acuity for aspheric IOLs, however, the authors supposed that the difference (-0.01 logMAR) was not clinically relevant. Comparing contrast sensitivity, a significant advantage was achieved with aspheric IOLs, especially under mesopic conditions.¹⁰⁵

This is a consequence of the inherent relation between spherical aberration and pupil diameter. Under a mesopic illumination condition the pupil diameter is larger and thus, spherical aberration has a higher impact on retinal image quality after implantation of both spherical and aspheric IOLs. However, it was shown that degradation of image quality with increasing pupil diameter was more pronounced in eyes with spherical IOLs (Figure 32).¹⁰²

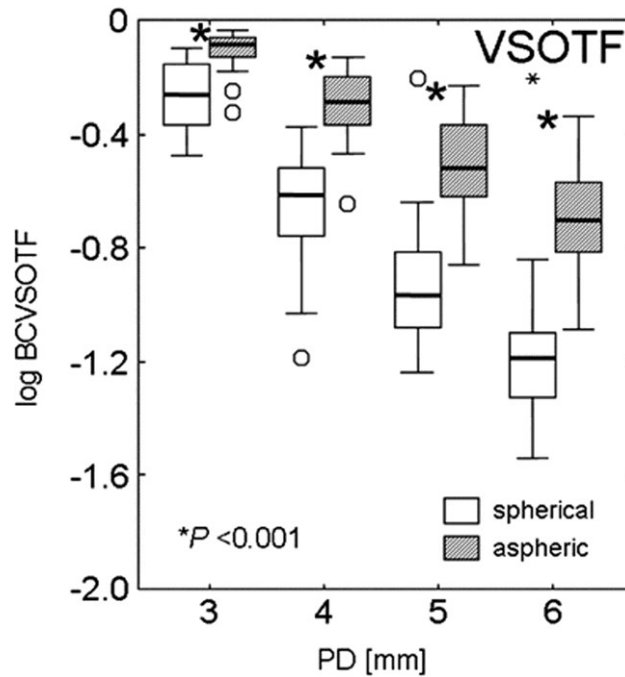


Figure 32: Image quality after implantation of spherical or aspheric intraocular lenses as a function of pupil diameter. Box plots of postoperative retinal image quality at different pupil diameters. BCVSOTF=visual Strehl ratio based on the optical transfer function, simulated for best correction, PD=pupil diameter. Reprinted by permission from Elsevier, *Ophthalmology*, Kohnen 2009¹⁰²

As only some of the clinical studies reported superior functional results after aspheric IOL implantation, this relationship between spherical aberration and pupil diameter was brought forward as a reason for the discrepant findings. It was suggested that pupil diameters were too small for providing visually significant spherical aberration differences.^{104,106} In eyes with a pupil diameter smaller than 3.7 mm no advantages may be achieved by the use of aspheric IOLs.¹⁰⁷

Decentration of the IOL in the capsular bag is another factor that may theoretically decrease efficiency of aspheric IOLs. However, when IOL tilt and decentration are within normal limits, they do not compromise the correction of spherical aberration by the aspheric IOL.¹⁰⁸

Despite improved image quality and contrast sensitivity, aspheric IOLs may also lead to decreased depth of focus. In an optical system with complete correction of aberrations, a sharp image is produced only if the image is perfectly focused. With some defocus, image

quality decreases. In the presence of aberrations, image quality may be compromised, but a certain tolerance for defocus is provided as there is a series of focal points instead of a single focal point. Thus, higher residual spherical aberration after cataract surgery with implantation of spherical IOLs could improve the depth of focus compared to aspheric IOLs.^{51,109,110} As a consequence, pseudophakic patients may have good uncorrected intermediate and near vision leading to increased independency of reading glasses.

This can particularly be observed in hyperopic patients, as short axial length is associated with good near vision after monofocal IOL implantation¹¹¹. One possible explanation is that the magnitude of spherical aberration increases with dioptric IOL power.¹¹²

Hence, the aim of the study was to evaluate, whether hyperopic patients with short axial length and high dioptric IOL power may achieve a higher depth of focus with better near and intermediate visual acuity after monofocal IOL implantation than emmetropic patients.

3 Depth of focus after implantation of spherical or aspheric intraocular lenses in hyperopic and emmetropic patients

The following section is being reproduced in large parts identically from the publication of Gernot Steinwender and co-authors “Depth of focus after implantation of spherical or aspheric intraocular lenses in hyperopic and emmetropic patients“ with explicit permission of the respective journal (Journal of Cataract & Refractive Surgery).¹¹³ Several additional graphs have been added for better explanation of differences between study groups, which were omitted in the published manuscript due to journal restrictions. The work constitutes the original work of the author (Gernot Steinwender).

3.1 Introduction

In modern cataract surgery, the aim is not only restoring visual acuity, but also providing the best quality of vision to patients. Therefore, modern intraocular lenses (IOLs) which basically add spherical refractive power after removal of the cataractous human lens were developed to offer better optical quality than a healthy human crystalline lens.^{114,115}

Higher-order aberrations (HOA), and mainly spherical aberration (SA) can lead to degradation of high-resolution imaging of the eye.¹¹⁶ In the presence of SA, rays entering in the peripheral part of the pupil are focused to a different point than rays entering in the near of the pupil center. An increase in the amount of SA leads to an impairment of optical function.¹¹⁷ Classical spherical IOLs induce positive SA whereas aspheric designed IOLs compensate for the positive SA of the cornea. These aspheric IOLs have no SA or a negative amount of SA, calculated for an averaged corneal profile of a population with normal untreated corneas. Previous studies showed that, compared to spherical IOLs, aspheric IOLs provide better contrast sensitivity due to decreasing SA.¹⁰⁵

However, the induction of multiple focal points on the focal axis by SA may lead to better depth of focus^{51,109,110,118}, which may result in a satisfactory near and/or intermediate visual acuity in some patients after monofocal IOL implantation. Therefore, retaining a certain amount of residual SA after cataract surgery may be the best compromise between visual quality and depth of focus.¹¹⁹ Further factors associated the amplitude of the apparent

accommodation in patients with monofocal IOLs are pupil diameter^{44,111} and corneal astigmatism^{8,9}.

Another study reported that also short axial length is associated with good near vision after monofocal IOL implantation.¹¹¹ The findings of Lim et al seem to back up our own clinical observation, that hyperopic patients were more often spectacle-independent after implantation of monofocal IOLs than emmetropic or myopic patients. This might be attributed to a higher magnitude of postoperative SA with increasing dioptric power of the IOL¹¹², leading to a higher defocus tolerance.

The aim of our study was to analyse, whether hyperopic patients with short axial length and high dioptric IOL power may achieve a higher depth of focus after monofocal IOL implantation than emmetropic patients. Therefore, we conducted a prospective, double-masked study with both, hyperopic and emmetropic cataract patients randomized to receive either a spherical or an aspheric IOL.

3.2 Patients and methods

Patients having phacoemulsification for age-related cataract between September 2013 and June 2015 at the Department of Ophthalmology of the Medical University of Graz, Austria, were comprised in this randomized, double-masked study.

The study followed the tenets of the Declaration of Helsinki and written informed consent was obtained from all patients enrolled in the study. The study was approved by the university's ethics committee.

Inclusion criterion was uncomplicated age-related cataract with the potential acuity of 20/20 or better, and exclusion criteria were coexisting ocular pathology, such as corneal opacities or irregularities, concurrent medication apart from ocular lubricants, corneal astigmatism more than 1.5 diopters (D), postoperative refractive spherical equivalent (SE) more than 2.0 D, postoperative corrected distance visual acuity (CDVA) less than 20/25, amblyopia, previous intraocular surgery or laser treatment, retinal complications, or incomplete follow-up.

A complete ophthalmic examination, including slitlamp, dilated fundus evaluation and applanation tonometry was performed preoperatively. Partial coherence interferometry (IOL Master, Carl Zeiss Meditec, Jena, Germany) was used to measure axial length (AL); if not possible due to dense cataract, measurements were obtained by ultrasonography.

According to calculated IOL power, patients were divided into a hyperopic (greater than or equal to 22.0 D) and an emmetropic group (18.0 to 21.5 D) and subsequently randomized by an online software (Randomizer for Clinical Trials, Version 1.8.4, Institute for Medical Informatics, Statistics and Documentation, Medical University of Graz, Austria) to receive either an aspheric Tecnis ZA9003 (Abbott Medical Optics) IOL with negative spherical aberration of 0.27 μm or a spherical Sensar AR40e (Abbott Medical Optics, Ettlingen, Germany) with spherical aberration. Both IOL models have an identical design with three-piece open loop haptics and an optic diameter of 6 mm, and are of the same hydrophobic acrylic material.

All surgeries were performed by 2 experienced surgeons (N.A., B.V.) using a 2.5 mm clear corneal incision with an auxiliary paracentesis 90° apart and a divide-and-conquer phacoemulsification technique. A continuous curvilinear capsulorhexis with an approximate diameter of 5.0 mm was created by a bent needle and IOLs were implanted into the capsular bag. All eyes were targeted for emmetropia and IOL power was calculated using the SRK/T formula with optimized A constants.

Three month postoperatively, corrected distance visual acuity (CDVA) and uncorrected distance visual acuity (UDVA) were measured using an Early Treatment Diabetic Retinopathy Study (ETDRS) logMAR visual acuity chart at 4 m under photopic conditions (target luminance of 85 cd/m²). Radner Reading visual acuity chart (Precision Vision, La Salle, USA) were used to measure corrected near visual acuity (CNVA) at 40 cm under photopic conditions.

As a measure of depth of focus, distance-corrected intermediate visual acuity (DCIVA) was the primary outcome measure of the study. DCIVA at 1 m and distance-corrected near visual acuity (DCNVA) at 40 cm were tested using the Radner Reading visual acuity chart under photopic conditions. Defocus curves were determined by reading ETDRS logMAR visual acuity charts at 4 m under photopic conditions through different levels of defocus induced with trial lenses (between -1.5 D and 1.5 D in steps of 0.5 D). Contrast sensitivity

testing was performed by the same investigators (G.S., S.S.); the investigators were unaware of which IOL model was implanted, and patients were also masked to IOL type. Anterior and posterior corneal surface aberrations were measured by Scheimpflug imaging (Pentacam, Oculus, Wetzlar, Germany) and included root mean square (RMS) values of corneal HOA and corneal SA for a central 5 mm zone.

Pupillometry and total eye wavefront analysis were obtained based on Hartmann-Shack technology using the WASCA aberrometer (Carl Zeiss Meditec). After measuring pupil diameter under photopic (85 cd/m²) and mesopic (3 cd/m²) conditions, pupils were dilated with 2 drops of tropicamide 0.5% given 15 minutes apart. Fifteen minutes after the last tropicamide drop was instilled, wavefront measurements including RMS values for total eye HOA and total eye SA were obtained. Aberrations were analysed to the sixth Zernike order and for a 5 mm pupil.

Contrast sensitivity was measured with distance correction under photopic (85 cd/m²) and mesopic (3 cd/m²) conditions using the Pelli-Robson contrast sensitivity test (Clement Clarke International, London, United Kingdom). Testing was performed at a viewing distance of 3 m, corresponding to a spatial frequency of approximately 3 cycles per degree (cpd).⁴³ To exclude the known influence of pupil size on contrast sensitivity, testing occurred in mydriasis with a 5.0 mm artificial pupil in the trial frame in front of the eye.¹⁷

For statistical analysis of visual acuity we used the logarithm of the minimal angle of resolution (logMAR) and for analysis of contrast sensitivity we used the log base 10 values (logCS). Categorical data is displayed as frequency with percentage and continuous data is given as mean with standard deviation. Sample size was calculated to provide 80% statistical power at the 5% level to detect a 0.10-difference in logMAR of DCIVA with a standard deviation of the mean difference of 0.15. All visual and refractive data were analysed with a two-way analysis of variances (ANOVA) to assess differences among spherical and aspheric IOLs as well as differences between hyperopic and emmetropic eyes. Parameters not meeting the assumptions of an ANOVA were rank transformed and analysed. All calculations were performed using IBM SPSS Statistics (Release 24.0.0.0 2016, Armonk, USA: International Business Machines Corporation). A P value less than 0.05 was considered statistically significant.

3.3 Results

Sixty-two eyes of 62 patients (38 women [61%] and 24 men[39%]) were included in this study. Mean age of patients was 67.9 years \pm 9.4 (SD). Table 1 shows pre- and postoperative patient characteristics for the aspheric and spherical groups.

Table 1: Patient characteristics for aspheric and spherical IOL group.

Patient Characteristics	Aspheric IOL Group	Spherical IOL Group	P-value
Eyes [n]	34 (54.8%)	28 (45.2%)	
Age [years]	66.2 \pm 9.2	69.9 \pm 9.3	0.130
Axial length [mm]	23.07 \pm 0.91	23.23 \pm 0.69	0.195
Mean K-value [D]	43.21 \pm 1.35	43.02 \pm 1.36	0.595
IOL-power [D]	22.57 \pm 2.74	22.02 \pm 1.36	0.244
Corneal astigmatism [D]	0.70 \pm 0.39	0.59 \pm 0.41	0.303
Photopic pupil diameter [mm]	3.2 \pm 0.6	2.9 \pm 0.4	0.010*
Mesopic pupil diameter [mm]	4.5 \pm 0.8	4.2 \pm 0.8	0.182
RMS corneal HOA [μ m]	0.40 \pm 0.16	0.48 \pm 0.31	0.601
RMS corneal SA [μ m]	0.16 \pm 0.07	0.16 \pm 0.07	0.923
RMS total eye HOA [μ m]	0.35 \pm 0.15	0.32 \pm 0.15	0.565
RMS total eye SA [μ m]	0.01 \pm 0.11	0.10 \pm 0.08	<0.001*

Values are presented as mean \pm standard deviation. D=diopeters, HOA=higher-order aberrations, IOL=intraocular lens, K-value=keratometry value, RMS=root mean square, SA=spherical aberrations. *= Statistically significant ($P \leq 0.05$). Reprinted by permission from Elsevier Inc., *Journal of Cataract and Refractive Surgery*, Steinwender¹¹³

Table 2 shows the postoperative refractive outcome for the both groups.

Table 2: Refractive outcome for aspheric and spherical IOL group.

Refractive Outcome	Aspheric IOL Group	Spherical IOL Group	P-value
UDVA [logMAR]			
MRSE [D]	-0.26 ± 0.62	-0.35 ± 0.67	0.602
CDVA [logMAR]	-0.05 ± 0.06	-0.06 ± 0.05	0.592
CNVA [logMAR]	0.10 ± 0.10	0.11 ± 0.07	0.465
DCIVA [logMAR]	0.21 ± 0.09	0.14 ± 0.08	0.004*
DCNVA [logMAR]	0.50 ± 0.09	0.43 ± 0.10	0.001*
Photopic CS [logCS]	1.23 ± 0.27	1.12 ± 0.23	0.073
Mesopic CS [logCS]	0.90 ± 0.19	0.83 ± 0.16	0.057

Values are presented as mean ± standard deviation. CDVA=corrected distance visual acuity, CNVA=corrected near visual acuity, CS=contrast sensitivity, DCIVA=distance corrected intermediate visual acuity, DCNVA=distance corrected near visual acuity, IOL=intraocular lens, logCS=logarithm of contrast sensitivity, logMAR= logarithm of the minimal angle of resolution, MRSE=manifest refractive spherical equivalent, UDVA=uncorrected distance visual acuity. *= Statistically significant ($P \leq 0.05$). Reprinted by permission from Elsevier Inc., *Journal of Cataract and Refractive Surgery*, Steinwender¹¹³

There were no significant differences between the aspheric and spherical IOL group for age, axial length, mean keratometry value (K-value), IOL-power, corneal astigmatism, and mean mesopic pupil diameter. Mean photopic pupil diameter was significantly larger in the aspheric IOL group ($p = 0.010$).

No significant differences between IOL groups were found regarding corneal aberrations and total eye HOA, however, total eye SA were higher in the spherical IOL group than in the aspheric IOL group ($P < 0.001$).

Depth of focus was significantly better in the spherical IOL group (DCIVA 0.14 ± 0.08 , DCNVA 0.43 ± 0.10) than in the aspheric group (DCIVA 0.21 ± 0.09 , DCNVA 0.50 ± 0.09) ($P = 0.004$, $P = 0.001$, respectively).

Photopic and scotopic contrast sensitivity, as well as UDVA, CDVA, CNVA did not differ significantly between the aspheric and spherical IOL groups.

Subgroup analysis of hyperopic and emmetropic eyes for each IOL group:

Patient characteristics for hyperopic and emmetropic subgroups with an aspheric IOL are shown in Table 3.

Table 3: Patient characteristics for hyperopic and emmetropic subgroup with an aspheric IOL.

Patient Characteristics	Aspheric IOL Group		
	Hyperopes	Emmetropes	P-value
Eyes [n]	15	19	
Age [years]	67.9 ± 8.6	64.8 ± 9.7	0.319
Axial length [mm]	22.45 ± 0.90	23.56 ± 0.57	<0.001*
Mean K-value [D]	43.20 ± 1.35	43.22 ± 1.39	0.968
IOL-power [D]	25.00 ± 2.33	20.66 ± 0.85	<0.001*
Corneal astigmatism [D]	0.64 ± 0.35	0.75 ± 0.42	0.421
Photopic pupil diameter [mm]	3.2 ± 0.4	3.2 ± 0.7	0.936
Mesopic pupil diameter [mm]	4.7 ± 0.5	4.3 ± 1.0	0.170
RMS corneal HOA [µm]	0.38 ± 0.15	0.41 ± 0.18	0.649
RMS corneal SA [µm]	0.18 ± 0.07	0.14 ± 0.08	0.025*
RMS total eye HOA [µm]	0.34 ± 0.11	0.35 ± 0.17	0.940
RMS total eye SA [µm]	-0.01 ± 0.08	0.04 ± 0.12	0.362

Values are presented as mean ± standard deviation. D=diopeters, HOA=higher-order aberrations, IOL=intraocular lens, K-value=keratometry value, RMS=root mean square, SA=spherical aberrations. *= Statistically significant ($P \leq 0.05$). Reprinted by permission from Elsevier Inc., *Journal of Cataract and Refractive Surgery*, Steinwender¹¹³

Refractive outcome for hyperopic and emmetropic subgroups with an aspheric IOL is shown in Table 4.

Table 4: Refractive outcome for hyperopic and emmetropic subgroup with an aspheric IOL.

Refractive Outcome	Aspheric IOL Group		P-value
	Hyperopes	Emmetropes	
UDVA [logMAR]			
MRSE [D]	-0.31 ± 0.61	-0.22 ± 0.65	0.679
CDVA [logMAR]	-0.06 ± 0.05	-0.05 ± 0.06	0.605
CNVA [logMAR]	0.08 ± 0.09	0.11 ± 0.10	0.388
DCIVA [logMAR]	0.21 ± 0.09	0.21 ± 0.09	0.878
DCNVA [logMAR]	0.50 ± 0.11	0.50 ± 0.07	0.891
Photopic CS [logCS]	1.28 ± 0.26	1.19 ± 0.28	0.338
Mesopic CS [logCS]	0.96 ± 0.15	0.84 ± 0.21	0.032*

Values are presented as mean ± standard deviation. CDVA=corrected distance visual acuity, CNVA=corrected near visual acuity, CS=contrast sensitivity, DCIVA=distance corrected intermediate visual acuity, DCNVA=distance corrected near visual acuity, IOL=intraocular lens, logCS=logarithm of contrast sensitivity, logMAR= logarithm of the minimal angle of resolution, MRSE=manifest refractive spherical equivalent, UDVA=uncorrected distance visual acuity. *= Statistically significant ($P \leq 0.05$). Reprinted by permission from Elsevier Inc., *Journal of Cataract and Refractive Surgery*, Steinwender¹³

Patient characteristics for hyperopic and emmetropic subgroups with a spherical IOL are shown in Table 5.

Table 5: Patient characteristics for hyperopic and emmetropic subgroups with a spherical IOL.

Patient Characteristics	Spherical IOL Group		P-value
	Hyperopes	Emmetropes	
Eyes [n]	14	14	
Age [years]	66.8 ± 10.5	73.1 ± 6.8	0.072
Axial length [mm]	22.90 ± 0.60	23.57 ± 0.62	0.011*
Mean K-value [D]	42.88 ± 1.17	43.16 ± 1.56	0.587
IOL-power [D]	23.14 ± 0.84	20.89 ± 0.63	<0.001*
Corneal astigmatism [D]	0.52 ± 0.21	0.66 ± 0.55	0.376
Photopic pupil diameter [mm]	2.9 ± 0.4	2.8 ± 0.4	0.529
Mesopic pupil diameter [mm]	4.3 ± 0.7	4.2 ± 0.9	0.729
RMS corneal HOA [µm]	0.43 ± 0.28	0.53 ± 0.34	0.195
RMS corneal SA [µm]	0.16 ± 0.05	0.16 ± 0.08	0.953
RMS total eye HOA [µm]	0.28 ± 0.13	0.37 ± 0.15	0.089
RMS total eye SA [µm]	0.09 ± 0.08	0.11 ± 0.07	0.534

Values are presented as mean ± standard deviation. D=diopeters, HOA=higher-order aberrations, IOL=intraocular lens, K-value=keratometry value, RMS=root mean square, SA=spherical aberrations. *= Statistically significant ($P \leq 0.05$). Reprinted by permission from Elsevier Inc., *Journal of Cataract and Refractive Surgery*, Steinwender¹¹³

Refractive outcome for hyperopic and emmetropic subgroups with a spherical IOL is shown in Table 6.

Table 6: Refractive outcome for hyperopic and emmetropic subgroups with a spherical IOL.

Refractive Outcome	Spherical IOL Group		P-value
	Hyperopes	Emmetropes	
UDVA [logMAR]	0.15 ± 0.14	0.19 ± 0.17	0.464
MRSE [D]	-0.46 ± 0.66	-0.25 ± 0.69	0.389
CDVA [logMAR]	-0.07 ± 0.05	-0.05 ± 0.05	0.344
CNVA [logMAR]	0.11 ± 0.08	0.11 ± 0.06	0.795
DCIVA [logMAR]	0.14 ± 0.07	0.14 ± 0.09	0.501
DCNVA [logMAR]	0.42 ± 0.09	0.43 ± 0.11	0.533
Photopic CS [logCS]	1.21 ± 0.22	1.03 ± 0.20	0.044*
Mesopic CS [logCS]	0.88 ± 0.16	0.77 ± 0.13	0.069

*Values are presented as mean ± standard deviation. CDVA=corrected distance visual acuity, CNVA=corrected near visual acuity, CS=contrast sensitivity, DCIVA=distance corrected intermediate visual acuity, DCNVA=distance corrected near visual acuity, IOL=intraocular lens, logCS=logarithm of contrast sensitivity, logMAR= logarithm of the minimal angle of resolution, MRSE=manifest refractive spherical equivalent, UDVA=uncorrected distance visual acuity. *= Statistically significant (P ≤ 0.05). Reprinted by permission from Elsevier Inc., Journal of Cataract and Refractive Surgery, Steinwender¹³*

There was a significant difference in axial length between the hyperopic and emmetropic subgroup in both, the group with aspheric and the group with spherical IOLs (p < 0.001, p = 0.011, respectively, Figure 33).

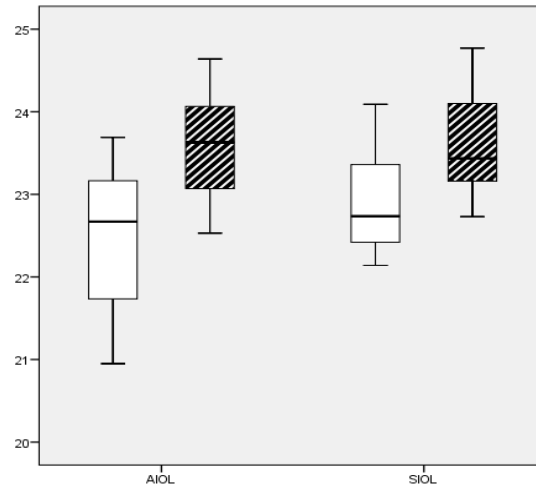


Figure 33: Axial length [mm]. Box plot diagram for emmetropic (diagonally hatched boxes) and hyperopic subgroups (white boxes).

AIOL=aspheric intraocular lens, SIOL=spherical intraocular lens

Mean keratometry values did not differ significantly between the subgroups (Figure 34).

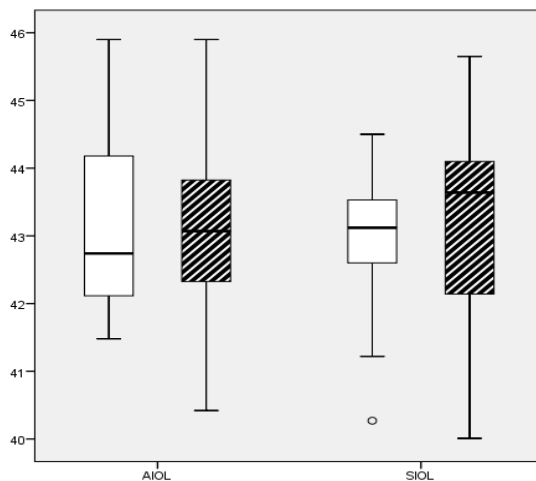


Figure 34: Mean K-value [D]. Box plot diagram for emmetropic (diagonally hatched boxes) and hyperopic subgroups (white boxes).

AIOL=aspheric intraocular lens, SIOL=spherical intraocular lens, K=keratometry

Figure 35 illustrates the significant differences in IOL-power between the hyperopic and emmetropic subgroups in both, the group with aspheric and the group with spherical IOLs ($p < 0.001$, $p < 0.001$, respectively).

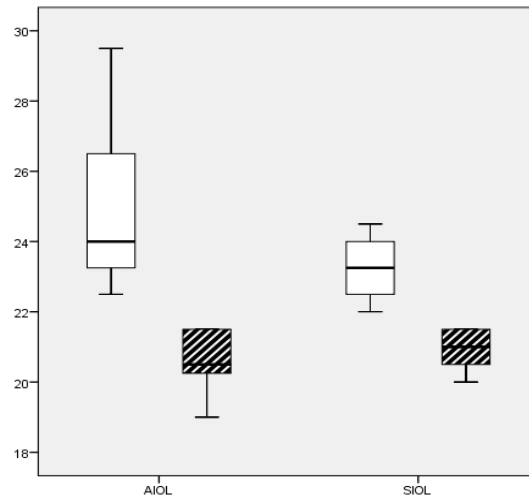


Figure 35: IOL-power [D]. Box plot diagram for emmetropic (diagonally hatched boxes) and hyperopic subgroups (white boxes).

AIOL=aspheric intraocular lens, SIOL=spherical intraocular lens

Corneal astigmatism did not differ significantly between the subgroups for both IOL models (Figure 36).

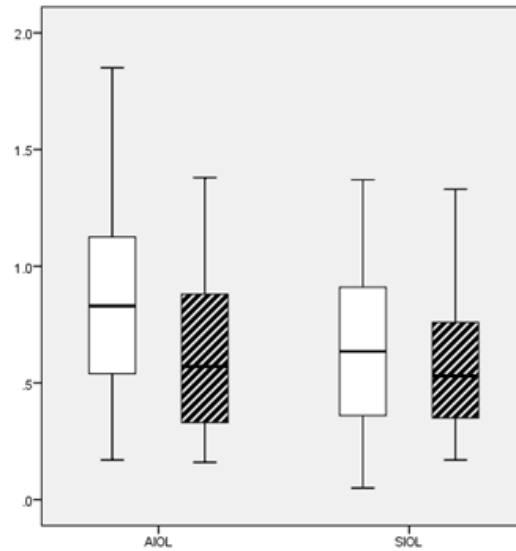


Figure 36: Corneal astigmatism [D]. Box plot diagram for emmetropic (diagonally hatched boxes) and hyperopic subgroups (white boxes).

AIOL=aspheric intraocular lens, SIOL=spherical intraocular lens

Photopic (Figure 37) and mesopic pupil diameter (Figure 38) did not differ significantly between the hyperopic and emmetropic subgroups in eyes with aspheric and spherical IOLs ($p = 0.936$, $p = 0.170$, $p = 0.529$, $p = 0.729$, respectively), although there was a significant difference in photopic pupil diameter between the IOL groups ($p = 0.010$).

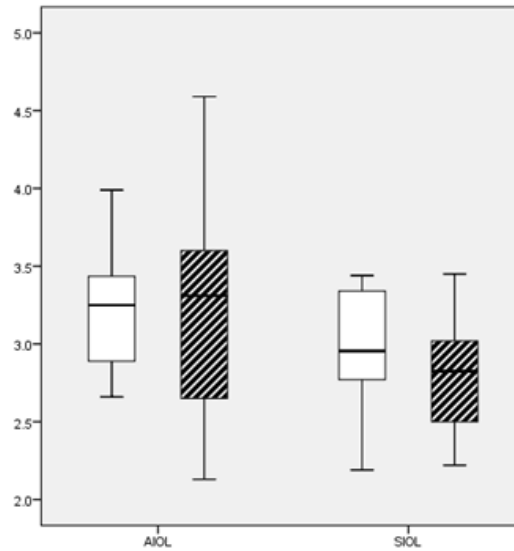


Figure 37: Photopic pupil diameter [mm]. Box plot diagram for emmetropic (diagonally hatched boxes) and hyperopic subgroups (white boxes).

AIOL=aspheric intraocular lens, SIOL=spherical intraocular lens

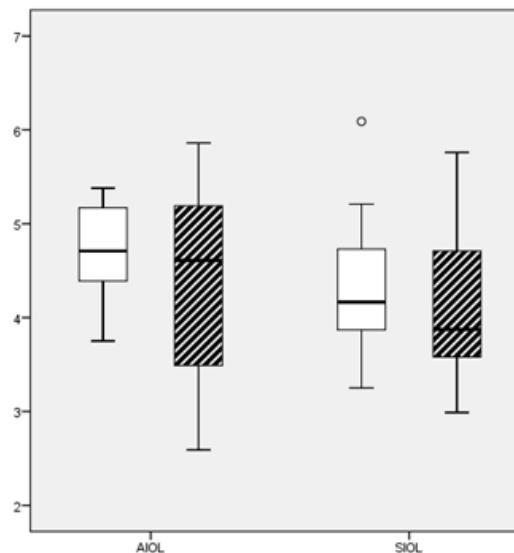


Figure 38: Mesopic pupil diameter [mm]. Box plot diagram for emmetropic (diagonally hatched boxes) and hyperopic subgroups (white boxes).

AIOL=aspheric intraocular lens, SIOL=spherical intraocular lens

Corneal higher-order aberrations (Figure 39) showed no significant differences between the hyperopic and emmetropic subgroup in eyes with aspheric or spherical IOLs ($p = 0.649$, $p = 0.195$, respectively).

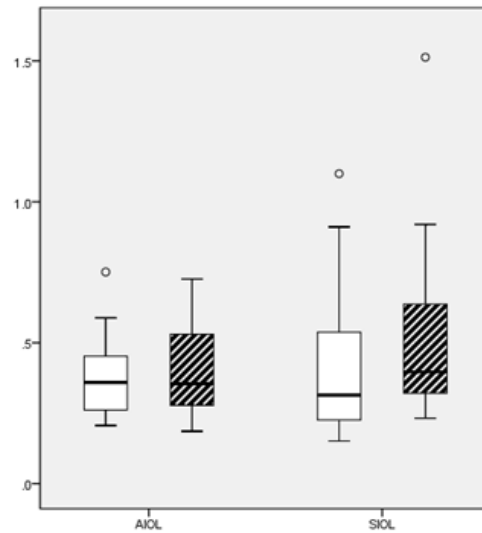


Figure 39: RMS corneal higher-order aberrations [μm]. Box plot diagram for emmetropic (diagonally hatched boxes) and hyperopic subgroups (white boxes). AIOL=aspheric intraocular lens, SIOL=spherical intraocular lens

Corneal spherical aberration (Figure 40) was significantly higher in the hyperopic subgroup compared to the emmetropic subgroup in eyes with aspheric IOLs ($p = 0.025$), whereas there was no significant difference between the subgroups in eyes with spherical IOLs ($p = 0.953$).

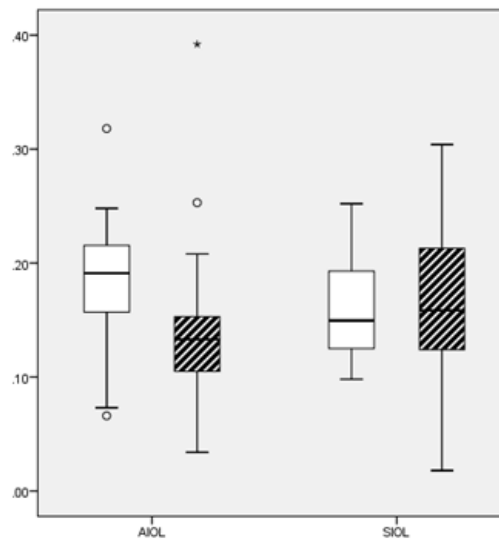


Figure 40: RMS corneal spherical aberration [μm]. Box plot diagram for emmetropic (diagonally hatched boxes) and hyperopic subgroups (white boxes). AIOL=aspheric intraocular lens, SIOL=spherical intraocular lens

Subgroup analysis of total eye higher-order aberrations (Figure 41) and total eye spherical aberration (Figure 42) revealed no significant differences ($p = 0.940$, $p = 0.089$, $p = 0.362$, $p = 0.534$, respectively).

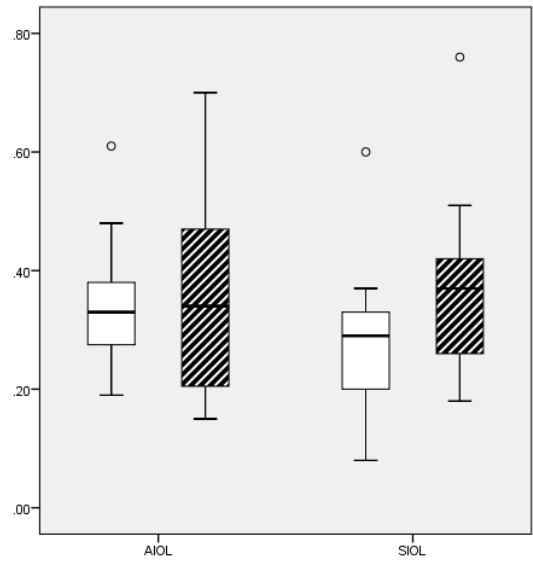


Figure 41: RMS total eye higher-order aberrations [μm]. Box plot diagram for emmetropic (diagonally hatched boxes) and hyperopic subgroups (white boxes). AIOL=aspheric intraocular lens, SIOL=spherical intraocular lens

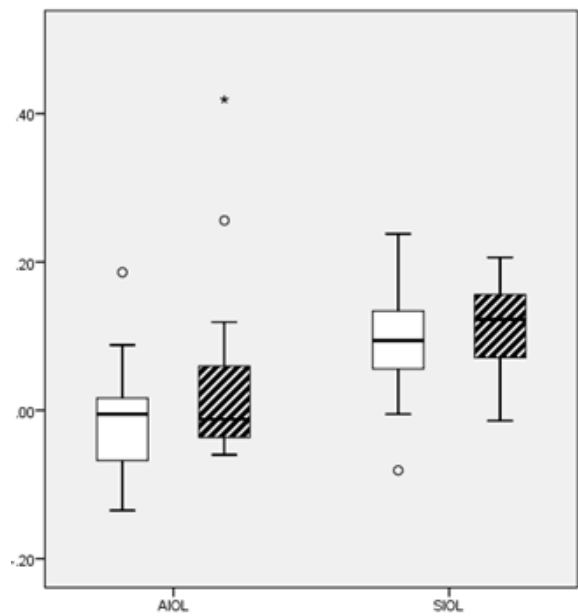


Figure 42: RMS total eye spherical aberration [μm]. Box plot diagram for emmetropic (diagonally hatched boxes) and hyperopic subgroups (white boxes). AIOL=aspheric intraocular lens, SIOL=spherical intraocular lens

No significant differences between subgroups for aspheric and spherical IOLs were found in uncorrected distance visual acuity (Figure 43), manifest refractive spherical equivalent (Figure 44), and corrected near visual acuity (Figure 45).

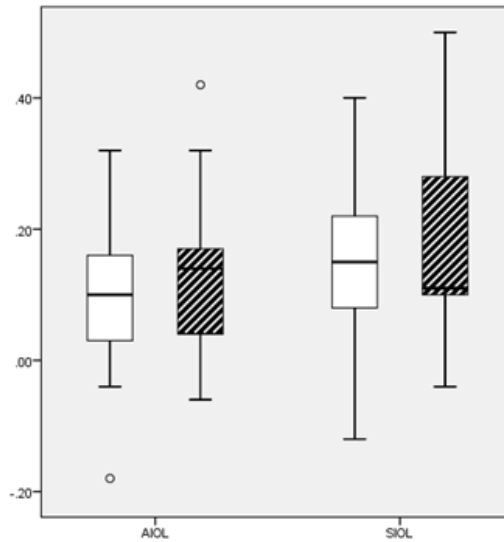


Figure 43: Uncorrected distance visual acuity (UDVA) [logMAR]. Box plot diagram for emmetropic (diagonally hatched boxes) and hyperopic subgroups (white boxes). AIOL=aspheric intraocular lens, SIOL=spherical intraocular lens

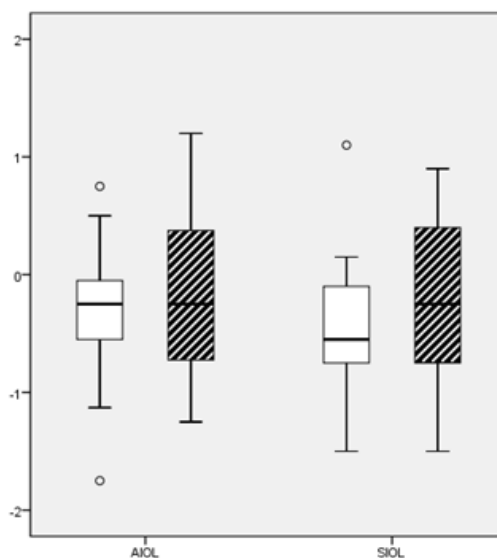


Figure 44: Manifest refractive spherical equivalent (MRSE) [D]. Box plot diagram for emmetropic (diagonally hatched boxes) and hyperopic subgroups (white boxes). AIOL=aspheric intraocular lens, SIOL=spherical intraocular lens

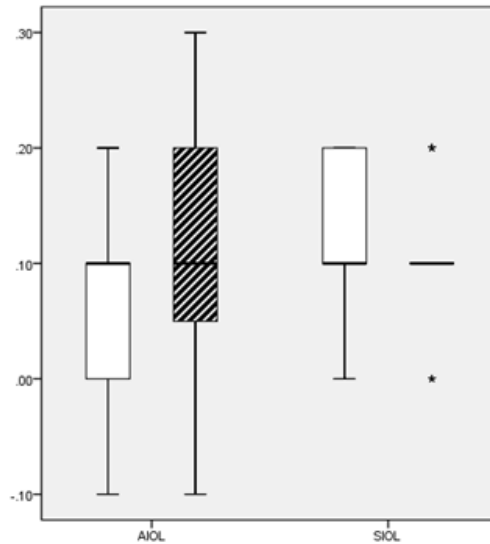


Figure 45: Corrected near visual acuity (CNVA) [logMAR]. Box plot diagram for emmetropic (diagonally hatched boxes) and hyperopic subgroups (white boxes).

AIOL=aspheric intraocular lens, SIOL=spherical intraocular lens

Despite the previously described significantly better results for spherical IOLs compared to aspheric IOLs regarding DCIVA (Figure 46) and DCNVA (Figure 47) as measures of depth of focus, subgroup analysis in both IOL groups revealed no further differences between hyperopic and emmetropic eyes ($p = 0.501$, $p = 0.878$, $p = 0.533$, $p = 0.891$, respectively).

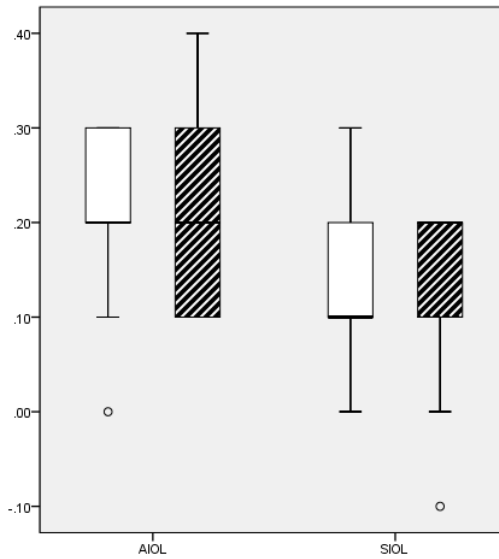


Figure 46: Distance corrected intermediate visual acuity (DCIVA) [logMAR]. Box plot diagram for emmetropic (diagonally hatched boxes) and hyperopic subgroups (white boxes).

AIOL=aspheric intraocular lens, SIOL=spherical intraocular lens

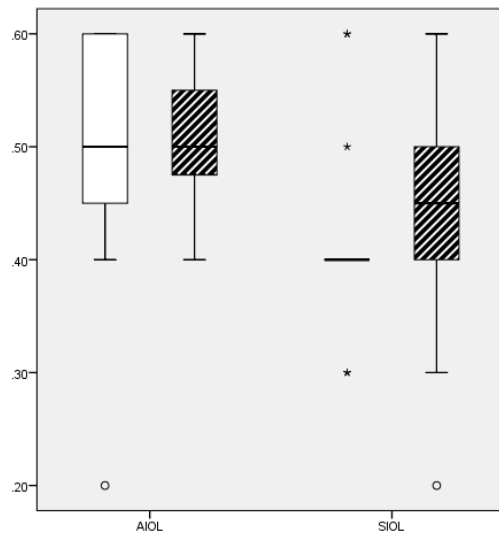


Figure 47: Distance corrected near visual acuity (DCNVA). Box plot diagram for emmetropic (diagonally hatched boxes) and hyperopic subgroups (white boxes).

AIOL=aspheric intraocular lens, SIOL=spherical intraocular lens

While differences in photopic and mesopic contrast sensitivity between eyes with aspheric IOLs and eyes with spherical IOLs showed a trend to better results for aspheric IOLs without reaching statistical significance ($p = 0.073$, $p = 0.057$), hyperopic eyes demonstrated significantly better photopic contrast sensitivity in a subgroup analysis of eyes with spherical IOLs ($p = 0.044$, Figure 48) and significantly better mesopic contrast sensitivity in a subgroup analysis of eyes with aspheric IOLs ($p = 0.032$, Figure 49).

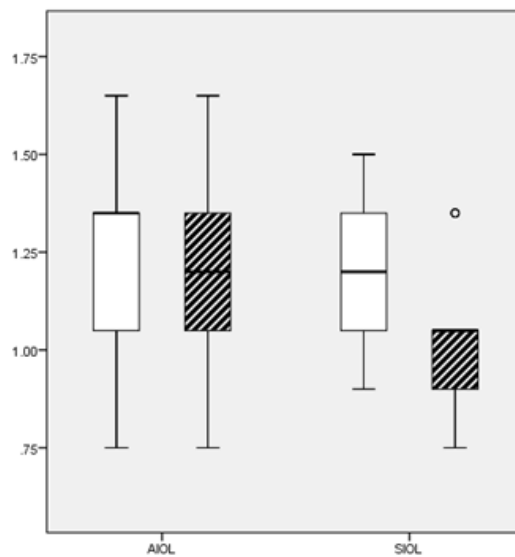


Figure 48: Photopic contrast sensitivity [logCS]. Box plot diagram for emmetropic (diagonally hatched boxes) and hyperopic subgroups (white boxes). AIOL=aspheric intraocular lens, SIOL=spherical intraocular lens

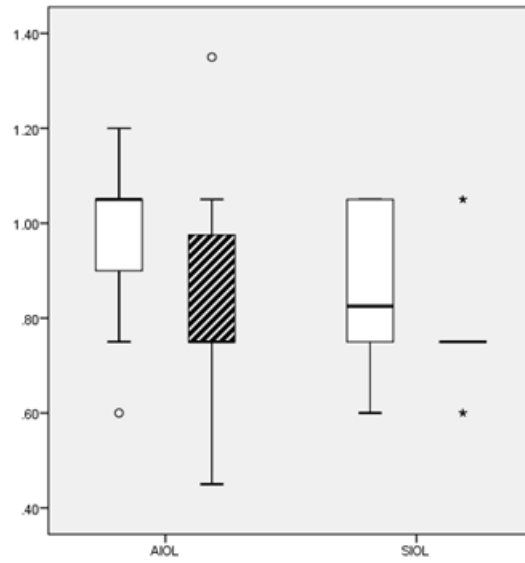


Figure 49: Mesopic contrast sensitivity [logCS]. Box plot diagram for emmetropic (diagonally hatched boxes) and hyperopic subgroups (white boxes). Aiol=aspheric intraocular lens, Siol=spherical intraocular lens

The refractive outcome for hyperopic eyes with the IOL types is displayed in Table 7.

Table 7: Refractive outcome for the hyperopic patient group.

Refractive Outcome	Aspheric IOL Group	Spherical IOL Group	P-value
UDVA [logMAR]	0.10 ± 0.13	0.15 ± 0.14	0.137
MRSE [D]	-0.31 ± 0.61	-0.46 ± 0.66	0.602
CDVA [logMAR]	-0.06 ± 0.05	-0.07 ± 0.05	0.592
CNVA [logMAR]	0.08 ± 0.09	0.11 ± 0.08	0.465
DCIVA [logMAR]	0.21 ± 0.09	0.14 ± 0.07	0.004*
DCNVA [logMAR]	0.50 ± 0.11	0.42 ± 0.09	0.001*
Photopic CS [logCS]	1.28 ± 0.26	1.21 ± 0.22	0.073
Mesopic CS [logCS]	0.96 ± 0.15	0.88 ± 0.16	0.057

*Values are presented as mean ± standard deviation. CDVA=corrected distance visual acuity, CNVA=corrected near visual acuity, CS=contrast sensitivity, D=diopeters, DCIVA=distance corrected intermediate visual acuity, DCNVA=distance corrected near visual acuity, logCS=logarithm of contrast sensitivity, logMAR= logarithm of the minimal angle of resolution, MRSE=manifest refractive spherical equivalent, UDVA=uncorrected distance visual acuity. *= Statistically significant (P ≤ 0.05). Reprinted by permission from Elsevier Inc., Journal of Cataract and Refractive Surgery, Steinwender¹¹³*

Defocus curves for the aspheric and spherical IOL group are shown in Figure 50. Whereas corrected distance visual acuity is similar for both IOLs, the curve of the spherical IOL group is flatter to the right side reflecting better tolerance to defocus and hence better visual acuity at intermediate and near distance.

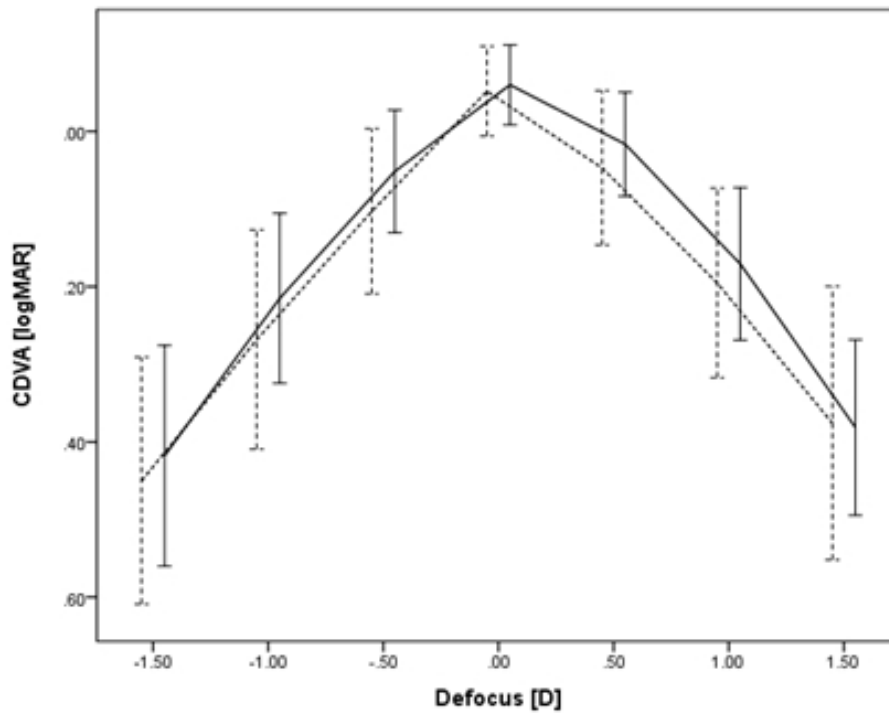


Figure 50: Defocus curves of eyes with aspheric (dashed line) and spherical IOLs (solid line): corrected distance visual acuity (CDVA) in different diopter steps of defocus with error bars (± 1 standard deviation). Reprinted by permission from Elsevier Inc., *Journal of Cataract and Refractive Surgery*, Steinwender¹¹³

Defocus curves of hyperopic eyes with the 2 IOL models are displayed in Figure 51, and defocus curves of emmetropic eyes with the 2 IOL models are displayed in Figure 52. The advantageous flatter slope on the right side of the curve of the spherical IOL group is shown for both hyperopic and emmetropic eyes.

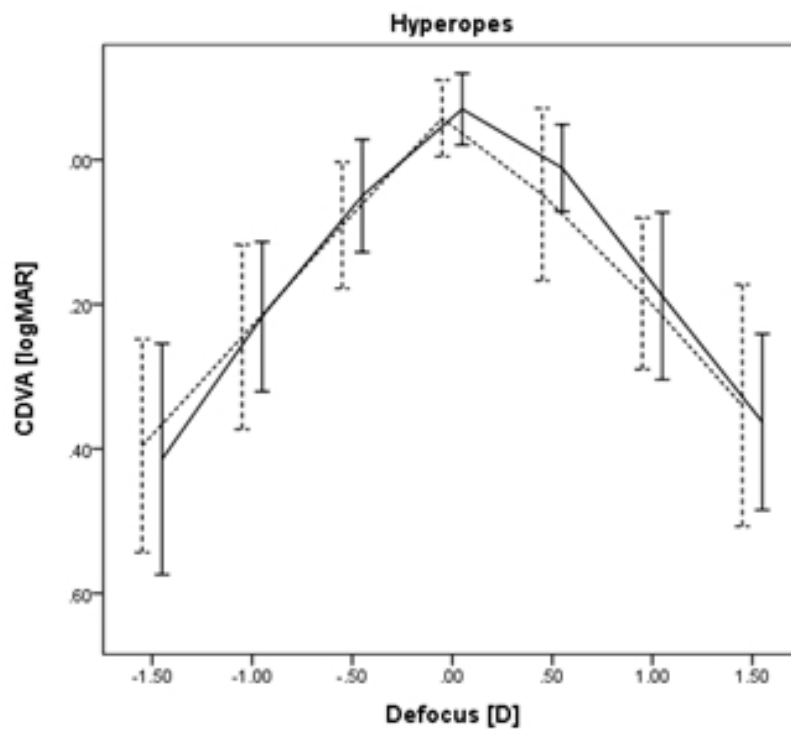


Figure 51: Defocus curves of hyperopic eyes with aspheric (dashed line) and spherical IOLs (solid line): corrected distance visual acuity (CDVA) in different diopter steps of defocus with error bars (± 1 standard deviation). Reprinted by permission from Elsevier Inc., *Journal of Cataract and Refractive Surgery*, Steinwender¹¹³

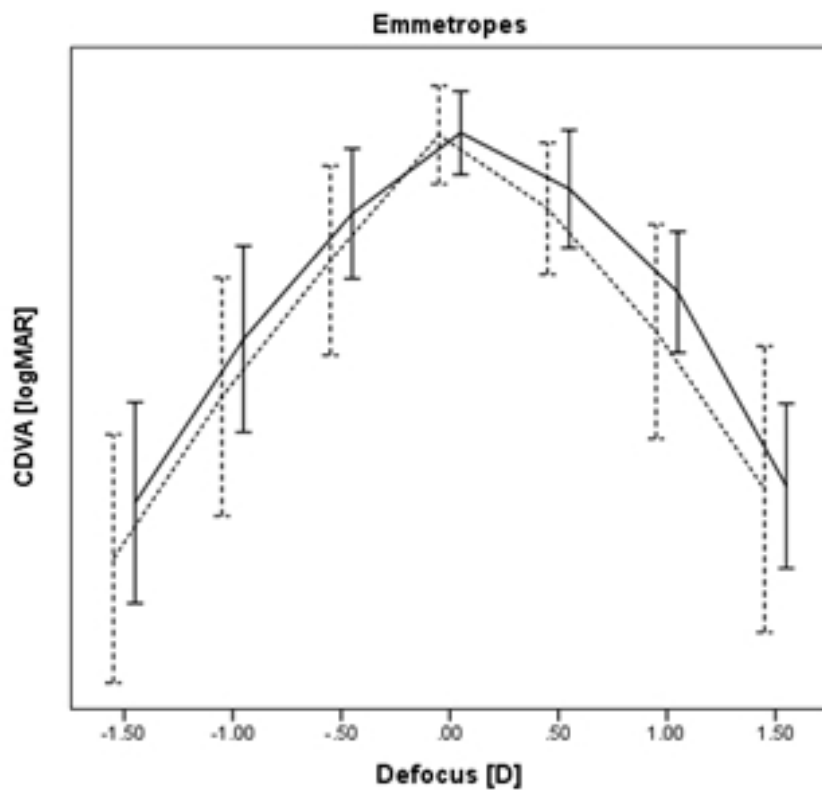


Figure 52: Defocus curves of emmetropic eyes with aspheric (dashed line) and spherical IOLs (solid line): corrected distance visual acuity (CDVA) in different diopter steps of defocus with error bars (± 1 standard deviation). Reprinted by permission from Elsevier Inc., *Journal of Cataract and Refractive Surgery*, Steinwender¹¹³

Comparing hyperopic and emmetropic eyes regardless of the IOL type, no significant differences in functional (UDVA, CDVA, CNVA, DCIVA, DCNVA) and refractive outcome (corneal HOA, corneal SA, total eye HOA, total eye SA) were found.

3.4 Discussion

In the present study, we compared the optical quality of eyes with an aspheric IOL with negative spherical aberration and eyes with a spherical IOL with spherical aberration.

Previous studies have compared visual acuity, contrast sensitivity, and postoperative spherical aberration of eyes with aspheric IOLs to eyes with spherical IOLs.^{118,120–122} A recent meta-analysis including 43 randomized clinical trials found no clinically relevant difference in CDVA; however, contrast sensitivity was better with an aspheric IOL, especially under mesopic conditions.¹⁰⁵ These findings were explained by less total eye spherical aberration and fewer total eye HOA after implantation of aspheric IOLs.¹²³

We used IOLs from the same manufacturer to minimize bias from different IOL materials or haptic designs: the spherical Sensar AR40e IOL and its aspheric counterpart, the Tecnis ZA9003 IOL. Outcome measures were CDVA, depth of focus (DCIVA, DCNVA), visual function in terms of mesopic and photopic contrast sensitivity, and corneal and total eye spherical aberration and HOAs. Since corneal spherical aberration did not differ significantly between the aspheric IOL and the spherical IOL group (Figure 40), it can be assumed that any difference in total eye spherical aberration can be attributed to IOL function inside the eye. The reduced magnitude of total eye spherical aberration in the aspheric IOL (Figure 42) group did not result in an improvement of CDVA or contrast sensitivity (Figure 48 and 49).

Only one previous study compared the same IOL models we used in our study. In accordance to our results, Van Gaalen et al found a significantly lower amount of spherical aberration after implantation of aspheric IOLs.¹²⁴ However, they did not observe a statistically significant difference in depth of focus and contrast sensitivity between the 2 IOL types. This deviation might be explained by differences in testing methodology (computerized contrast sensitivity testing at several defocus levels) and furthermore, by a different photopic pupil size between IOL groups in our study (Figure 37). There is a known association between pupil size and apparent accommodation after implantation of monofocal IOLs.⁴⁴ The difference in postoperatively measured photopic pupil size in our cohorts might be partially attributed to a statistically non-significant difference in mean patient age (Table 5), which is inversely correlated to pupil size.¹²⁵

Depth of focus after implantation of aspheric and spherical IOLs was investigated by several previous studies. Cheng et al observed that HOA, including spherical aberration, coma and secondary astigmatism increase depth of focus.¹²⁶ So, even though aberrations

may decrease image quality, they also enhance the tolerance to defocus. The rationale behind is that an optical system with spherical aberration induces a series of focal points instead of a single focal point, increasing the depth of focus along the focal line on which they lie. Rocha and colleagues, who used the same testing method for evaluation of depth of focus than we used in our study, reported results concordant with our data. As we did in our study, they observed a significantly reduced amount of spherical aberration with a degradation of DCIVA and DCNVA in the aspheric IOL group (Figure 42, 46, 47).⁵¹ These findings are in agreement with those by Nanavaty et al, who reported a decreased depth of focus in aspheric IOLs by comparing aberrometer-computed depth of focus values.¹¹⁰ Analyzing adaptive optics visual stimulation, Ruiz-Alcocer and colleagues proposed, that the best compromise between distance visual acuity and depth of focus may be a certain magnitude of spherical aberration.¹¹⁹ This assumption is supported by our presented defocus curves (Figure 50), as CDVA is comparable between IOL groups whereas the flatter slope of the spherical IOL curve reflects advantageous depth of focus. Santhiago et al reported contradictory results with no significant differences in depth of focus between aspheric and spherical IOLs.¹²¹ This may be due to the type of aspheric IOL they used in their study, which is considered aberration-neutral with theoretically no spherical aberration, whereas the aspheric IOL we used in our study (Tecnis ZA9003), has a negative spherical aberration of 0.27 μm . Another study of Thiagarajan et al comparing an aberration-neutral IOL with the spherical Sensar AR40e IOL, also found no significant differences in depth of focus.¹²²

The lack of difference in contrast sensitivity between the aspheric IOL group and the spherical IOL group in our study may be a consequence of the fact, that although there were differences in total eye spherical aberration (Figure 42), the total eye HOAs did not differ (Figure 41). Our results are in line with those reported by Van Gaalen et al, who found no differences in contrast sensitivity in a comparison of the same IOLs we used in our study.¹²⁴ Nevertheless, there was a tendency to decreased photopic and mesopic contrast sensitivity values with spherical IOLs ($p = 0.073$, $p = 0.057$, respectively, Figure 48 and Figure 49) in our data, which might have reached statistical significance with higher statistical power due to larger cohorts.

We conclude that our findings confirm the hypothesis, that some residual spherical aberration in the pseudophakic eye is a better choice for enhancing optical quality after cataract surgery.

As in our clinical experience hyperopic patients were more often spectacle-independent after cataract surgery with monofocal IOLs than emmetropic or myopic patients, another aim of our study was to analyze, whether hyperopic eyes achieve a different quality of vision after implantation of a spherical or aspheric IOL.

This clinical observation was consistent with previous findings of Lim and colleagues, who showed an association between good near vision after monofocal IOL implantation and short axial length.¹¹¹ The advantage of short axial length was explained by an inverse effect of axial length and accommodation for a given amount of IOL-movement. This effect was reported by Nawa et al: if an IOL implanted in the capsular bag moved forward 1.0 mm, the achieved accommodation was proportionately higher in shorter eyes compared to longer eyes.¹²⁷ Recently, Savini et al described another interesting observation regarding IOL position: they showed that the effective lens position (ELP) is the factor that actually influences the near focal distance with multifocal IOLs.¹²⁸ In their study, in short hyperopic eyes a shorter near focal distance was calculated than in longer eyes, mainly caused by a short ELP. Probably, the influence of ELP on spherical aberration is comparable to its influence on the near add power in multifocal IOLs.

However, we did not find significant differences in distance corrected intermediate or near visual acuity between the hyperopic and emmetropic subgroups, neither in the aspheric nor in the spherical IOL group. We suppose that the effect of ELP on spherical aberration is too small to reach clinical and statistical significance. Possible reasons for the discrepancy between the findings of Lim et al and our data may also be longer axial length values in their study compared to ours, and furthermore, the relatively small sample size in our subgroups which represents a limitation of our study.

Previously, Padmanabhan et al described an association between the magnitude of spherical aberration and the dioptric IOL power after implantation of spherical IOLs.¹¹² However, their observation deviates from our results as total eye spherical aberration did not differ significantly between hyperopic and emmetropic patients in our cohort. This contradiction may be attributed to lower IOL powers (10 to 26 D) in their study compared to ours (18 to 29.5 D).

In our study, a higher amount of corneal spherical aberration in hyperopic eyes compared to emmetropic eyes in the aspheric IOL group (Figure 40) was not reflected in a significant difference in total eye spherical aberration (Figure 42). Interestingly, analyzing contrast sensitivity in the subgroups with spherical IOLs, we observed a worse performance in emmetropic eyes which might be attributed to a nonsignificant trend of increased total eye

HOA in the emmetropic eyes compared to the hyperopic eyes (Figure 41). A possible reason for increased HOA could be a higher percentage of IOL tilt or decentration in this subgroup, but, unfortunately we had no access to any mean of measurement of those parameters.

In conclusion, we found that implantation of a monofocal spherical IOL lead to increased depth of focus without significant impairment of distance visual acuity or contrast sensitivity. To our knowledge, this is the first study analyzing whether hyperopic patients with short axial length and high dioptric IOL power may achieve a higher depth of focus. Nevertheless, we found no significant differences in depth of focus between hyperopic and emmetropic eyes after both, implantation of spherical and aspheric intraocular lenses.

4 Bibliography

1. Azar D, Azar N, Brodie S, et al. *Basic and Clinical Science Course (American Academy of Ophthalmology)*. Vol 3 Clinical Optics. 1st ed. San Francisco; 2013.
2. Williams KM, Verhoeven VJM, Cumberland P, et al. Prevalence of refractive error in Europe: the European Eye Epidemiology (E(3)) Consortium. *Eur J Epidemiol*. 2015;30(4):305-315. doi:10.1007/s10654-015-0010-0
3. Williams KM, Bertelsen G, Cumberland P, et al. Increasing Prevalence of Myopia in Europe and the Impact of Education. *Ophthalmology*. 2015;122(7):1489-1497. doi:10.1016/j.ophtha.2015.03.018
4. Pan C-W, Ramamurthy D, Saw S-M. Worldwide prevalence and risk factors for myopia: Prevalence and risk factors for myopia. *Ophthalmic Physiol Opt*. 2012;32(1):3-16. doi:10.1111/j.1475-1313.2011.00884.x
5. Flitcroft DI. The complex interactions of retinal, optical and environmental factors in myopia aetiology. *Prog Retin Eye Res*. 2012;31(6):622-660. doi:10.1016/j.preteyeres.2012.06.004
6. Baumeister M, Kohnen T. Akkommodation und Presbyopie: Teil 1: Physiologie der Akkommodation und Entwicklung der Presbyopie. *Ophthalmol*. 2008;105(6):597-610. doi:10.1007/s00347-008-1761-8
7. Kohnen T. *Refraktive Chirurgie*. Dordrecht: Springer; 2011. <http://public.eblib.com/choice/publicfullrecord.aspx?p=770138>. Accessed July 20, 2018.
8. Datiles MB, Gancayco T. Low myopia with low astigmatic correction gives cataract surgery patients good depth of focus. *Ophthalmology*. 1990;97(7):922-926.
9. Sawusch MR, Guyton DL. Optimal astigmatism to enhance depth of focus after cataract surgery. *Ophthalmology*. 1991;98(7):1025-1029.
10. Michelitsch M, Ardjomand N, Vidic B, Wedrich A, Steinwender G. Prävalenz und Altersabhängigkeit von kornealem Astigmatismus bei Patienten vor Kataraktchirurgie. *Ophthalmol*. 2017;114(3):247-251. doi:10.1007/s00347-016-0323-8
11. Bühren J, Kohnen T. Anwendung der Wellenfrontanalyse in Klinik und Wissenschaft: Vom irregulären Astigmatismus zu Aberrationen höherer Ordnung –

- Teil I: Grundlagen. *Ophthalmol.* 2007;104(10):909-925. doi:10.1007/s00347-007-1626-6
12. Oshika T, Klyce SD, Applegate RA, Howland HC. Changes in corneal wavefront aberrations with aging. *Invest Ophthalmol Vis Sci.* 1999;40(7):1351-1355.
 13. Smith G, Cox MJ, Calver R, Garner LF. The spherical aberration of the crystalline lens of the human eye. *Vision Res.* 2001;41(2):235-243.
 14. Packer M, Fine IH, Hoffman RS. Wavefront technology in cataract surgery. *Curr Opin Ophthalmol.* 2004;15(1):56-60.
 15. Artal P, Berrio E, Guirao A, Piers P. Contribution of the cornea and internal surfaces to the change of ocular aberrations with age. *J Opt Soc Am A Opt Image Sci Vis.* 2002;19(1):137-143.
 16. Barbero S, Marcos S, Jiménez-Alfaro I. Optical aberrations of intraocular lenses measured in vivo and in vitro. *J Opt Soc Am A Opt Image Sci Vis.* 2003;20(10):1841-1851.
 17. van Gaalen KW, Jansonius NM, Koopmans SA, Terwee T, Kooijman AC. Relationship between contrast sensitivity and spherical aberration: comparison of 7 contrast sensitivity tests with natural and artificial pupils in healthy eyes. *J Cataract Refract Surg.* 2009;35(1):47-56. doi:10.1016/j.jcrs.2008.09.016
 18. Liang J, Grimm B, Goetz S, Bille JF. Objective measurement of wave aberrations of the human eye with the use of a Hartmann-Shack wave-front sensor. *J Opt Soc Am A Opt Image Sci Vis.* 1994;11(7):1949-1957.
 19. Mrochen M, Kaemmerer M, Mierdel P, Krinke HE, Seiler T. Principles of Tscherning aberrometry. *J Refract Surg Thorofare NJ 1995.* 2000;16(5):S570-571.
 20. Koh S, Maeda N, Kuroda T, et al. Effect of tear film break-up on higher-order aberrations measured with wavefront sensor. *Am J Ophthalmol.* 2002;134(1):115-117.
 21. Montés-Micó R, Alió JL, Muñoz G, Pérez-Santonja JJ, Charman WN. Postblink changes in total and corneal ocular aberrations. *Ophthalmology.* 2004;111(4):758-767. doi:10.1016/j.optha.2003.06.027
 22. Zernike von F. Beugungstheorie des schneidenverfahrens und seiner verbesserten form, der phasenkontrastmethode. *Physica.* 1934;1(7-12):689-704. doi:10.1016/S0031-8914(34)80259-5
 23. Thibos LN, Applegate RA, Schwiegerling JT, Webb R, VSIA Standards Taskforce Members. Vision science and its applications. Standards for reporting the optical aberrations of eyes. *J Refract Surg Thorofare NJ 1995.* 2002;18(5):S652-660.

24. Smolek MK, Klyce SD. Zernike polynomial fitting fails to represent all visually significant corneal aberrations. *Invest Ophthalmol Vis Sci.* 2003;44(11):4676-4681.
25. Schwiegerling J, Greivenkamp JE, Miller JM. Representation of videokeratographic height data with Zernike polynomials. *J Opt Soc Am A Opt Image Sci Vis.* 1995;12(10):2105-2113.
26. Applegate RA, Marsack JD, Ramos R, Sarver EJ. Interaction between aberrations to improve or reduce visual performance. *J Cataract Refract Surg.* 2003;29(8):1487-1495.
27. Nio YK, Jansonius NM, Fidler V, Geraghty E, Norrby S, Kooijman AC. Spherical and irregular aberrations are important for the optimal performance of the human eye. *Ophthalmic Physiol Opt J Br Coll Ophthalmic Opt Optom.* 2002;22(2):103-112.
28. Nio YK, Jansonius NM, Wijdh RHJ, et al. Effect of methods of myopia correction on visual acuity, contrast sensitivity, and depth of focus. *J Cataract Refract Surg.* 2003;29(11):2082-2095.
29. Marsack JD, Thibos LN, Applegate RA. Metrics of optical quality derived from wave aberrations predict visual performance. *J Vis.* 2004;4(4):8. doi:10.1167/4.4.8
30. Applegate RA, Sarver EJ, Khemsara V. Are all aberrations equal? *J Refract Surg Thorofare NJ 1995.* 2002;18(5):S556-562.
31. Ferris FL, Bailey I. Standardizing the measurement of visual acuity for clinical research studies: Guidelines from the Eye Care Technology Forum. *Ophthalmology.* 1996;103(1):181-182.
32. Laidlaw DAH. Development of a clinically feasible logMAR alternative to the Snellen chart: performance of the “compact reduced logMAR” visual acuity chart in amblyopic children. *Br J Ophthalmol.* 2003;87(10):1232-1234. doi:10.1136/bjo.87.10.1232
33. Gupta N, Wolffsohn JSW, Naroo SA. Comparison of near visual acuity and reading metrics in presbyopia correction. *J Cataract Refract Surg.* 2009;35(8):1401-1409. doi:10.1016/j.jcrs.2009.03.026
34. Radner W. Reading charts in ophthalmology. *Graefes Arch Clin Exp Ophthalmol.* 2017;255(8):1465-1482. doi:10.1007/s00417-017-3659-0
35. Radner W, Obermayer W, Richter-Mueksch S, Willinger U, Velikay-Parel M, Eisenwort B. The validity and reliability of short German sentences for measuring reading speed. *Graefes Arch Clin Exp Ophthalmol Albrecht Von Graefes Arch Klin Exp Ophthalmol.* 2002;240(6):461-467. doi:10.1007/s00417-002-0443-5

36. Radner W. Near vision examination in presbyopia patients: Do we need good homologated near vision charts? *Eye Vis Lond Engl*. 2016;3:29. doi:10.1186/s40662-016-0061-7
37. Bach M, Wesemann W, Kolling G, Bühren J, Krastel H, Schiefer U. Photopisches Kontrastsehen: Örtliche Kontrastempfindlichkeit. *Ophthalmol*. 2008;105(1):46-59. doi:10.1007/s00347-007-1605-y
38. Dalimier E, Dainty C. Use of a customized vision model to analyze the effects of higher-order ocular aberrations and neural filtering on contrast threshold performance. *J Opt Soc Am A Opt Image Sci Vis*. 2008;25(8):2078-2087.
39. Pesudovs K, Marsack JD, Donnelly WJ, Thibos LN, Applegate RA. Measuring visual acuity--mesopic or photopic conditions, and high or low contrast letters? *J Refract Surg Thorofare NJ* 1995. 2004;20(5):S508-514.
40. Williams D, Yoon GY, Porter J, Guirao A, Hofer H, Cox I. Visual benefit of correcting higher order aberrations of the eye. *J Refract Surg Thorofare NJ* 1995. 2000;16(5):S554-559.
41. Elliott DB, Sanderson K, Conkey A. The reliability of the Pelli-Robson contrast sensitivity chart. *Ophthalmic Physiol Opt J Br Coll Ophthalmic Opt Optom*. 1990;10(1):21-24.
42. Milling AF, O'connor AR, Newsham D. The importance of contrast sensitivity testing in children. *Br Ir Orthopt J*. 2014;11(0):9. doi:10.22599/bioj.79
43. Maaranen T, Mäntyjärvi M. Contrast sensitivity in patients recovered from central serous chorioretinopathy. *Int Ophthalmol*. 1999;23(1):31-35.
44. Elder MJ, Murphy C, Sanderson GF. Apparent accommodation and depth of field in pseudophakia. *J Cataract Refract Surg*. 1996;22(5):615-619.
45. Trindade F, Oliveira A, Frasson M. Benefit of against-the-rule astigmatism to uncorrected near acuity. *J Cataract Refract Surg*. 1997;23(1):82-85.
46. Nanavaty MA, Vasavada AR, Patel AS, Raj SM, Desai TH. Analysis of patients with good uncorrected distance and near vision after monofocal intraocular lens implantation. *J Cataract Refract Surg*. 2006;32(7):1091-1097. doi:10.1016/j.jcrs.2006.03.021
47. Nakazawa M, Ohtsuki K. Apparent accommodation in pseudophakic eyes after implantation of posterior chamber intraocular lenses. *Am J Ophthalmol*. 1983;96(4):435-438.

48. Oshika T, Mimura T, Tanaka S, et al. Apparent accommodation and corneal wavefront aberration in pseudophakic eyes. *Invest Ophthalmol Vis Sci.* 2002;43(9):2882-2886.
49. Uthoff D, Haigis W, Hepper D, Pözl M, Holland D. Evaluierung der Wertigkeit objektiver und subjektiver Verfahren zur Messung von pseudophaker Akkommodation. *Ophthalmol.* 2013;110(5):441-446. doi:10.1007/s00347-012-2695-8
50. Artola A, Patel S, Schimchak P, Ayala MJ, Ruiz-Moreno JM, Alió JL. Evidence for Delayed Presbyopia after Photorefractive Keratectomy for Myopia. *Ophthalmology.* 2006;113(5):735-741.e1. doi:10.1016/j.ophtha.2006.01.054
51. Rocha KM, Soriano ES, Chamon W, Chalita MR, Nosé W. Spherical aberration and depth of focus in eyes implanted with aspheric and spherical intraocular lenses: a prospective randomized study. *Ophthalmology.* 2007;114(11):2050-2054. doi:10.1016/j.ophtha.2007.01.024
52. Langenbacher A, Huber S, Nguyen NX, Seitz B, Gusek-Schneider GC, Kuchle M. Measurement of accommodation after implantation of an accommodating posterior chamber intraocular lens. *J Cataract Refract Surg.* 2003;29(4):677-685.
53. Langenbacher A, Seitz B, Huber S, Nguyen NX, Kuchle M. Theoretical and measured pseudophakic accommodation after implantation of a new accommodative posterior chamber intraocular lens. *Arch Ophthalmol Chic Ill 1960.* 2003;121(12):1722-1727. doi:10.1001/archopht.121.12.1722
54. Gupta N, Wolffsohn JSW, Naroo SA. Optimizing measurement of subjective amplitude of accommodation with defocus curves. *J Cataract Refract Surg.* 2008;34(8):1329-1338. doi:10.1016/j.jcrs.2008.04.031
55. Lenton L. Visual performance in a flight simulator: multifocal intraocular lenses in pilots. *BMJ Open Ophthalmol.* 2018;3(1):e000139. doi:10.1136/bmjophth-2017-000139
56. Myers GA, Stark L. Topology of the near response triad. *Ophthalmic Physiol Opt J Br Coll Ophthalmic Opt Optom.* 1990;10(2):175-181.
57. Pieh S, Kellner C, Hanselmayer G, et al. Comparison of visual acuities at different distances and defocus curves. *J Cataract Refract Surg.* 2002;28(11):1964-1967.
58. Pascolini D, Mariotti SP. Global estimates of visual impairment: 2010. *Br J Ophthalmol.* 2012;96(5):614-618. doi:10.1136/bjophthalmol-2011-300539

59. Brian G, Taylor H. Cataract blindness--challenges for the 21st century. *Bull World Health Organ.* 2001;79(3):249-256.
60. Fishkind WJ, ed. *Phacoemulsification and Intraocular Lens Implantation: Mastering Techniques and Complications in Cataract Surgery: With 643 Illustrations.* Second edition. New York Stuttgart Delhi: Thieme; 2017.
61. Leaming DV. Practice styles and preferences of ASCRS members--1997 survey. *J Cataract Refract Surg.* 1998;24(4):552-561.
62. Kohnen T, Dick B, Jacobi KW. Comparison of the induced astigmatism after temporal clear corneal tunnel incisions of different sizes. *J Cataract Refract Surg.* 1995;21(4):417-424.
63. Gimbel HV, Neuhann T. Development, advantages, and methods of the continuous circular capsulorhexis technique. *J Cataract Refract Surg.* 1990;16(1):31-37.
64. Assia EI, Apple DJ, Tsai JC, Lim ES. The elastic properties of the lens capsule in capsulorhexis. *Am J Ophthalmol.* 1991;111(5):628-632.
65. Faust KJ. Hydrodissection of soft nuclei. *J - Am Intra-Ocul Implant Soc.* 1984;10(1):75-77.
66. Kelman CD. Phaco-emulsification and aspiration. A new technique of cataract removal. A preliminary report. *Am J Ophthalmol.* 1967;64(1):23-35.
67. Findl O. Intraocular Lens Materials and Design. In: *Achieving Excellence in Cataract Surgery A Step-by-Step Approach.* Vol Chapter 12. 1st ed. ; 2009.
68. Miyake K, Ota I, Miyake S, Maekubo K. Correlation between intraocular lens hydrophilicity and anterior capsule opacification and aqueous flare. *J Cataract Refract Surg.* 1996;22 Suppl 1:764-769.
69. Werner L. Glistenings and surface light scattering in intraocular lenses. *J Cataract Refract Surg.* 2010;36(8):1398-1420. doi:10.1016/j.jcrs.2010.06.003
70. Hu J, Sella R, Afshari NA. Dysphotopsia: a multifaceted optic phenomenon. *Curr Opin Ophthalmol.* 2018;29(1):61-68. doi:10.1097/ICU.0000000000000447
71. Zhao Y, Yang K, Li J, Huang Y, Zhu S. Comparison of hydrophobic and hydrophilic intraocular lens in preventing posterior capsule opacification after cataract surgery: An updated meta-analysis. *Medicine (Baltimore).* 2017;96(44):e8301. doi:10.1097/MD.00000000000008301
72. Schmidbauer JM, Werner L, Apple DJ, et al. Postoperative Trübung von Hinterkammerlinsen - eine Übersicht123. *Klin Monatsblätter Für Augenheilkd.* 2001;218(9):586-594. doi:10.1055/s-2001-17635

73. Abhilakh Missier KA, Nuijts RMM., Tjia KF. Posterior capsule opacification: Silicone plate-haptic versus AcrySof intraocular lenses. *J Cataract Refract Surg.* 2003;29(8):1569-1574. doi:10.1016/S0886-3350(02)02046-1
74. Apple DJ, Escobar-Gomez M, Zaugg B, Kleinmann G, Borkenstein AF. Modern Cataract Surgery: Unfinished Business and Unanswered Questions. *Surv Ophthalmol.* 2011;56(6):S3-S53. doi:10.1016/j.survophthal.2011.10.001
75. Findl O, Buehl W, Menapace R, Sacu S, Georgopoulos M, Rainer G. Long-term effect of sharp optic edges of a polymethyl methacrylate intraocular lens on posterior capsule opacification: a randomized trial. *Ophthalmology.* 2005;112(11):2004-2008. doi:10.1016/j.optha.2005.06.021
76. Shah A, Spalton DJ, Gilbert C, et al. Effect of intraocular lens edge profile on posterior capsule opacification after extracapsular cataract surgery in a developing country. *J Cataract Refract Surg.* 2007;33(7):1259-1266. doi:10.1016/j.jcrs.2007.03.044
77. Findl O, Drexler W, Menapace R, et al. Accurate determination of effective lens position and lens-capsule distance with 4 intraocular lenses. *J Cataract Refract Surg.* 1998;24(8):1094-1098.
78. Findl O, Buehl W, Bauer P, Sycha T. Interventions for preventing posterior capsule opacification. Cochrane Eyes and Vision Group, ed. *Cochrane Database Syst Rev.* February 2010. doi:10.1002/14651858.CD003738.pub3
79. Holladay JT, Lang A, Portney V. Analysis of edge glare phenomena in intraocular lens edge designs. *J Cataract Refract Surg.* 1999;25(6):748-752.
80. Erie JC, Bandhauer MH, McLaren JW. Analysis of postoperative glare and intraocular lens design. *J Cataract Refract Surg.* 2001;27(4):614-621.
81. Buehl W, Findl O, Menapace R, et al. Effect of an acrylic intraocular lens with a sharp posterior optic edge on posterior capsule opacification. *J Cataract Refract Surg.* 2002;28(7):1105-1111.
82. Fedorov SN, Kolinko AI, Kolinko AI. [A method of calculating the optical power of the intraocular lens]. *Vestn Oftalmol.* 1967;80(4):27-31.
83. Lundström M, Barry P, Henry Y, Rosen P, Stenevi U. Evidence-based guidelines for cataract surgery: Guidelines based on data in the European Registry of Quality Outcomes for Cataract and Refractive Surgery database. *J Cataract Refract Surg.* 2012;38(6):1086-1093. doi:10.1016/j.jcrs.2012.03.006

84. Hoffmann PC, Hütz WW, Eckhardt HB, Heuring AH. [Intraocular lens calculation and ultrasound biometry: immersion and contact procedures]. *Klin Monatsbl Augenheilkd.* 1998;213(3):161-165. doi:10.1055/s-2008-1034967
85. Preussner P-R. [Accuracy limits in IOL calculation: current status]. *Klin Monatsbl Augenheilkd.* 2007;224(12):893-899. doi:10.1055/s-2007-963734
86. Norrby S. Sources of error in intraocular lens power calculation. *J Cataract Refract Surg.* 2008;34(3):368-376. doi:10.1016/j.jcrs.2007.10.031
87. Olsen T. Prediction of the effective postoperative (intraocular lens) anterior chamber depth. *J Cataract Refract Surg.* 2006;32(3):419-424. doi:10.1016/j.jcrs.2005.12.139
88. Leinonen J, Laakkonen E, Laatikainen L. Repeatability (test-retest variability) of refractive error measurement in clinical settings. *Acta Ophthalmol Scand.* 2006;84(4):532-536. doi:10.1111/j.1600-0420.2006.00695.x
89. Aristodemou P, Knox Cartwright NE, Sparrow JM, Johnston RL. Intraocular lens formula constant optimization and partial coherence interferometry biometry: Refractive outcomes in 8108 eyes after cataract surgery. *J Cataract Refract Surg.* 2011;37(1):50-62. doi:10.1016/j.jcrs.2010.07.037
90. Koch DD, Hill W, Abulafia A, Wang L. Pursuing perfection in intraocular lens calculations: I. Logical approach for classifying IOL calculation formulas. *J Cataract Refract Surg.* 2017;43(6):717-718. doi:10.1016/j.jcrs.2017.06.006
91. Hoffmann PC, Hütz WW. Analysis of biometry and prevalence data for corneal astigmatism in 23 239 eyes. *J Cataract Refract Surg.* 2010;36(9):1479-1485. doi:10.1016/j.jcrs.2010.02.025
92. Wang Q, Jiang W, Lin T, Wu X, Lin H, Chen W. Meta-analysis of accuracy of intraocular lens power calculation formulas in short eyes: IOL power calculation in short eyes. *Clin Experiment Ophthalmol.* 2018;46(4):356-363. doi:10.1111/ceo.13058
93. Carifi G, Aiello F, Zygoura V, Kopsachilis N, Maurino V. Accuracy of the Refractive Prediction Determined by Multiple Currently Available Intraocular Lens Power Calculation Formulas in Small Eyes. *Am J Ophthalmol.* 2015;159(3):577-583. doi:10.1016/j.ajo.2014.11.036
94. Gökce SE, Zeiter JH, Weikert MP, Koch DD, Hill W, Wang L. Intraocular lens power calculations in short eyes using 7 formulas. *J Cataract Refract Surg.* 2017;43(7):892-897. doi:10.1016/j.jcrs.2017.07.004

95. Packer M, Fine IH, Hoffman RS, Piers PA. Prospective randomized trial of an anterior surface modified prolate intraocular lens. *J Refract Surg Thorofare NJ* 1995. 2002;18(6):692-696.
96. Koch DD, Wang L. Custom optimization of intraocular lens asphericity. *Trans Am Ophthalmol Soc.* 2007;105:36-41; discussion 41-42.
97. Yeu E, Wang L, Koch DD. The Effect of Corneal Wavefront Aberrations on Corneal Pseudoaccommodation. *Am J Ophthalmol.* 2012;153(5):972-981.e2. doi:10.1016/j.ajo.2011.10.019
98. Wang L, Dai E, Koch DD, Nathoo A. Optical aberrations of the human anterior cornea. *J Cataract Refract Surg.* 2003;29(8):1514-1521. doi:10.1016/S0886-3350(03)00467-X
99. Wang L, Santaella RM, Booth M, Koch DD. Higher-order aberrations from the internal optics of the eye. *J Cataract Refract Surg.* 2005;31(8):1512-1519. doi:10.1016/j.jcrs.2004.01.048
100. Wang L, Koch DD. Ocular higher-order aberrations in individuals screened for refractive surgery. *J Cataract Refract Surg.* 2003;29(10):1896-1903. doi:10.1016/S0886-3350(03)00643-6
101. Montés-Micó R, Ferrer-Blasco T, Cerviño A. Analysis of the possible benefits of aspheric intraocular lenses: Review of the literature. *J Cataract Refract Surg.* 2009;35(1):172-181. doi:10.1016/j.jcrs.2008.09.017
102. Kohnen T, Klaproth OK, Bühren J. Effect of intraocular lens asphericity on quality of vision after cataract removal: an intraindividual comparison. *Ophthalmology.* 2009;116(9):1697-1706. doi:10.1016/j.opthta.2009.03.052
103. Nanavaty MA, Spalton DJ, Gala KB. Fellow-eye comparison of 2 aspheric microincision intraocular lenses and effect of asphericity on visual performance. *J Cataract Refract Surg.* 2012;38(4):625-632. doi:10.1016/j.jcrs.2011.10.039
104. Kasper T, Bühren J, Kohnen T. Visual performance of aspherical and spherical intraocular lenses: intraindividual comparison of visual acuity, contrast sensitivity, and higher-order aberrations. *J Cataract Refract Surg.* 2006;32(12):2022-2029. doi:10.1016/j.jcrs.2006.07.029
105. Schuster AK, Tesarz J, Vossmerbaeumer U. The impact on vision of aspheric to spherical monofocal intraocular lenses in cataract surgery: a systematic review with meta-analysis. *Ophthalmology.* 2013;120(11):2166-2175. doi:10.1016/j.opthta.2013.04.011

106. Kasper T, Bühren J, Kohnen T. Intraindividual comparison of higher-order aberrations after implantation of aspherical and spherical intraocular lenses as a function of pupil diameter. *J Cataract Refract Surg.* 2006;32(1):78-84. doi:10.1016/j.jcrs.2005.11.018
107. Eom Y, Yoo E, Kang S-Y, Kim H-M, Song J-S. Change in Efficiency of Aspheric Intraocular Lenses Based on Pupil Diameter. *Am J Ophthalmol.* 2013;155(3):492-498.e2. doi:10.1016/j.ajo.2012.09.024
108. Baumeister M, Bühren J, Kohnen T. Tilt and decentration of spherical and aspheric intraocular lenses: Effect on higher-order aberrations. *J Cataract Refract Surg.* 2009;35(6):1006-1012. doi:10.1016/j.jcrs.2009.01.023
109. Marcos S, Barbero S, Jiménez-Alfaro I. Optical quality and depth-of-field of eyes implanted with spherical and aspheric intraocular lenses. *J Refract Surg Thorofare NJ 1995.* 2005;21(3):223-235.
110. Nanavaty MA, Spalton DJ, Boyce J, Saha S, Marshall J. Wavefront aberrations, depth of focus, and contrast sensitivity with aspheric and spherical intraocular lenses: fellow-eye study. *J Cataract Refract Surg.* 2009;35(4):663-671. doi:10.1016/j.jcrs.2008.12.011
111. Lim DH, Han JC, Kim MH, Chung E-S, Chung T-Y. Factors affecting near vision after monofocal intraocular lens implantation. *J Refract Surg Thorofare NJ 1995.* 2013;29(3):200-204. doi:10.3928/1081597X-20130129-06
112. Padmanabhan P, Yoon G, Porter J, Rao SK, Roy J, Choudhury M. Wavefront aberrations in eyes with Acrysof monofocal intraocular lenses. *J Refract Surg Thorofare NJ 1995.* 2006;22(3):237-242.
113. Steinwender G, Strini S, Glatz W, et al. Depth of focus after implantation of spherical or aspheric intraocular lenses in hyperopic and emmetropic patients. *J Cataract Refract Surg.* 2017;43(11):1413-1419. doi:10.1016/j.jcrs.2017.08.012
114. Packer M, Fine IH, Hoffman RS. Aspheric intraocular lens selection: the evolution of refractive cataract surgery. *Curr Opin Ophthalmol.* 2008;19(1):1-4. doi:10.1097/ICU.0b013e3282f2d791
115. Holladay JT, Piers PA, Koranyi G, van der Mooren M, Norrby NES. A new intraocular lens design to reduce spherical aberration of pseudophakic eyes. *J Refract Surg Thorofare NJ 1995.* 2002;18(6):683-691.

116. Bellucci R, Morselli S, Piers P. Comparison of wavefront aberrations and optical quality of eyes implanted with five different intraocular lenses. *J Refract Surg Thorofare NJ 1995*. 2004;20(4):297-306.
117. Li J, Xiong Y, Wang N, et al. Effects of spherical aberration on visual acuity at different contrasts. *J Cataract Refract Surg*. 2009;35(8):1389-1395. doi:10.1016/j.jcrs.2009.03.033
118. Denoyer A, Denoyer L, Halfon J, Majzoub S, Pisella P-J. Comparative study of aspheric intraocular lenses with negative spherical aberration or no aberration. *J Cataract Refract Surg*. 2009;35(3):496-503. doi:10.1016/j.jcrs.2008.11.032
119. Ruiz-Alcocer J, Pérez-Vives C, Madrid-Costa D, García-Lázaro S, Montés-Micó R. Depth of focus through different intraocular lenses in patients with different corneal profiles using adaptive optics visual simulation. *J Refract Surg Thorofare NJ 1995*. 2012;28(6):406-412. doi:10.3928/1081597X-20120518-03
120. Nochez Y, Majzoub S, Pisella P-J. Effect of residual ocular spherical aberration on objective and subjective quality of vision in pseudophakic eyes. *J Cataract Refract Surg*. 2011;37(6):1076-1081. doi:10.1016/j.jcrs.2010.12.056
121. Santhiago MR, Netto MV, Barreto J, Gomes BAF, Oliveira CD, Kara-Junior N. Optical quality in eyes implanted with aspheric and spherical intraocular lenses assessed by NIDEK OPD-Scan: a randomized, bilateral, clinical trial. *J Refract Surg Thorofare NJ 1995*. 2011;27(4):287-292. doi:10.3928/1081597X-20100714-01
122. Thiagarajan M, McClenaghan R, Anderson DF. Comparison of visual performance with an aspheric intraocular lens and a spherical intraocular lens. *J Cataract Refract Surg*. 2011;37(11):1993-2000. doi:10.1016/j.jcrs.2011.05.046
123. Schuster AK, Tesarz J, Vossmerbaeumer U. Ocular wavefront analysis of aspheric compared with spherical monofocal intraocular lenses in cataract surgery: Systematic review with metaanalysis. *J Cataract Refract Surg*. 2015;41(5):1088-1097. doi:10.1016/j.jcrs.2015.04.005
124. van Gaalen KW, Koopmans SA, Jansonius NM, Kooijman AC. Clinical comparison of the optical performance of aspheric and spherical intraocular lenses. *J Cataract Refract Surg*. 2010;36(1):34-43. doi:10.1016/j.jcrs.2009.06.040
125. Winn B, Whitaker D, Elliott DB, Phillips NJ. Factors affecting light-adapted pupil size in normal human subjects. *Invest Ophthalmol Vis Sci*. 1994;35(3):1132-1137.
126. Cheng X, Bradley A, Thibos LN. Predicting subjective judgment of best focus with objective image quality metrics. *J Vis*. 2004;4(4):310-321. doi:10.1167/4.4.7

127. Nawa Y, Ueda T, Nakatsuka M, et al. Accommodation obtained per 1.0 mm forward movement of a posterior chamber intraocular lens. *J Cataract Refract Surg.* 2003;29(11):2069-2072.
128. Savini G, Hoffer KJ, Lombardo M, Serrao S, Schiano-Lomoriello D, Ducoli P. Influence of the effective lens position, as predicted by axial length and keratometry, on the near add power of multifocal intraocular lenses. *J Cataract Refract Surg.* 2016;42(1):44-49. doi:10.1016/j.jcrs.2015.07.044